Unconventional import pathways of the dually localised proteins Thioredoxin 1 and Glutathione peroxidase 3 into the mitochondrial intermembrane space

Eleanor Dickson-Murray BSc (Hons)

Submitted in fulfilment of the requirements for the degree of MSc (Research) Biochemistry - Molecular, Cell and Systems Biology

Institute of Molecular, Cell and Systems Biology

College of Medical, Veterinary and Life Sciences

University of Glasgow

September 2021

Abstract

Mitochondria are essential organelles, underpinning a variety of vital cellular functions. However, mitochondrial DNA (mtDNA) encodes for only 13 proteins and therefore the remaining ~1000 proteins in the proteome of *Saccharomyces cerevisiae* require import into the organelle. All the proteins of the intermembrane space (IMS), a sub-compartment of mitochondria, require import. The main import pathway to the IMS is the mitochondrial import and assembly (MIA) pathway. As well as being the interface between the matrix and the cytosol, the IMS is the site of disulfide bond formation through oxidative folding by the MIA pathway. However, unlike other locations where disulfide bond formation occurs, i.e. the endoplasmic reticulum (ER) and the bacterial periplasm, no reductive pathway has yet been detailed for the IMS. As the major IMS import pathway, the MIA pathway, is subject to redox regulation, it is of interest to investigate proteins that may have a role in balancing the redox environment of the IMS. Having been previously identified as being dually localised between the IMS and the cytosol, the import pathways of the oxidase Glutathione peroxidase 3 (Gpx3) and the reductase Thioredoxin 1 (Trx1) remain unknown. The first part of this thesis focused on investigating the import pathway of Trx1, however as the project developed aims shifted to optimising the import protocol of Trx1. Whilst the import could not be optimised, parameters were identified that can be excluded from having a major role in this import pathway. The second part of this thesis focused on the import pathway of Gpx3 and components that may be involved. The role of the abundant outer membrane proteins Om14 and Om45 were specifically investigated in both a post and co-translational manner with the use of ribosome-stalled Gpx3 RNA. Whilst in a post-translational manner, no effect was observed in the import of Gpx3 into mitochondria containing no Om45, in a co-translational system an increase in import was observed. This preliminary result suggests that Om45 may play a role in the import of Gpx3 and warrants further investigation in the future. Furthering understanding of the nuances involved in the various protein import pathways into mitochondria will ultimately aid the developments of therapeutics for mitochondrial diseases.

Table of Contents

List of Tables

List of Figures

Acknowledgements

Firstly, I would like to sincerely thank my supervisor Professor Kostas Tokatlidis for the opportunity to undertake this masters in his lab. I would not be where I am today in my scientific career without his support, guidance and belief in my abilities. I have hugely enjoyed the opportunity to work as part of his lab and I will always be indebted for the confidence he has instilled in me.

Secondly, I would like Dr Eaglesfield and Dr Edwards (Tokatlidis lab Post Docs) for their time and guidance with the lab practical side of this report. It was a pleasure to work alongside them and their enthusiasm for the field of mitochondrial biology was infectious. I would also like to thank Tokatlidis lab members, past and present, for their help and for creating a welcoming and supportive atmosphere in the lab.

Finally, I would like to say thank you to Stefan and Roza (Tokatlidis lab masters students) for all their support and camaraderie this year. From the early morning mitoprep starts to the late nights finishing an experiment and all the ice-cream trips in between, I have had the best time working with you both and I am excited to see where this masters takes us.

Declaration

I declare that the research conducted in this thesis is the result of my own work unless it is otherwise stated through explicit reference. The work in this thesis has not been submitted for any other degree at the University of Glasgow or any other institution.

List of Abbreviations

0_2^-: superoxide anion

AAC: ADP/ATP carrier

Ab: antibody

ADP: adenosine diphosphate

AIF: apoptosis inducing factor

ATP: adenosine triphosphate

bITS: ß-like IMS targeting signal

CC1p: cytochrome *c* peroxidase

CCCP: carbonyl cyanide m-chlorophenyl hydrazone

CCHL: cytochrome *c* haem lyase

CJ: cristae junction

DTT: dithiothreitol

ER: endoplasmic reticulum

ETC: electron transport chain

FAD: flavin adenine dinucleotide

FT: flow through

G6P: glucose-6-phosphate

G6PD: glucose-6-phosphate dehydrogenase

Glr: glutathione reductase

Gpx3: glutathione peroxidase 3

Grx: glutaredoxin

GSH: glutathione

H_20_2: hydrogen peroxide

Hsp: heat shock protein

IMM: inner mitochondrial membrane

IMS: intermembrane space

IPTG: Isopropyl ß-D-1-thiogalactopyranoside

ITS: intermembrane space targeting signal

List of Abbreviations

MIA: mitochondrial import and assembly

Mim1: mitochondrial protein import 1

MPP: mitochondrial-processing peptidase

mtDNA: mitochondrial DNA

mtHsp70: matrix heat shock protein 70

MTS: matrix targeting signal

N18: 18-amino acid N-terminal extension

NAC: nascent chain-associated complex

NADPH: nicotinamide adenine dinucleotide phosphate

OH^-: hydroxyl radical

OMM: outer mitochondrial membrane

OXA: oxidase assembly

OXPHOS: oxidative phosphorylation

P: pellet

PAM: presequence translocated associated motor

PK: proteinase K

PMSF: phenylmethylsulfonylfluoride

Prx1: peroxiredoxin 1

RNS: reactive nitrogen species

ROS: reactive oxygen species

RRL: rabbit reticulocyte lysate

S: supernatant

SAM: sorting and assembly machinery

SB: sample buffer

SDS: sodium dodecyl sulfate

SOD1: superoxide dismutase 1

TCA: trichloroacetic acid

TIM: translocase of the inner membrane

TNT: coupled transcription and translation

TOM: translocase of the outer membrane

Trr1: thioredoxin reductase 1

Trx1: thioredoxin 1

TX: triton-X

VDAC: voltage dependent anion channel

WT: wild type

ΔΨ: inner mitochondrial membrane potential

Chapter 1: Introduction

1.1 Mitochondria

Mitochondria are essential double membraned organelles that are involved in a diverse range of vital cellular functions. Nicknamed the 'powerhouse of the cell', mitochondria are derived from a common ancestral organelle whose origins came from the integration of an endosymbiotic α-proteobacterium into an early eukaryotic cell (Sagan, 1967). Mitochondria are involved in the energetics, metabolism and regulation of cells. They synthesise energy in the form of ATP via oxidative phosphorylation (OXPHOS) with the components of OXPHOS, respiratory complexes I-IV and F1F0 ATP synthase, being present in the inner mitochondrial membrane (IMM) (Kühlbrandt, 2015). Mitochondria are also the site of a variety of metabolic processes such as the citric acid cycle, the urea cycle and fatty acid regulation. In addition to this central role in energy production, mitochondria are responsible for the beginning of the synthesis of heme (a precursor of haemoglobin), are a hub for amino acid synthesis and biosynthesise iron-sulfur clusters which are protein co-factors. Furthermore, mitochondria contribute to the synthesis of the lipids phosphatidylethanolamine and cardiolipin, the latter being the major lipid in the IMM (Voelker, 2004). Lastly, mitochondria are also involved in the initiation of cell death through the release of cytochrome *c* (Stehling and Lill, 2013; Spinelli and Haigis, 2018; Bock and Tait, 2020).

Mitochondria contain around 1000 different proteins in *Saccharomyces cerevisiae* (*S. cerevisiae*) and roughly 1400 in humans, yet the yeast and human mitochondrial genome encode for just 7 and 13 proteins respectively (Calvo and Mootha, 2010). The proteins encoded by the mitochondrial genome are components of respiratory subunits (Wiedemann and Pfanner, 2017). Therefore, 99% of mitochondrial proteins are nuclear encoded and require import into their correct location within the organelle. Additionally, there is crosstalk between the two genomes to prevent excess protein translation in a variety of forms, for example through oxidative energy production and metabolic signals (Poyton and McEwen, 1996). There is also emerging evidence to support the idea of localised protein synthesis at the outer mitochondrial membrane (OMM) with specific interactions between ribosomes and the translocase of the outer membrane

(TOM) complex (Gold *et al.*, 2017). As the majority of proteins are imported, furthering understanding of protein import and the nuances of the various import pathways involved will ultimately aid therapeutic treatment of mitochondrial diseases. Mitochondria are closely integrated in many cellular processes and have an increased mutation rate in comparison to nuclear DNA. This results in mitochondria being linked to a range of diseases such as cancer, cell death, ageing, diabetes and neurodegenerative diseases (Zong, Rabinowitz and White, 2016; Haas, 2019; Monzio Compagnoni *et al.*, 2020; Skuratovskaia *et al.*, 2020).

1.2 Mitochondria structure

Mitochondria are around 0.1-0.5μM in width and ~102μM in length with two aqueous sub-compartments separated by two phospholipid bilayers (Frey and Mannella, 2000). These two bilayers differ in composition and function with the IMM containing a greater amount of cardiolipin than the OMM. Additionally, the IMM is impermeable in comparison to the semi-permeable OMM, described in more detail below (figure 1).

1.2.1 The outer mitochondrial membrane

The OMM separates the mitochondria from the cytoplasm and is a semi-permeable membrane. It allows for the free diffusion of small molecules up to 5kDa through channels called porins. The OMM contains several channels, the main channel is Porin1, also referred to as Voltage dependent anion channel (VDAC), and the TOM complex. Interestingly, recent evidence has uncovered potential novel roles of Porin1; firstly as a coupling factor which assists the transport of metabolite carrier proteins (Ellenrieder *et al.*, 2019). Secondly in regulating the trimeric to dimeric state of the TOM complex through an interaction with Tom22 receptor (Edwards and Tokatlidis, 2019; Sakaue *et al.*, 2019).

1.2.2 The intermembrane space (IMS)

Surrounded by the OMM and the IMM, the intermembrane space (IMS) is the smallest sub-compartment of mitochondria. The IMS can be further sub-divided

into the boundary IMS and the cristae space, the latter of which is formed by invaginations of the IMM. The cristae space is separated from the boundary IMS by cristae junctions (CJs) and contact sites describe where the OMM and the IMM physically contact each other (Mannella, 2006; Habich, Salscheider and Riemer, 2019). This small compartment is the interface between the mitochondrial matrix and the cytosol, exchanging various proteins, lipids, metabolites and metal ions, all of which play a role in redox regulation (Frey and Mannella, 2000). This 'controlled leakiness' of the IMS is due to the presence of porins in the OMM, facilitating communication between the mitochondria and the rest of the cell (Nuebel, Manganas and Tokatlidis, 2016). The IMS contains ~51 proteins in yeast and ~ 53 in humans, none of which are encoded by the mitochondrial genome and therefore require import (Vögtle *et al.*, 2012; Rath *et al.*, 2020). IMS proteins are involved in process such as the assembly and stability of respiratory chain complexes, protein folding and the initiation of cell death through the release of cytochrome *c* (Bock and Tait, 2020; Edwards, Gerlich and Tokatlidis, 2020). The IMS provides a redox active space which is more oxidising than the cytosol, and this allows for the formation of disulfide bonds through oxidative folding. Additionally, the redox environment of the IMS is maintained separately from the cytosol and the matrix (Hu, Dong and Outten, 2008). There are ~6 known import pathways to the IMS with a number of IMS proteins exhibiting dual localisation between the cytosol and the IMS, reinforcing that communication occurs between these two locations (Vögtle *et al.*, 2012; Nuebel, Manganas and Tokatlidis, 2016; Edwards, Gerlich and Tokatlidis, 2020).

1.2.3 The inner mitochondrial membrane

Unlike the OMM, the IMM is impermeable, highly charged and has a more protein rich composition due to the presence of the respiratory chain. It contains a range of proteins to help facilitate import to the matrix such as the translocase of the inner membrane (TIM) complexes 22 and 23. The IMM can bend inwards to form cristae, giving rise to cristae junctions and intracristae spaces. Recent research demonstrates that different cristae in the same mitochondria can have different membrane potentials, with the cristae junctions providing electrical insulation (Wolf *et al.*, 2019).

1.2.4 The matrix

This second sub-compartment has an overall negative charge and contains the majority of mitochondrial proteins and the mitochondrial DNA (mtDNA). The matrix is the site of key mitochondrial pathways such as Fe-S cluster synthesis, the TCA cycle, OXPHOS and is involved in the regulation of calcium dynamics which play a role in cell death.

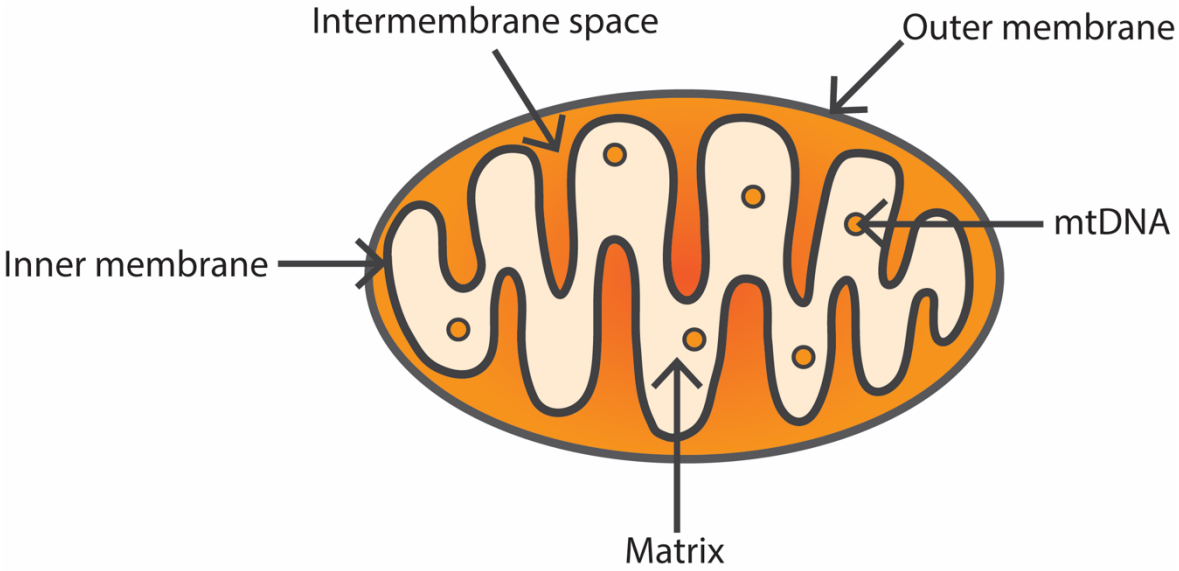

Figure 1: The structure of the mitochondrion. The different subcompartments and the location of mtDNA are annotated.

1.3 Mitochondrial import pathways

As mentioned previously, the majority of mitochondrial proteins require import into mitochondria and to cope with this, mitochondria have at least five different and sophisticated pathways. The five main pathways that are currently known are; (i) the presequence pathway, (ii) the carrier pathway, (iii) the ß-barrel pathway, (iv) insertion of α-helical transmembrane segment containing proteins and (v) the mitochondrial import and assembly pathway (MIA), the latter will discussed in section 1.4. The vast majority of these proteins all translocate through the TOM channel.

1.3.1 The translocase of the outer membrane (TOM)

The TOM complex is the general import channel in the OMM, through which the majority of precursor proteins translocate from the cytosol to their correct sub-compartments. The TOM complex is comprised of the ß-barrel channel protein Tom40, the 3 protein receptors (Tom22, Tom20 and Tom70) and 3 non-essential smaller Tom proteins (Tom5, Tom6 and Tom7) (Hill *et al.*, 1998; Shiota *et al.*, 2015; Wiedemann and Pfanner, 2017). Tom20 is the initial receptor for incoming precursors that contain a cleavable presequence and Tom70 recognises precursors of hydrophobic IMM and OMM proteins (Abe *et al.*, 2000; Young, Hoogenraad and Hartl, 2003; Grevel, Pfanner and Becker, 2019). Tom22 has a dual role: firstly in recruiting Tom20 and Tom70 to the complex, and secondly in aiding the transfer of the preprotein from the receptors to the Tom40 channel (Yamano *et al.*, 2008). The three small Tom proteins (Tom5, 6 and 7) play a role in the stability of the TOM complex but are not essential (Wiedemann and Pfanner, 2017). Recently the structure of the dimeric and trimeric TOM complex complexes of *S. cerevisiae* were visualised by cryo-electron microscopy and revealed detailed interactions between components of the complexes (Tucker and Park, 2019). The trimeric state of the TOM complex is the most common and preferentially imports IMM and matrix proteins. Whereas the dimeric form of the complex is less common, lacks Tom22 and is believed to preferentially import Mia40 substrates. The change between dimer-trimer conversion of the TOM complex is controlled by VDAC (Por1 in yeast), which cooperates with Tom6 (Sakaue *et al.*, 2019; Edwards, Eaglesfield and Tokatlidis, 2021). Interestingly it was reported that the TOM complex can form tetramers and even larger oligomers. The authors suggested that clustering of TOM complexes may allow for fine tuning of protein import activity, however the function of these oligomeric complexes is yet to be eluded (Tucker and Park, 2019).

1.3.2 The presequence pathway to the matrix

Most matrix proteins are synthesised in the cytosol and contain an N-terminal presequence that targets them to the matrix, the matrix targeting signal (MTS). The presequence pathway is the route for the majority of proteins (~70%) destined for the matrix and for a fraction of IMM proteins (figure 2B). Presequences are located at the N-terminus of preproteins and are ~15-30 amino acids long, forming a positively charged amphipathic helix which is usually

cleaved (Roise and Schatz, 1988). Proteins destined for the IMM contain a hydrophobic sorting signal in addition to the MTS that arrests translocation in the TIM23 complex, this is known as the stop/transfer mechanism (Glick *et al.*, 1992).

The pathway to the matrix firstly involves cytosolic chaperones that bind the precursor protein to keep the protein in an import competent, unfolded state as the Tom40 channel is ~20Å wide. The Tom20 receptor is the initial receptor for the incoming preprotein with negative patches of the receptor interacting with the positive presequence. Additionally, the cytosolic domain of Tom20 forms an alpha helix which contains a groove that aids in the translocation of the presequence (Abe *et al.*, 2000; Yano, Terada and Mori, 2004). From the Tom20 receptor, the preprotein is transferred through the Tom40 channel and pulled through the channel into the mitochondrial by a gradation of affinities, known as the acid chain hypothesis (Komiya *et al.*, 1998). Additionally, Tom22 has a domain in the IMS that is negatively charged, further encouraging translocation of the positive presequence (Yano, Terada and Mori, 2004).

In the IMS, the presequence precursors interact with the translocase of the inner membrane (TIM) 23 complex. TIM23 has a channel size of ~14-15Å and is formed by Tim50, Tim21, Tim23, Tim17, Tim44, Pam18, Pam16, Pam17 and Mge1 (Mokranjac and Neupert, 2010). Tim50 is the first component that binds the preprotein emerging in the IMS aided by Tim21 (Geissler *et al.*, 2002). The IMS facing side of TIM23 is negatively charged and the membrane potential (~200mV) across the IMM is crucial for the translocation of the preprotein through Tim23. To drive translocation, the TIM23 complex recruits the presequence translocase associated motor (PAM) which contains the matrix heat shock protein 70 (mtHsp70) as a central subunit. Tim44 along with Pam16,17 and 18 (all associated with Tim23) play a role in regulating the activity and localisation of mtHsp70, with Tim44 acting as a binding site (Rassow *et al.*, 1994; Hutu *et al.*, 2008). The incoming polypeptide is bound by mtHsp70 which drives movement into the matrix. This process requires adenosine triphosphate (ATP), promoting the unidirectional movement of the preproteins. After import into the matrix, the positively charged presequence is cleaved by the mitochondrial-processing peptidase (MPP) (Braun and Schmitz, 1997).

1.3.3 Insertion into the IMM

The carrier pathway involves the import of hydrophobic IMM proteins that do not contain a presequence (figure 2C). Most of these proteins are metabolite carriers such as the ADP/ATP carrier (AAC), where an internal part of the protein acts as the presequence and insertion of the carrier is facilitated by the TIM23 complex (Wiedemann, Pfanner and Ryan, 2001). The mitochondrial carrier family functions as metabolite transporters, and in humans are involved in several disorders. The family ranges from 30-35kDa in size and they have a common topology of 6 transmembrane domains in a 3x2 helix model (Kuan and Saier, 2008).

Chaperones are key in this import pathways at all stages to ensure that the preprotein does not fold prematurely. Cytosolic chaperones from the Hsp70 and Hsp90 families bind to the hydrophobic precursor carrier proteins to prevent their aggregation (stage I) (Young, Hoogenraad and Hartl, 2003). The chaperone-preprotein complex is then recognised by Tom70 which binds the hydrophobic internal signal (stage II). Tom70 contains binding sites for both the precursor protein and the cytosolic chaperons: the precursor protein is then passed to Tom40 (Wiedemann, Pfanner and Ryan, 2001). After translocating through the Tom40 channel, the carrier preprotein binds the hexameric Tim9-Tim10 complex (themselves imported by the MIA pathway) as it begins to emerge into the IMS. The Tim9-Tim10 complex acts as a chaperone where Tim10 binds the hydrophobic segments of the substrate, with the C-terminal end of Tom10 being crucial for complex formation and Tim9 having more of a structural role (stage III) (Koehler *et al.,* 1998; Vasiljev *et al.,* 2004; Webb *et al.,* 2006). Tim9 and Tim10 are essential, ATP-independent chaperones, instead energy is provided by protein-protein interactions. There is a second hexameric chaperone complex in the IMS, Tim8-Tim13, which is homologous to Tim9-Tim10 however, the latter is the major IMS chaperone system (Curran *et al.,* 2002). Tim9-Tim10 transfer the AAC protein to the TIM22 complex which forms a twin pore translocase (Rehling *et al.,* 2003). Tim54 and Tim18 are integral membrane proteins that are associated with Tim22; Tim54 has a large domain in the IMS which is thought to serve as a docking site for the incoming chaperone-carrier protein complex. Stage IV of the carrier import pathway is the insertion of the preprotein into the Tim22 channel, with activation of the Tim22 channel involving internal targeting signals of the precursor and a membrane electrochemical potential (Rehling *et*

al., 2003). Finally, the AAC protein is laterally released in the lipid phase of the IMM following dimerization and maturation (stage V) (Chacinska *et al.*, 2009). Overall the carrier pathway relies on binding specificity for hydrophobic segments, both by the Tom70 receptor and by the Tim9-Tim10 chaperones before the lateral insertion of the carrier into the IMM by TIM22. However, it has been recently reported that the carrier pathway is more flexible than previously thought. Recent research has shown that the pathway can transport transmembrane helices that are paired or non-paired, being able to direct the precursors' N-terminal into the IMS or the matrix. This suggests that there could be a greater number of substrates for this pathway than previously thought (Rampelt *et al.*, 2020).

A second IMM insertion pathway, the stop transfer pathway, includes the presence of a hydrophobic sorting signal behind the MTS. This sorting signal acts to arrest translocation in the TIM23 complex, leading to lateral release of the protein into the lipid bilayer of the IMM (Glick *et al.*, 1992; van der Laan *et al.*, 2007). This lateral release of proteins is controlled by the small hydrophobic protein Mgr2 which interacts with preproteins in the TIM23 complex (Ieva *et al.*, 2014). Lastly, these IMM preproteins without a hydrophobic will translocate into the matrix. These preproteins are inserted into the IMM from the matrix side by the oxidase assembly (OXA) export machinery. The OXA machinery also plays a role in the biogenesis and assembly of hydrophobic proteins that are encoded by mtDNA, with two subunits of the TIM22 complex relying on OXA for their correct insertion, and therefore activity, in the IMM (Stiller *et al.*, 2016).

1.3.4 ß-barrel pathway to the OMM

All proteins of the OMM are synthesised in the cytosol and the OMM contains two major types of proteins, α-helical proteins and ß-barrel proteins. The former is anchored in the OMM by one or more transmembrane hydrophobic α-helical segments (figure 2D). The latter contains multiple transmembrane ß-strands for insertion into the lipid phase. Note that the IMM contains α-helical proteins only (Chacinska *et al.*, 2009; Schmidt, Pfanner and Meisinger, 2010).

The most common mitochondrial ß-barrel proteins are Porin1 and Tom40: ß-barrel precursors are firstly targeted to the TOM complex before then passing through Tom40 into the IMS. When in the IMS, the Tim9-Tim10 and Tim8-Tim13

chaperones bind the precursor proteins and participate in their transport (Hoppins and Nargang, 2004; Wiedemann *et al.,* 2004). The chaperone complexes guide the precursor proteins to the sorting and assembly machinery (SAM) complex where the ß-barrel precursors are then inserted into a hydrophilic environment within the SAM complex. Finally, the ß-barrel precursors are released into the lipid phase (Wiedemann *et al.,* 2003; Kutik *et al.,* 2008). The SAM complex has been recently reported to exist in two different complexes, one contains Mdm10 and the other contains a second Sam50 subunit (Takeda *et al.,* 2021).

This pathway of transfer to the TOM complex and then the SAM complex mediates the insertion of typical ß-barrel proteins such as Porin1, however, there is a more complicated pathway for the Tom40 precursor protein. Tom40 preproteins require a pre-existing and mature Tom40 channel for their import into mitochondria with the central Tom40 channel requiring both correct assembly of itself and with other TOM complex components. The SAM complex has been shown to provide a platform for TIM components and as mentioned above, there is a population of SAM complexes that contain Mdm10 which promotes the assembly of Tom40 with other TOM α-helical receptor proteins such as Tom22. Tom40 then sequentially assembles with other TOM complex proteins to form the mature TOM complex (Meisinger *et al.,* 2004; Chacinska *et al.,* 2009; Thornton *et al.,* 2010; Yamano, Tanaka-Yamano and Endo, 2010).

1.3.5 Insertion of α-helical proteins in the OMM

There are different types of α-helical OMM proteins that differ in location of their transmembrane segments, which act as targeting signals for the proteins (figure 2A). Proteins that contain a sorting and anchoring single transmembrane segment at their N-terminus use the OMM protein mitochondrial import 1 (Mim1) for membrane insertion (Becker *et al.,* 2008). For example, Tom20 docking to the correct location in the TOM complex is catalysed by Mim1 (Hulett *et al.,* 2008). Precursor proteins with multiple transmembrane segments are inserted using Tom70 in a chaperone-like manner for transfer into the OMM (Otera *et al.,* 2007). Additionally, the precursor Tom22 proteins uses both TOM receptors and the SAM complex for insertion into its correct location. This precursor protein contains multiple internal sequences, a hydrophobic segment in the middle and

some hydrophilic parts. The TOM receptors are responsible for recognition of the precursor and the SAM complex is responsible for the integration of the precursor into the OMM (Stojanovski *et al.*, 2007).

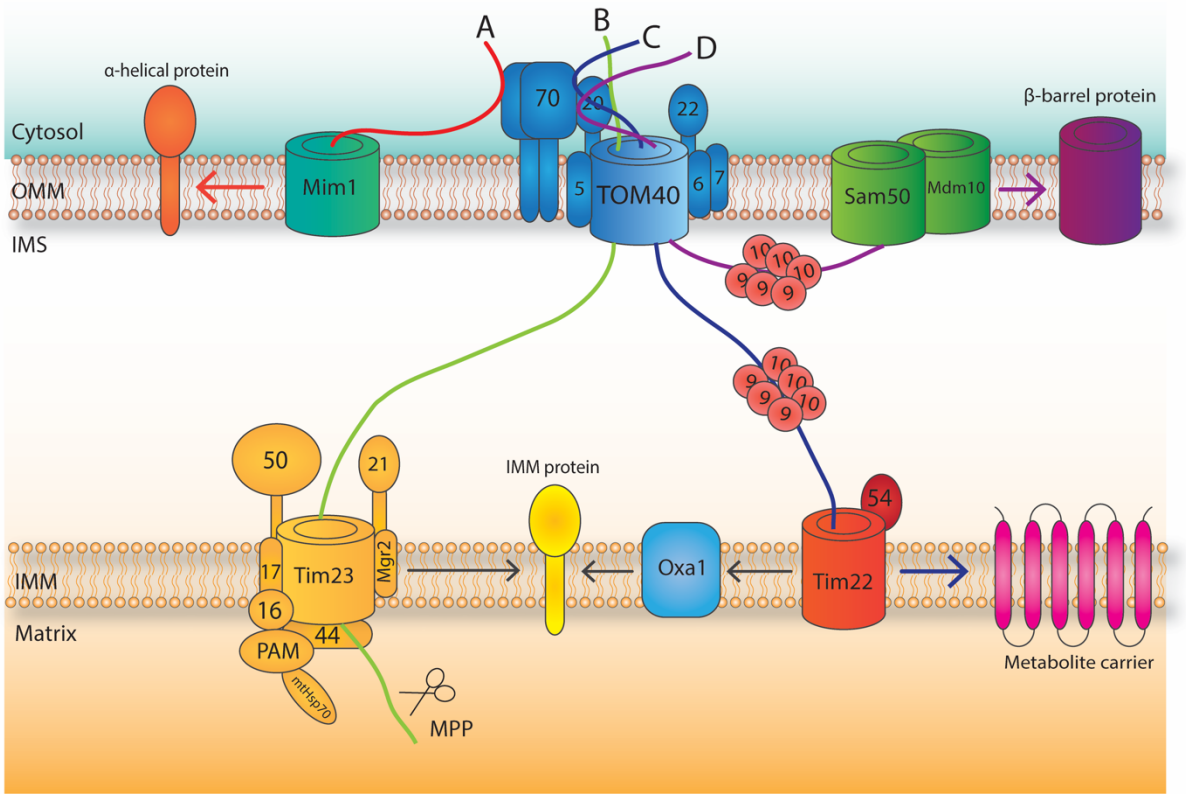

Figure 2: Overview of the main import pathways into the different compartments of mitochondria. (A) Alpha-helical outer membrane proteins utilise the Mim1 complex for their insertion into the IMM. (B) Matrix proteins typically follow the presequence pathway, which involves the TOM complex, the TIM complex and final processing by the matrix processing peptidase (MPP). (C) Hydrophobic IMM metabolite carrier proteins follow the carrier pathway, in which chaperones play a key role at every stage. (D) OMM beta-barrel proteins firstly pass through the TOM complex, before being inserted into the OMM via the SAM complex.

1.4 The import and assembly pathways of mitochondrial IMS proteins

As mentioned previously, the IMS is the smallest sub-compartment of the mitochondria and importantly it provides a redox active space that is more oxidising than the cytosol. This redox active space allows for the formation of disulfide bonds, with the redox active environment of the IMS being maintained

separately from the cytosol and the matrix (Hu, Dong and Outten, 2008). The disulfide bonds are formed in substrate proteins that enter the IMS in a reaction where the thiol groups of two cysteine residues are oxidised, forming a covalently linked intramolecular disulfide. It is through oxidative folding, via the MIA pathway, where a protein acquires its native disulfide bonds and therefore its native 3D structure (Chacinska *et al.*, 2004; Lu *et al.*, 2004). Most proteins in the IMS are of low molecular mass (~7-25kDa), have a simple structure (with a helix-loop-helix being the most common organisation) and lack a presequence (Vögtle *et al.*, 2012; Backes and Herrmann, 2017). It is interesting to note that all proteins destined for the matrix are imported by one pathway that involves a common presequence and energy source (the membrane potential across the IMM). In sharp contrast, protein targeting to the IMS involves a range of pathways, various targeting signals and different energy sources (Edwards, Eaglesfield and Tokatlidis, 2021).

1.4.1 The mitochondrial IMS assembly machinery (MIA)

The MIA pathway in the IMS is responsible for introducing disulfide bonds into imported proteins through oxidative folding and once folded, the protein is retained in the IMS in an oxidised state. The MIA pathway is composed of two essential proteins, the oxidoreductase Mia40 (CHCHD4 in mammals) (Chacinska *et al.*, 2004; Naoé *et al.*, 2004) and the FAD-dependent sulfhydryl oxidase Erv1 (ALR in humans) (Mesecke *et al.*, 2005) (figure 3D).

Mia40 contains six strictly conserved cysteine residues that are organised as a redox sensitive CPC motif and two CX9C motifs. The two CX9C motifs stabilise the proteins and form a hydrophobic cleft of two anti-parallel helices to bind the substrate. The solvent-exposed CPC motif constitutes the redox active cysteine pair of Mia40 that accepts electrons shuttled from the substrate protein, and introduces the disulfide bond whilst switching between a reduced and oxidised state (Naoé *et al.*, 2004; Banci *et al.*, 2009; Kawano *et al.*, 2009). In higher eukaryotes, Mia40 is soluble in the IMS, whereas in fungi and yeast it is anchored to the IMM by its N-terminus (although this membrane anchor is not essential for function). Although this report focuses on the yeast Mia40, ~75% homology exists between the human and yeast homologs of Mia40 (Hofmann *et al.*, 2005; Fischer and Riemer, 2013). With it previously reported that CHCHD4 and ALR, the human

homologous of yeast Mia40 and Erv1 respectively, can complement their yeast counterparts for the function of oxidative biogenesis of mitochondrial IMS proteins (Sztolsztener *et al.*, 2013). Typically, Mia40 substrates are of small mass (between 8-22kDa), contain a hydrophobic intermembrane space targeting signal (ITS) and contain either twin CX3C or CX9C motifs (Gabriel *et al.*, 2007; Terziyska *et al.*, 2007; Sideris *et al.*, 2009). However, other non-typical Mia40 substrates exist that contain a different pattern of cysteine residues, such as the protein Mix23 which has a CX13C/CX14C motif. Overall this demonstrates that the MIA pathway interacts with substrates that contain a broad range of cysteine motifs (Vögtle *et al.*, 2012).

The other essential component of the MIA pathway is Erv1, a 22 kDa conserved flavin-linked sulfhydryl oxidase that is present in a dimeric form in the IMS. Cells that are mutated or depleted of Erv1 have reduced levels of small IMS proteins, such as the Tims, and this highlights the importance of Erv1 in the import of IMS proteins (Mesecke *et al.*, 2005). Erv1 family members have a core domain of ~100 amino acids arranged in a four-helix bundle structure with flavin adenine dinucleotide (FAD) bound non-covalently for stabilisation. The stabilising proximal disulfide (C130/133) is located in the FAD-binding domain and contains the redox active CXXC motif (Wu *et al.*, 2003). Located at the N-terminus is the first cysteine pair, C30/33, which is the shuttle disulfide and interacts with Mia40. The third pair, C159/176, is the structural disulfide which is recognised by Mia40 during the import of Erv1. This N-terminal shuttle domain of Erv1 is sufficient and necessary for the noncovalent interaction of Mia40 and Erv1 (Hofhaus *et al.*, 2003; Lionaki *et al.*, 2010; Kallergi *et al.*, 2012; Banci *et al.*, 2013; Manganas, MacPherson and Tokatlidis, 2017; Ceh-Pavia *et al.*, 2020). The role of Erv1 in the disulfide relay is to re-oxidise Mia40 and this mechanism will be described below in greater detail. However, Erv1 itself is not a classical Mia40 substrate and is imported by the MIA pathway via a CXXC motif (Terziyska *et al.*, 2007; Kallergi *et al.*, 2012). Recently it has been reported that Erv1 is perhaps not as active as previously thought and is a moderately efficient enzyme, using both O_2 and cytochrome *c* as electron acceptors. However, the researchers reason that this moderate efficiency could be due to the slower kinetics of protein import and disulfide bond formation which places no pressure on the requirement for a higher catalytic efficiency (Tang *et al.*, 2020).

To reach the IMS proteins must pass first through the OMM, and in the MIA pathway proteins are translocated through the TOM complex in an unfolded, reduced import competent conformation (Lu *et al.,* 2004). During translocation into the IMS, substrate proteins can bind Mia40 via specific docking cysteines which further drives the import process (Milenkovic *et al.,* 2007; Sideris and Tokatlidis, 2007). The ITS, an internal peptide of 9 amino acids that forms an amphipathic helix, is involved in the interaction between Mia40 and the substrate protein. The ITS itself is sufficient for crossing the OMM and fits complementary to the cleft of Mia40 through hydrophobic interactions (Milenkovic *et al.*, 2009; Sideris *et al.*, 2009). The 'substrate docking' model details the mechanism of interaction between Mia40 and its substrates, with the first 'sliding' step involving positioning of the preprotein's ITS in the cleft of Mia40. The close proximity and correct orientation of the ITS in the hydrophobic cleft results in the formation of a transient intermolecular bond between Mia40 and the substrate, this is facilitated by the CPC motif of Mia40 (Sideris *et al.,* 2009; Banci *et al.,* 2010). The 'docking' step involves the formation of a transient disulfide intermediate between the CPC second cysteine of Mia40 and the docking cystiene of the substrate. An intramolecular disulfide within the substrate is formed when the transient intermolecular disulfide is subject to nucleophilic attack by the other cysteine of the substrate. This results in the release of the substrate from Mia40 in an oxidised, stably-folded conformation which can now be retained in the IMS. The CPC motif of Mia40 is left in a reduced state and requires re-oxidation to restore its capacity to import substrate proteins (Banci *et al.*, 2009; Sideris *et al.,* 2009; Manganas, MacPherson and Tokatlidis, 2017).

Erv1 can then re-oxidise Mia40 for another cycle of disulfide bond formation, interacting with Mia40 in a manner termed the 'substrate mimicry' model. The N-terminal of oxidised Erv1, ~72 residues, interacts with the hydrophobic binding groove of Mia40 in a similar manner to the ITS of the substrate, it then accepts electrons via the N-terminal redox active CPC motif (Banci *et al.*, 2011, 2013). Erv1 can then transfer these electrons either directly to oxygen which results in the production of hydrogen peroxide (H_20_2) in the IMS or to cytochrome *c* and complex IV of the respiratory chain (Allen *et al.,* 2005; Bihlmaier *et al.,* 2007; Dabir *et al.,* 2007; Daithankar, Farrell and Thorpe, 2009; Kojer *et al.,* 2012).

Alternative final electron acceptors, for example Osm1, in yeast allow the process to proceed under anaerobic conditions (Neal *et al.,* 2017).

A non-essential protein that is involved in the MIA pathway is the soluble IMS protein Hot13, instead this protein has an ancillary role. Conserved amongst eukaryotes, Hot13 contains 10 cysteines and has the capacity to bind zinc through a CHY zinc-finger domain (Curran *et al.,* 2004). Hot13 has been proposed to maintain Mia40 in a zinc-free state thereby allowing for a more efficient re-oxidation by Erv1. Mutants in Hot13 have impaired import of Mia40 substrates and when compared to wild type (WT) cells, have a greater level of reduced Mia40 whilst having no difference in overall levels of Mia40 and Erv1. The current model suggests that Hot13 acts as a metal chaperone to transfer zinc ions from Mia40 allowing for re-oxidation by Erv1 (Mesecke *et al.,* 2008).

Additionally, Mia40 requires and interacts with endogenous Mia40 for its own import into the IMS despite not being a classical substrate of the MIA pathway. The import of Mia40 occurs in kinetically distinct steps; firstly Mia40 translocates through the TOM complex where it is then inserted into the IMM by the TIM23 complex. Secondly, the core of Mia40 is folded with assistance from Mia40 through oxidation of the structural CX9C motif. Finally, an interaction with Erv1 oxidises the CPC motif which results in a folded and active Mia40 (Chatzi *et al.,* 2013; Edwards, Gerlich and Tokatlidis, 2020).

The MIA pathway is responsible for inserting disulfide bonds into proteins and shares similarities with the disulfide relay systems in the endoplasmic reticulum (ER) and bacterial periplasm. However, unlike the locations of other disulfide relay systems, no reductive pathway has been described in the process of disulfide bond formation in the IMS. Thioredoxin 1 (Trx1) and thioredoxin reductase 1 (Trr1) have both been previously identified in the IMS which raises questions around a potential regulatory role on the redox state of this sub-compartment, and any influence either directly or indirectly on Mia40 which will be further detailed in section 1.4.5 (Vögtle *et al.,* 2012).

1.4.2 The stop-transfer pathway to the IMS

Another well characterised IMS pathway is the stop-transfer pathway which is unique as it involves IMS preproteins that contain a cleavable bipartite

presequence (figure 3A). The first part of this bipartite signal is similar to the MTS, it is positively charged and recognised by the TOM receptors to aid translocation through the OMM. The second part of this signal is a transmembrane segment which gives rise to the 'stop' half of this pathway (Backes and Herrmann, 2017). After translocation through the TOM complex, the Tim50 receptor sorts the bipartite signal of the preprotein into the TIM23 complex. Here, the hydrophobic transmembrane segment arrests translocation in the TIM23 channel, preventing import into the matrix. Finally, the transmembrane segment is laterally released and inserted into the lipid bilayer. To facilitate this import process, the TIM23 complex is in a specific conformation known as $TIM23^{SORT}$ which contains Tim23, Tim21 and Tim17 but lacks the import motor Pam18. This import motor inhibits the lateral release of proteins and is present in the $TIM23^{MOTOR}$ conformation of the complex, which lacks Tim21 (Schendzielorz *et al.,* 2018). Within this pathway there are two key cleavage events: the first involves the cleavage of the matrix targeting portion of this bipartite signal by MPP. The second proteolytic cleavage event occurs between the mature protein and the transmembrane part of the bipartite sequence, which releases the mature protein into the IMS. This second cleavage event is carried out by the IMM proteases Imp1 and Imp2 (Glick *et al.,* 1992; Esser *et al.,* 2004; Herrmann and Hell, 2005; Edwards, Gerlich and Tokatlidis, 2020). Examples of proteins which utilise this pathway include cytochrome *b2* and the apoptosis inducing factor (AIF) (Glick *et al.,* 1992; Esaki *et al.,* 1999; Hangen *et al.,* 2015).

An unconventional variation of the traditional stop-transfer pathway is used by the yeast Peroxiredoxin 1 (Prx1) which has been shown to be dually localised to the IMS and the matrix. Prx1 translocation can be arrested in the TIM23 complex due to the presence of a small hydrophobic sorting signal in the presequence. It has previously been suggested that the localisation of Prx1 is dependent on which peptidase carriers out the second proteolytic cleavage, matrix localisation is dependent on Oct1 and IMS localisation by Imp2 (Gomes *et al.,* 2017).

1.4.3 Cytochrome *c* import pathway

The most abundant IMS protein is cytochrome *c*, a key component of the respiratory chain transferring electrons from complex III to complex IV and

release of this protein initiates the apoptotic signalling cascade (Liu *et al.,* 1996; Hüttemann *et al.,* 2011). Cytochrome *c* utilises cytochrome *c* haem lyase (CCHL) as a trans site receptor to facilitate the incorporation of a haem group to the protein (Dumont *et al.,* 1991; Backes and Herrmann, 2017). The precursor of cytochrome *c* is apocytochrome *c*, which is not bound to haem and enters the mitochondria through the TOM complex. The only components of the TOM complex required for import of cytochrome *c* are the Tom22 receptor and the Tom40 channel (Wiedemann *et al.,* 2003). Once in the IMS, apocytochrome *c* interacts with CCHL which introduces the haem co-factor to cytochrome *c* (figure 3C). This addition of haem results in the release of a functional, active holocytochrome *c* which is located on the IMS side of the IMM (Diekert et al., 2001; Wiedemann *et al.,* 2003). Additionally, apocytochrome *c*, which lacks haem, can cross the OMM through the TOM complex in either direction, demonstrating that the addition of haem by CCHL folds and traps the protein in the IMS (Diekert et al., 2001; Backes and Herrmann, 2017). To date, a recognition signal or an IMS targeting signal in cytochrome *c* has yet to be discovered.

1.4.4 Cytochrome *c* haem lyase import pathway

As mentioned above, CCHLs are responsible for catalysing the covalent attachment of the haem group to *c* type cytochromes. In yeast two CCHL proteins exist, the soluble cytochrome *c* and the membrane bound cytochrome c_1, both are found in the IMS. Neither contain a cleavable N-terminal presequence and import is independent on ATP hydrolysis and the electrochemical potential across the IMM (Lill *et al.,* 1992; Steiner *et al.,* 1995). The highly conserved targeting sequence for haem lyases is hydrophilic, containing both positively and negatively charged amino acids (Diekert *et al.,* 1999). This targeting signal is ~60 residues long, found in the third quarter of the protein and contains two highly conserved motifs. Additionally, this signal can efficiently direct non-mitochondrial proteins to the IMS, similar to the MTS. The haem lyase presequence is recognised by the Tom22 and Tom22 receptors, and then translocated through the Tom40 channel. Once through the TOM complex, CCHLs folds and binds to the IMM with the IMS targeting signal suggested to play a role in binding to the IMM (Diekert *et al.,* 1999; Herrmann and Hell, 2005; Edwards, Gerlich and Tokatlidis, 2020) (figure 3B). However questions still

remain around whether IMS proteins have a role in the retention and/or folding of CCHL.

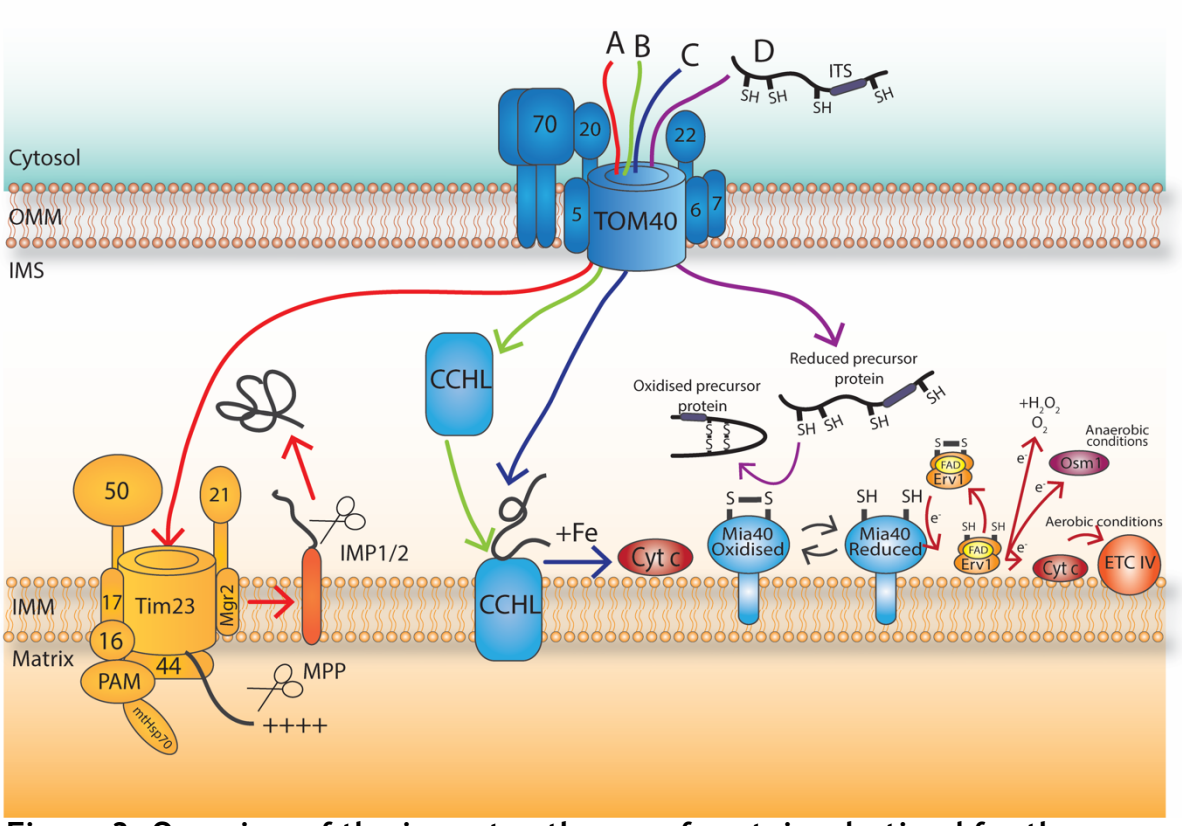

Figure 3: Overview of the import pathways of proteins destined for the intermembrane space. (A) The stop-transfer pathway which involves the TIM23 complex and two proteolytic cleavage events. (B) The import pathway of cytochrome *c* haem lyase (CCHL) which then binds to the IMM, facing the IMS side. (C) The import pathway of cytochrome *c* which requires CCHL. (D) The import pathway of MIA substrates.

1.4.5 Unconventional and unknown import pathways to the IMS – Thioredoxin 1 and Glutathione peroxidase 3

There are a number of proteins that are dually localised between the IMS and the cytosol, those relevant to this report will be discussed in this section. Dual localisation of proteins allows for adaptability of the mitochondria, especially under stress conditions where the action of an antioxidant protein is required quickly to maintain homeostasis. The dually localised protein can be imported rapidly instead of waiting for synthesis to be completed. The import pathway and function of both Trx1 and glutathione peroxidase 3 (Gpx3) into mitochondria remain to be discovered.

1.4.5.1 Thioredoxin 1 (Trx1)

The thioredoxin system is comprised of thioredoxin (Trx), thioredoxin reductase (Trr) and NADPH as an electron donor. S. cerevisiae contains 3 thioredoxins (Trx1, Trx2 and Trx3) and 2 Thioredoxin reductases (Trr1 and Trr2). Trx3 and Trr2 are located in the mitochondrial matrix while Trx1 and Trx2 are responsible for the cytosolic pathway. The thioredoxin system is involved in regulating oxidative stress through providing electrons to the peroxiredoxins for the removal of reactive oxygen species (ROS) and reactive nitrogen species (RNS). Thioredoxins are ~12kDa reductases that contain a conserved CGPC motif at their active site and catalyse the disulfide exchange of proteins. Other proteins that modify thiol states, such as glutaredoxins, also contain the characteristic thioredoxin fold which is comprised of three alpha helices that surround four beta sheets with an active CX_2C motif (Cardenas-Rodriguez and Tokatlidis, 2017). The reaction that Trx catalyses is a bimolecular nucleophilic substitution reaction which involves the transfer of a disulfide bond from the substrate protein to Trx. This disulfide bond has no structural function, instead acting as a redox switch with oxidised Trx being more stable than the reduced active form (Collet and Messens, 2010). The reaction catalysed by Trx starts with nucleophilic attack of the target proteins CGPC motif which results in a mixed disulfide between Trx and the substrate protein. Finally, the substrate protein is released in a reduced state and Trx is left oxidised. Oxidised Trx is recycled to its reduced active form by Trr using NADPH, priming Trx for another cycle (Collet and Messens, 2010).

Trx1 has a molecular weight of 11.2 kDa and along with Trr1, has been identified as being dually localised in both the IMS and the cytosol (Vögtle *et al.,* 2012), raising the possibility that Trx1 is involved in influencing the IMS redox environment. Kritsiligkou *et al* suggested that in the IMS a H_2O_2 detoxification system may be required as this ROS is a by-product of both the electron transport chain (ETC) and the Mia40-Erv1 oxidative folding machinery. The dual localisation of Trx1 could suggest that it has a role in maintaining the redox environment in the IMS and may provide the reducing power required for Gpx3 (Kritsiligkou *et al.,* 2017). Furthermore, disulfide bond formation is an error prone process and it seems logical that a reductase system would be present in

the IMS to allow for disulfide isomerisation as a means to achieve the correct disulfide bonds in proteins.

As mentioned previously, the MIA pathway facilitates the insertion of disulfide bonds into its substrates, trapping them in the IMS. If a Mia40 substrate is not released properly from Mia40 due to the formation of a mixed disulfide, the trapped substrate prevents other Mia40 substrates from being imported. To partially overcome this situation in the IMS, mammalian mitochondria contain the reducing enzyme glutaredoxin 1 (Grx1) which was shown to modulate the oxidation of COX17, a mammalian Mia40 (CHCHD4) substrate (Habich *et al.,* 2019). This furthers our speculation that Trx1 could have a similar role in yeast mitochondria, acting on Mia40 substrates to ensure the MIA pathway works optimally. However, this role may only be required for substrates with several cysteine residues, which may contain a more complex pattern of cysteine pairs. Additionally, the Grx and Trx reducing pathways can compensate for each other due to their overlapping functions and they are often found in the same locations, adding to the logic that Trx1 may mirror in yeast the role of Grx in mammalian cells (Reinhardt *et al.,* 2020). Interestingly, Trx1 has previously been shown to directly interact with Mia40 in a large proteomic screen and can reduce Mia40 in the cytosol, maintaining it in an import competent, unfolded state (Nakao *et al.,* 2015).

Previous work in the Tokatlidis lab has suggested that Trx1 may interact with Mia40, affecting its redox state and influencing the balance between an oxidised and reduced population of Mia40 in the IMS. Trx1 is also capable of interacting with Erv1 *in vitro* and as Trx1 has a broad substrate specificity in the cytosol, it is likely to be interacting with other proteins in this sub-compartment. Interaction between Trx1 and both of the major components of the redox regulated MIA machinery is interesting due to the central role if the MIA pathway in protein import into the IMS (unpublished data, Tokatlidis lab) (Cárdenas Rodríguez, 2019).

In summary, the exact function of Trx1 in the IMS remains to be detailed, although it seems logical that a reductive function in the IMS could mirror its function in the cytosol, but with a different set of substrates, and may even have additional roles. The import mechanism of Trx1 and Trr1 into the IMS are also unknown and questions around the state of Trx1 during import and through

which OMM channel it may translocate through remain open. Recently the structures of the TOM channel and the SAM channel have been solved by cryo-electron microscopy, which allows for greater insight into these channels, and any alternative topologies they adopt (Tucker and Park, 2019; Takeda *et al.,* 2021).

1.4.5.2 Glutathione peroxidase 3 (Gpx3)

Glutathione peroxidase 3 (Gpx3, also called Orp1 and Hyr1) is a thiol peroxidase and its presence in the IMS was identified in the same study as Trx1 (Vögtle *et al.,* 2012). Within cells, Gpx3 acts as a sensor for H_20_2, promoting the oxidation of the transcription factor Yap1. Oxidation of Yap1 occurs when there is an increased level of H_20_2 which directly oxidises Cys36 of Gpx3, which forms a transient intermolecular disulfide with Cys598 of Yap1 which is oxidised and activated. Yap1 can now translocate to the nucleus where it induces the anti-oxidant response which involves the transcription of anti-oxidant genes. This pathway is attenuated by thioredoxin which reduces the disulfide in Gpx3 that is formed by an increase in H_20_2 levels (Delaunay *et al.,* 2002).

Gpx3 has a MW of ~26 kDa and undergoes alternative translation under H_20_2 stress to form an 18-amino acid N-terminal (N18) extended version of the protein and this N18 extended protein was identified as being targeted to the mitochondrial IMS (Gerashchenko, Lobanov and Gladyshev, 2012; Kritsiligkou *et al.,* 2017). The N-terminal 18 amino acid extension of Gpx3 is encoded by a non-AUG codon and is capable of targeting other proteins to mitochondria both *in vivo* and *in organello*. Cells lacking Gpx3 were reported to have aberrant mitochondrial morphology, a decrease in protein import and a lower electrochemical potential across the IMM. All of these phenotypes were able to be reversed by expressing the N18 mitochondrial targeted Gpx3. However, Gpx3 in the cytosol which lacks the N18 extension, can also be imported into mitochondria, with the import pathways of the extended and non-extended forms being mostly unaffected by a lack of Mia40. This suggests that Gpx3 has an unconventional import pathway as its import is independent of the essential protein Mia40. Furthermore, Gpx3 can interact with Mia40 to oxidise its reduced form and maintain the redox state of Mi40 as oxidised with Gpx3 becoming rapidly reduced following incubation with Mia40 (Kritsiligkou *et al.,* 2017).

Overall, this data suggests a mitochondria-specific role of Gpx3 in the IMS where it could interact with the IMS-localised Trx1 as the source of the reducing power for Gpx3 in this compartment, essentially mirroring the redox system of the cytosol.

1.5 Influences on the redox state and redox regulation in the IMS

As mentioned previously, the IMS provides a redox active space that is more oxidising that the cytosol, and this redox active space allows for the formation of disulfide bonds through oxidative folding. The MIA pathway in the IMS is unique as it is the only import pathway that chemically modifies its substrates resulting in intramolecular disulfide bonds. This subjects the major IMS protein import pathway to regulation by the redox environment which is determined by all the reductive and oxidative reactions that take place. ROS and RNS are produced in such reactions and whilst they are beneficial for cell signalling at low levels, are damaging at high levels. Damaging effects of ROS/RNS include DNA modification, protein oxidation and lipid oxidation, all of which are detrimental to cell function and can lead to cell death (Schieber and Chandel, 2014; Manganas, MacPherson and Tokatlidis, 2017). The balance between the production and removal of these reactive species has a direct influence on the environment of the cell and therefore vital cellular processes such as protein biogenesis. As ~99% of mitochondrial proteins require import, protein biogenesis is essential to the viability and function of mitochondria (Cardenas-Rodriguez and Tokatlidis, 2017). Redox signalling is crucial as it allows cells to rapidly adapt to a range of environmental stimuli with cellular redox status being maintained by several anti-oxidant systems, primarily the Trx and Grx systems. Additionally, redox signals that are produced by the essential functions of mitochondria allow for the organelle to be integrated into the wider cellular context through the free diffusion of small molecules between the IMS and the cytosol via the semi-permeable OMM (Collins *et al.,* 2012). The redox environment of the IMS is maintained separately from the cytosol and the matrix, with various factors influencing each compartment (Hu, Dong and Outten, 2008).

In addition to protein modulators of the redox environment in the IMS, there are also small molecules that play a role in redox regulation, small molecules that will be discussed below include hydrogen peroxide (H_2O_2) and glutathione (GSH). H_20_2, along with the superoxide anion (O_2^-) and the hydroxyl radical (OH^-) are classified as types of ROS and are all associated with oxidative stress (Schieber and Chandel, 2014). ROS can act as signalling molecules by oxidising cysteine residues and forming disulfide bonds which results in the alteration of a protein's structure and therefore function. The reductases Trx and Grx can reduce these disulfide bonds, and this reversibility allows for the rapid alteration of protein function in response to ROS (Cremers and Jakob, 2013; Schieber and Chandel, 2014).

1.5.1 Glutathione (GSH) in the IMS (reducing)

GSH is a component of the glutaredoxin system which also contains glutaredoxins (Grx) and GSH reductases. The glutaredoxin system is one of the major pathways that controls cellular redox homeostasis, the other being the thioredoxin pathway. The tripeptide GSH has various key roles in reducing disulfide bonds, synthesising iron sulfur clusters and detoxifying ROS. Participating in these reactions frequently leads to the oxidation of GSH to GSSG, which contains a disulfide bond that links two molecules of GSH together: targets of GSH are left reduced. GSSG can be reduced back to GSH by glutathione reductase (Glr) using electrons supplied by NADPH (Kojer *et al.,* 2012; Calabrese, Morgan and Riemer, 2017). GSH is synthesised in the cytosol and is presumed to be imported into the mitochondria through the TOM complex and porins although no GSH reductase has been identified in the IMS. Therefore, once GSH is oxidised to GSSG in the IMS it has been proposed to be exported back though the TOM complex and porins. However, evidence to support this efflux mechanism remains to be provided (Kojer *et al.,* 2012).

In cells, the majority of glutathione is in the reduced form GSH and the ratio of GSH to GSSG (GSH:GSSG) is an indicator of oxidative stress, with a greater level of stress increasing the ratio of GSSG:GSH. E_{GSH} in the matrix is regulated separately from the cytosol and the IMS and the local E_{GSH} has a role in maintaining the partially reduced redox state of Mia40 which is found to be around 70% oxidised. When Erv1 was depleted in cells, Mia40 was found to be

increasingly reduced which could be due to the GSH pool in this compartment (Kojer *et al.,* 2012).

In the IMS where disulfide bond formation takes place, GSH is responsible for recycling Grx back to its reduced active state. Reduced GSH can then reduce protein thiols and is therefore involved in thiol reduction. Additionally, GSH in the IMS has been shown to increase the speed of import into this sub-compartment whilst also proposed to have a proofreading function within the disulfide relay process. GSH was also shown to prevent/remove the formation of long lived complexes between Mia40 and its substrates (Bien *et al.,* 2010), but *in vivo* data on this mechanism is still lacking.

1.5.2 Hydrogen peroxide (H_2O_2) in the IMS (oxidising)

H_2O_2 is derived from the partial reduction of molecular oxygen and is more stable and less reactive than O_2^- because it does not contain unpaired electrons. H_20_2 is reactive as it contains a relatively weak O-O bond which is susceptible to decomposition and this results in the formation of OH^- which is very reactive (Patterson *et al.,* 2015; Magnani *et al.,* 2020). H_20_2 is generated in the IMS in several ways and is generally produced in places where there is a leakage of pairs of electrons, however there are various antioxidant defence systems in place to protect the cell from damage. In the IMS, the copper-zinc isoform of Superoxide dismutase 1 (SOD1) catalyses the rapid dismutation of two molecules of O_2^- to produce H_20_2 and O_2. Superoxide anions are also released to the IMS side of the IMM by various enzymes of the respiratory chain, notably complex III (Habich, Salscheider and Riemer, 2019). Additionally, the Erv1/ALR enzyme in its normal catalytic cycle also produces H_20_2 by passing electrons directly to molecular oxygen instead of to cytochrome *c*, which leads to the production of water (Bihlmaier *et al.,* 2007). This interaction between cytochrome *c* and Erv1 has been recently detailed where is was reported that a rapid collision-type interaction between the two prevents the production of H_2O_2 (Peker *et al.,* 2021). In the IMS Cytochrome *c* peroxidase (CC1p) reduces H_20_2 to water to remove the ROS, and it has recently been suggested that Gpx3 may also have a role in removing H_20_2 as thiol peroxidases are major antioxidants in cells (Dabir *et al.,* 2007; Kritsiligkou *et al.,* 2017). Interestingly, both CC1p and Gpx3 interact with components of the MIA pathway (Tang *et al.,* 2020).

In terms of signalling, H_20_2 can directly oxidise select cysteine residues to induce signalling and is thought to be broadly non-specific. Oxidating cysteine thiol groups can lead to structural changes in the protein, which can result in a change of function. As discussed previously, Trx1 can reduce these disulfide bonds and along with Trr1, has been identified in the IMS (Vögtle *et al.,* 2012). Additionally, there is the potential for high local concentrations of H_20_2 in the IMS to arise from the invaginations of the IMM and the presence of respiratory chain enzymes (Habich, Salscheider and Riemer, 2019). Overall, H_20_2 has an oxidising effect in the IMS and the design of mitochondrial targeted reagents that can independently induce O_2^- or H_20_2, therefore disrupting mitochondrial thiol homeostasis (mitoParaquat and MitoChlorodinitrobenzoic acid respectively), will allow for further study into the effects of specific ROS on mitochondrial proteins (Cvetko *et al.,* 2020).

1.5.3 Nicotinamide adenine dinucleotide phosphate (NADPH)

Nicotinamide adenine dinucleotide phosphate (NADPH) functions as a cofactor and electron donor in cells. In the cytosol, the enzyme Glr is dependent on NADPH to keep GSH reduced, therefore NADPH is crucial to maintain redox homeostasis. Additionally, NADPH is used by both the two main thiol reducing pathways in the cell, the thioredoxin pathway and the glutaredoxin pathway. The NADPH used by these pathways is produced by glucose-6-phosphate dehydrogenase (G6PD) as its final electron donor in the pentose phosphate pathway, which synthesises precursors for nucleic acids (Cardenas-Rodriguez and Tokatlidis, 2017). However this pathway resides in the cytosol and it will be interesting in the future to elucidate further links between the effects of potential reducing systems in the IMS on Mia40 and on the cellular redox state. Although there is a role for cytosolic NADPH generation, and NADPH dependent Glr1 in regulating the pool of GSH in the IMS through porins in the OMM of mitochondria (Kojer *et al.,* 2012).

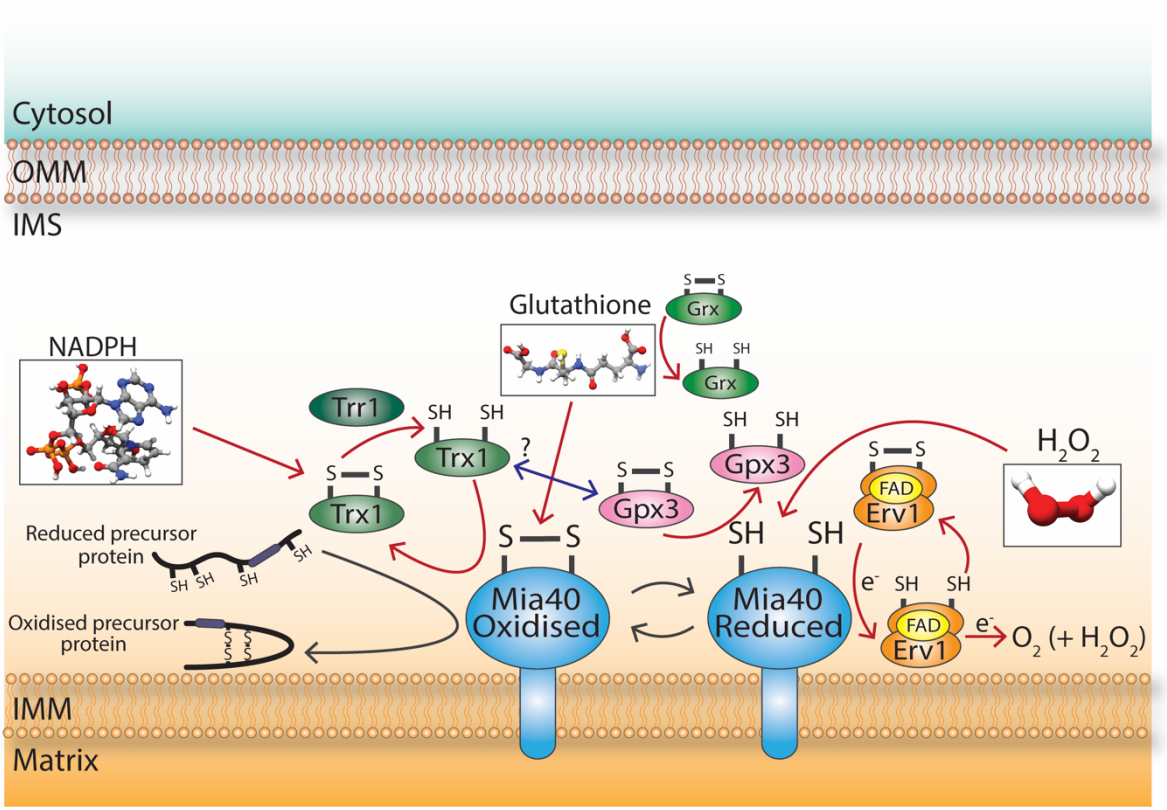

Figure 4: Overview of the various influences on the redox state of the intermembrane space. There are multiple influences on the redox state of the intermembrane space including small molecules such as glutathione (reducing), NADPH and hydrogen peroxide (oxidising). Protein influences on the redox state of the intermembrane space include thioredoxin 1 (Trx1) and glutathione peroxidase 3 (Gpx3) which have a reducing and oxidising effect respectively.

Chapter 2: Aims

The overall main aim of this project was to characterise the unconventional import pathways of the IMS dually localised proteins Gpx3 and Trx1, building upon work carried out by previous lab members of the Tokatlidis lab. However, as the project developed the aims shifted towards improving methods to optimise the import protocol of Trx1.

The second half of this project focuses on the import mechanism of Gpx3, investigating potential components involved in the import pathway using appropriate null mutant yeast strains. Gpx3 ribosome-stalled RNA was utilised to investigate the import in a co-translational environment rather than the post-translational environment in the standard import protocol.

To answer these aims, the following specific experimental objectives were set:

1. Investigate, through biochemical techniques such as radiolabelled protein import and pull down assays, the import mechanism and components involved of Gpx3 and Trx1.
2. Optimise the import mechanism of Trx1 through the use of the Flexi TNT system.
3. Conduct radiolabelled protein import experiments with delta or gal strains of yeast mitochondria in order to assess the importance of components involved. In delta strains of yeast, the protein has been removed and is no longer present. In gal stains the protein is still present, however its levels have been reduced.
4. Use denaturing and/or reducing conditions of radiolabelled protein experiments to assess any differences in import.

Chapter 3: Materials and Methods

3.1 Materials

3.1.1 Antibodies

Table 1 lists the primary and secondary antibodies (Ab) used during this project. All antibodies described below were diluted in a 5% milk TBST solution unless stated otherwise.

Antibody	Company	Species raised in	Concentration	Source
α-Aconitase	Davids Biotechnologie	Rabbit polyclonal	1:10000	Gifted by Prof. G. Schatz
α-Erv1	Davids Biotechnologie	Rabbit polyclonal	1:1000	Lionaki et al., 2010
α-Gpx3	Davids Biotechnologie	Rabbit polyclonal	1:1000	Kritsikigkou et al., 2017
α-His	AbD Serotec (Bio-Rad)	Mouse monoclonal	1:5000	Purchased from Bio-Rad
α-Hsp70	Davids Biotechnologie	Rabbit polyclonal	1:10000	Gifted by Prof. N. Pfanner
α-Mia40	Davids Biotechnologie	Rabbit polyclonal	1:1000	Sideris et al., 2009
α-Om14	n/a	Rabbit polyclonal	1:1000	Gifted by Prof. N. Pfanner
α-Om45	n/a	Rabbit polyclonal	1:1000	Gifted by Prof. N. Pfanner
α-Porin1	Davids Biotechnologie	Rabbit polyclonal	1:10000	Gifted by Prof. N. Pfanner

α-Tom40	Davids Biotechnologie	Rabbit polyclonal	1:1000	Tokatlidis lab
α-Trx1	Davids Biotechnologie	Rabbit polyclonal	1:1000	Tokatlidis lab
α-Mouse (2*) igG DryLight 800CW	Bio-Rad	Goat polyclonal	1:10000 in TBST	Purchased from Bio-Rad
α-Rabbit (2*) igG DryLight 680	Invitrogen	Goat polyclonal	1:10000 in TBST	Purchased from Invitrogen

Table 1: List of antibodies used in this report, 2* indicates secondary antibodies.

3.1.2 Plasmids

Table 2 details the plasmids used in this project and are stored in glycerol stocks by the Tokatlidis lab. Genes were cloned into pSP plasmids in order to be used in TNT ^{35}S-Methionine protein radiolabelling. For protein expression and purification the pET plasmid was used.

Insert	Plasmid
Su9-DHFR	pSP64-Su9DHFR
Tim10	pSP64-Tim10
AAC	pGEM-AAC
Trx1	pSP64-Trx1 pSP64-Trx1 His pET24-Trx1 His
Trx1 C30S	pSP64-Trx1C30S
Trx1 C30/35S	pSP64-Trx1 C30/35S
Trx1 G81A	pET24–Trx1G81A
Trx1 K86A	pET24-Trx1K86A
Trr1	pSP64-Trr1
Gpx3	pSP64-Gpx3
Gpx3 C36/64/82S	pSP64-Gpx3 C36/64/82S

Table 2: Description of inserts and plasmids used in this report.

3.1.3 Primers

Primers in this study were purchased from Sigma-Aldrich and used for a PCR to generate Gpx3 stalled RNA for co-translation import assays (table 3). Primers were stored in ddH_2O at -20°C at a concentration of 100µM.

Primer name	Primer sequence 5'-3'	Description
Frw_SP6	CAATTAATACATAACCTTATGTATCATACACATACG	Forward primer, binds directly upstream of the SP6 plasmid
Rev_Gpx3_stall_MLKV	CACTTTCAGCATCTCGAGTTCCACCTCTTTCAAAAGTTCTTC	Reverse primer, binds to the last residue of Gpx3, therefore removing the stop codon

Table 3: Description of primers used in this report.

3.1.4 Yeast strains

Table 4 lists the strains of *Saccharomyces cerevisiae* (*S. cerevisiae*) that were used during this project. To prepare the mitochondria (described in detail in section 3.2.3.1), the strains were cultured on YPD and YPLac (detailed below). Additionally, the WT yeast strain D273-10B was grown in glucose rich media, termed glucose grown mitochondria, which results different proteins being expressed.

Yeast strain	Description	Source
D273-10B	Wild-type strain used for isolation of mitochondria	(Sherman, 1964)
BY4741	Wild-type strain, both gal and D strains are derived from this strain	(Brachmann et al., 1998)
Gal-Mia40	Conditional knock-out with the expression of Mia40 under the control of the Gal promoter	(Banci et al., 2009)
Gal-Erv1	Conditional knock-out with the expression of Erv1 under the control of the Gal promoter	(Lionaki et al., 2010)
ΔOm14	Om14 deletion	Ordered from Horizon Discovery Yeast Knockout collection
ΔOm45	Om45 deletion	Ordered from Horizon Discovery Yeast Knockout collection

Table 4: Description of yeast strains used in this report.

3.1.5 Bacterial strains

The Escherichia coli (E. coli) strain DH5a was used for cloning of genes and plasmids of interest. For recombinant protein expression and subsequent purification, BL21 (DE3) E. coli cells were used. Isopropyl-ß-d-thiogalactopyranoside at a concentration of 0.4mM was used to induce protein expression. Bacterial cells were grown in Luria-Bertani (LB) media, described below.

3.1.6 Media

Bacterial growth media

E. coli cells were grown in LB media, 1% (w/v) bactotryptone, 0.5% (w/v) yeast extract and 1% (w/v) NaCl, at 37°C. LB agar plates were prepared in the same way and contained 2% agar. Competent bacteria with the plasmid of interest were selected for by adding 30µg/µl of the antibiotic Kanamycin to the media. Sterilisation of bacterial media was achieved by a cycle of autoclaving, 121°C for 15 minutes.

Yeast growth media

Yeast cells were grown in YPLac media at 30°C as a starter culture for the large scale mito-prep. YPLac media contains 1% (w/v) yeast extract, 2% (w/v) peptone and 2% (w/v) lactic acid. For a volume of one litre; 10g yeast extract, 20g peptone and 20g lactic acid were added to 900ml dH_2O. The pH was then adjusted to 5.5 with KOH pellets, completed to a one litre volume and autoclaved for 15 minutes at 121°C to sterilise. To produce the glucose grown mitochondria, yeast cells were grown in yeast extract peptone dextrose (YPD) media. YPD media contains 1% yeast extract, 2% peptone and 2% sugar (glucose) and also sterilised as above.

3.2 Methods

3.2.1 Molecular biology assays

3.2.1.1 Plasmid DNA purification

QiaPrep Spin Miniprep (catalogue 12123 and 12125) and Midiprep kits (catalogue 12143 and 12145) were used to isolate plasmid DNA as per manufacturer's instructions. The concentration of each prep was measured on a NanoDrop Spectrophotometer (Thermo) then diluted to 1µg/µl in if appropriate in nuclease free water and stored at -20°C.

3.2.1.2 PCR and sequencing

Plasmid or vector DNA were used as template material for all PCR reactions in this report. The PCR reactions contained the following; 1µl of forward and reverse primer (10mM), 1µl of DNA (at 1µg/µl), 10µl of Q5 reaction buffer, 0.5µl Q5 DNA polymerase, 1µl dNTPs and 35.5µl nuclease free water. One cycle of PCR consisted of denaturation at 95°C for 30 sec, annealing at 58°C for 30 seconds and extension at 75°C for 1 minute with 35 cycles in total. DNA fragments were separated by Agarose gel electrophoresis (1.5% w/v agarose, 1X TAE buffer and 1X SYBR safe) for 1 hour at 80V with the addition of a DNA ladder (Promega). Following a PCR, the QiaQuick PCR clean-up kit (Qiagen) was used as per manufactures instructions and DNA concentrations were measured on a NanoDrop Spectrophotometer (Thermo).

Sequence analysis was carried out by Eurofins Genomics, with the results being analysed and compared to the desired sequence in the bioinformatic program CLC Genomics Workbench.

3.2.1.3 Production and Clean-up of RNA

RNA used in this report was generated using a RiboMAX™ large scale RNA production system from Promega (catalogue number P1280). Firstly a PCR was conducted to generate the desired product, or if using vector DNA, a DNA digest was carried out using the appropriate restriction enzymes (in this case Ecor1) prior to RNA production.

To synthesis RNA, in a 1.5ml eppendorf tube the following was added: 20µl 5X SP6 transcription buffer, 20µl 25mM rNTPs, 25µl linear DNA at 111ng/µl, 10µl SP6 enzyme mix and 25µl nuclease free water. The contents were mixed gently by pipetting and incubated at 37°C for 3.5 hours. After the incubation period, 2µl was removed for a pre-DNase treatment control. Five units of DNase was added to the eppendorf and the reaction left for another 15 minutes at 37°C, after which a further 2µl was removed for a post-DNase treatment control. To both samples, 8µl of water and 2µl of loading dye were added. To visualise the samples, 100ml of 1.5% agarose gel was made using agarose powder and TAE buffer with the addition of 10µl Sybr safe gel stain.

The RNA synthesised from the RiboMAX™ large scale RNA production system was cleaned-up. Firstly, one volume of acid-phenol-choloform-isamylalcholo (125:24:1) was added, vortexed for 1min and centrifuged 15,000 x g for 2min. The upper phase was transferred to a fresh tube and one volume of chloroform-isoamyl-alcohol (24:1) was added, vortexed for 1min and centrifuged 16,600g for 2min. The upper phase was transferred to a fresh eppendorf and 0.1 volume of sodium acetate (pH 5.2) and one volume of sodium acetate was added. This was mixed gently by pipetting, left on ice for 5min and centrifuged 16,600g for 10min. The pellet was washed with 200µl of 70% ethanol, centrifuged for 5 min at 16,600g and dried on a heat block at 60°C for 25min. Finally, the pellet was re-dissolved in 50µl nuclease free water. The concentration was measured on a NanoDrop Spectrophotometer (Thermo) and diluted if appropriate to 1µg/µl. The RNA was aliquoted and stored at -80°C.

3.2.2 Biochemical methods

3.2.2.1 SDS-PAGE and western blotting

Either 12%-14% Tris-Tricine or 12-14% Tris-Glycine SDS-PAGE were used to separate proteins by their MW. The percentage of the gel depended on the MW of the POI (tables 5 and 6). Samples were resuspended in 2X Laemmli sample buffer (SB) (4% 10% w/v SDS, 20% glycerol, 120mM Tris-Cl pH 6.8, 0.02% bromophenol blue, ß-mercaptoethanol 13µl/1ml of 2x SB).

Tris-Tricine gels were ran at 120V for 15 minutes (so to allow proteins to enter the separating gel) then 150V for ~1hr or until the dye front began to run-off the gel. Tris-Glycine gels were ran at 80V for 15 minutes through the stacking then at 120V for ~1hr as above. The Tris-Tricine upper tank buffer contain 100mM Tris-HCl, 100mM tricine, 0.1% SDS and was adjusted to a pH of 8.25: the Tris-Tricine lower tank buffer contained 200mM Tris-HCl adjusted to pH 8.9. The Tris-Glycine gel tanks contained 1X SDS running buffer (make from 1 litre 10X stock; 30.2g Tris, 144g glycine, 10g SDS and the pH adjusted to 8.3). Once the gel run was completed, the majority of gels were transferred a onto nitrocellulose membrane for western blotting. Additionally, gels were either silver stained or Coomassie stained.

To probe for multiple proteins, each membrane was be cut. To determine protein transfer prior to cutting the membrane ponceau stain (5% acetic acid, 0.1% ponceau stain) was added for ~1 minute then rinsed in ddH_2O. Western blotting onto a nitrocellulose membrane was performed using a semi-dry transfer (BioRad) at 25V for 25 minutes. Three pieces of Whatmann paper were pre-soaked in Transfer buffer (25mM Tris, 190mM glycine, 20% methanol, 0.1% SDS), the pre-soaked nitrocellulose membrane was placed on top, followed by the gel and three more pieces of pre-soaked Whatmann paper.

The membrane was then blocked in 5% Milkfresh skimmed milk in TBST (150mM NaCl, 100mM Tris-HCL pH 7.4, 0.01% Tween-20) for one hour at room temperature on a Stuart See-Saw rocker SSLA4. The milk solution was poured off and the primary antibody added for one hour with gentle rocking. Membranes were then washed for 10 minutes in TBST at room temperature with gentle rocking three time. The secondary antibody was then added in TBST for one hour, room temperature with gentle rocking. Lastly, three TBST washes were conducted as previously then the membranes were scanned via the LI-COR odyssey CLX.

	Stacking	Separating	Separating
	5%	12%	15%
ddH_2O	1.4ml	1.6ml	1.1ml
30% acrylamide mix	0.33ml	2.0ml	2.5ml
1.5M Tris pH8.8	0.25ml	1.3ml	1.3ml
10% SDS	0.02ml	0.05ml	0.05ml
10% ammonium persulfate	0.02ml	0.05ml	0.05ml
TEMED	0.002ml	0.005ml	0.002ml
Total	2ml	5ml	5ml

Table 5: Recipe for casting 12% and 15% Tris-glycine gels for SDS-PAGE.

	Stacking	Separating	Separating 14%
	5%	12%	14%
Acryl/Bis-acryl total 40%	0.25ml	3ml	3.5ml
Tricine gel buffer	0.5ml	3.3ml	3.3ml
Glycerol 87%	-	1.3ml	1.3ml
ddH_2O	1.21ml	2.29ml	1.79ml
10% ammonium persulfate	35µl	100µl	100µl
TEMED	3.5µl	10µl	10µl
Total	2ml	10ml	10ml

Table 6: Recipe for casting 12% and 14% Tris-tricine gels for SDS-PAGE.

3.2.2.2 Coomassie staining

Coomassie buffer (30% methanol, 10% acetic acid, 0.2% Coomassie blue R-250) was added to the gel and incubated with gentle rocking for 5 minutes. The Coomassie buffer was poured off and de-staining buffer (15% methanol, 10% acetic acid) was added for one hour with gentle rocking. The stained gel was rinsed further for another hour or until bands are clear.

3.2.2.3 Silver Staining

All incubations and washes for this protocol were performed with gentle rocking. Once the SDS-PAGE has been completed, the gel is fixed overnight in gel fixing solution (10% acetic acid, 40% methanol). After fixing, the gel is rinsed in ddH_2O and incubated with $CuCl_2$ solution (1% $CuCl_2$ in ddH_2O) for 15 minutes and rinsed with ddH_2O. The gel is then incubated with washing solution (10% ethanol, 5% acetic acid) for 15 minutes, this step is repeated with a ddH_2O wash in-between. The gel is incubated further with $KMnO_4$ (0.004% w/v $KMnO_4$ in ddH_2O) for 15 minutes, rinsed twice for 15 minutes in washing solution (with a rinse in ddH_2O between washes as previously) and rinsed in ddH_2O for a further 10 minutes to remove any residual metal and by this step the gel should have a yellow hue, if not then further washes are required. The silver solution (0.1% $AgNO_3$ in ddH_2O) was added and the gel incubated for 15-20 minutes then rinsed under running ddH_2O for ~45 seconds. Then 100ml of developer solution (150mM K_2CO_3, 0.036%

formaldehyde) is added for 1 minute, poured off and 100ml of fresh developer solution added with gentle agitation until the desired band intensity is reached. To stop the reaction, the developing solution is decanted and the gel rinsed in ddH_2O. The gel can be stored in 5% acetic acid in ddH_2O.

3.2.2.4 Recombinant protein expression

Plasmid DNA of the pET24 plasmid containing His tagged Trx1 was transformed into BL21 DE3 cells and grown overnight on LB agar plates containing 100µg/ml of the antibiotic kanamycin. For the transformation, 3µl of His tagged Trx1 DNA (55.3 ng/µl) was added to the BL21 DE3 cells and left to incubate on ice for 20 minutes followed by a heat shock at 42°C for 35 seconds and another incubation on ice for 2 minutes. A volume of 500µl of fresh LB was added and left shaking in the incubator at 37°C for 45 minutes. The eppendorf was centrifuged at 16,600g for 1 minute, 100µl of the supernatant was left and the pellet resuspended in this volume. The whole volume was plated as mentioned above and left in the incubator at 37°C overnight. Two colonies from the transformed plate were then grown in a small scale liquid culture (5ml LB and 5µl of 100mg/ml kanamycin) to test protein expression. The two colonies were grown in the shaking incubator at 37°C and then induced with 0.4mM IPTG and placed back into the incubator for 2 hours. Before and after the IPTG was added, 1ml of the culture from both colonies was removed, centrifuged for 5 minutes at 8,000g and resuspended in 100µl 2X SB. To determine which of the two colonies expressed the most protein the samples were ran on 15% Tris-glycine gels at 120V and the gel was then Coomassie stained as described above. From this, the highest expressing colony was used for the large scale expression. The large scale expression was carried out using one litre of LB, 1ml of kanamycin and the remaining 3ml of the 5ml small scale culture were added. The optical density at wavelength 600 (OD_{600}) of the large scale culture was measured before incubation at 37°C, and the cells were grown until the OD_{600} reached 0.7-0.8. Expression was then induced with a final concentration of 0.4mM IPTG, incubated at 37°C for another hour and left overnight at 25°C. The cells were harvested by centrifugation at 4,000g for 10 minutes using a JLA 8.1000 rotor (Beckmann Coulter) and can either be stored at -20°C until use or resuspended in buffer A (0.3M NaCl, 0.05M Tris pH 7.4, 10% glycerol).

3.2.2.5 Histidine tagged protein purification

After resuspension in buffer A, additional buffer A is added to give a final volume of ~30ml and 60µl of 0.2M phenylmethylsulfonylfluoride (PMSF) is added. One mg of Lysozyme per ml of suspension was added and the cells lysed by five 30 second rounds of sonication on ice using a Soniprep 150 sonicator. The lysed cells are then centrifuged at 21,000g for 34 minutes at 4°C and SDS-PAGE samples from both the supernatant and pellet can be taken to identify whether or not the protein is soluble or in inclusion bodies. As His tagged Trx1 is known to be soluble, this step was not completed.

The 8ml NiNTA columns are stored in ethanol and to equilibrate the columns, the columns are washed with a 1M imidazole, then ddH_20 and finally with 30ml of equilibration buffer (0.3M NaCl, 0.05M Tris pH 7.4, 10% glycerol and 0.01M imidazole). SDS-PAGE samples (10µl sample and 10µl 2X SB) were taken from the supernatant and the concentration of imidazole in supernatant adjusted to a final concentration of 5mM. This was applied to equilibrated column and allowed to settle for a couple of minutes before the flow through (FT) is collected and SDS-PAGE samples taken as previously. Firstly the column is washed with 30ml wash buffer 1 (0.15M NaCl, 0.05M Tris pH 7.4, 10% glycerol and 0.015M imidazole), secondly with 30ml of wash buffer 2 (0.15M NaCl, 0.05M Tris pH 7.4, 10% glycerol and 0.025M imidazole) and thirdly with 30ml of wash buffer 3 (0.15M NaCl, 0.05M Tris pH 7.4, 10% glycerol and 0.04M imidazole). Samples are collected as above after each wash step and lastly the protein is eluted with 10ml of elution buffer (0.15M NaCl, 0.05M Tris pH 7.4, 10% glycerol and 0.25M imidazole). The SDS-PAGE samples collected throughout the purification steps were ran on a 15% Tris-glycine gel at 80V through the stacking and then 120V for the remainder, the gel was then Coomassie stained. The elution was dialysed overnight at 4°C with dialysis buffer (0.15M NaCl, 0.05M Tris pH 7.4, 10% glycerol) and the next day was concentrated to 2ml by centrifugation at 3500g at 4°C for one hour in Vivaspin protein concentrator spin column (Cytiva). The concentration of the protein was determined on a NanoDrop Spectrophotometer (Thermo) and diluted with 50mM HEPES-KOH pH7.4 to 2µg/µl and stored in 50µl aliquots at -20°C and -80°C.

3.2.2.6 Pull down of His-tagged Trx1

The NiNTA columns were calibrated as above and different amounts of Trx1 were bound to each column; 0µg, 5µg, 20µg and 50µg from a 10µg/ml Trx1 stock. The correct volume of Trx1 stock was added to each column, pipetted to mix and the total volume pipetted into a falcon and left rotating on a LABINCO L28 test tube rotator at 4°C for 2 hours. After 2 hours, the total volume was added back to the column and the flow through, FT, (termed Trx1 FT) collected to check if Trx1 has bound to the column. 200µg of WT mitochondria were solubilised in a 1% Triton-X, 50mM NaCl, 20mM Tris pH 8 buffer to give a concentration of 50µg/ml, 50µg of mitochondria were then added to each column, left to incubate for 5 minutes and the FT collected (termed mitochondria FT). The columns were washed with wash buffer (50mM NaCl, 0.05M Tris pH 7.4, 10% glycerol, 0.05M imidazole) and the FT collected (termed wash FT). Two ml of elution buffer (50mM NaCl, 0.05M Tris pH 7.4, 10% glycerol and 0.3M imidazole) was added to the columns, left for 5 minutes and the FT collected (termed elution FT) and split in half to be treated with reducing and non-reducing conditions. The Trx1 FT and elution FT were Trichloroacetic acid (TCA) precipitated as follows, 10% of the total volume in the eppendorf of TCA was added and incubated on ice for 30 minutes. The samples were then centrifuged at 4°C, 16,600g for 30 minutes and the resulting pellet washed with acetone and centrifuged as above for 5 minutes. The acetone was removed and the pellet resuspended in 2X SB. The samples were ran on a 1.5mm 14% Tris-Tricine gel and the gels silver stained as previously described.

3.2.2.7 *In vitro* radiolabelled protein translation

Radiolabelled protein precursors were produced using ^{35}S-Methionine in the TNT quick coupled transcription/translation system (Promega) as per the supplied instructions. For the import of Trx1 in this report, the TNT coupled Wheat Germ extract system was used and for the import of all other proteins, the TNT coupled Reticulate Lysate system was used. The gene of interest has been previously cloned into a vector (either pSP64 or pGEM) that contains the SP6 promoter to initiate transcription. Each TNT mix contained a DNA at a concentration of 2µg per 100µl to allow enough ^{35}S-labelled protein to be translated, and was incubated at 30°C for 90 minutes shielded from light. The

ribosomes were then removed from the TNT mix by ultracentrifugation in a TLA-100 rotor (Beckman Coulter) at 55,000rpm (116,717g) for 15 minutes at 4°C.

Alternatively, the Flexi® Rabbit Reticulocyte Lysate (RRL) System (Promega) was used to produce radiolabelled protein precursors from an RNA substrate. The Flexi® RRL system is more easily optimised than the standard TNT® quick coupled transcription/translation system as the concentrations of Mg^{2+} and K^{+} can be varied, along with whether the reducing agent DTT is included. Furthermore, the amount of glucose-6-phosphate (G6P) can be varied which allows for more control over the redox state. In a 50µl reaction the following components were added; 33µl Flexi® Rabbit Reticulocyte Lysate (RRL), 1µl 1mM amino acid mixture minus methionine, 2µl ^{35}S-Methionine 1,200Ci/mmol at 10mCi/ml, 1µl 25mM magnesium acetate, 1.4µl 2.5M potassium chloride, 1µl RNasin (40U/µl), 1-12µl RNA substrate (aim for 10µg RNA minimum in reaction) and 5µl 1mM G6P. The translation reaction was gently pipetted to mix and incubated at 30°C for 90 minutes shielded from light and the ribosomes removed by ultracentrifugation in a TLA-100 rotor at 55,000rpm for 15 minutes at 4°C. When using the Gpx3-ribosome stalled RNA in the Flexi RRL System, the TNT sample was layered over a 30% sucrose gradient with the sucrose dissolved in a magnesium acetate HEPES-KOH pH 7.4 buffer to give a final concentration of 15mM magnesium acetate and 50mM HEPES-KOH pH 7.4. Magnesium acetate was included in the buffer to prevent dissociation of the ribosome complex during the experiment as magnesium ions are important for maintaining the stability of the ribosome complex. A 1:1 ratio of gradient to TNT was added to an ultracentrifuge tube and centrifuged in a TLA-100 rotor (Beckman Coulter) at 70,000rpm (189,062) for 30 minutes at 4°C. The resulting ribosome pellet was then resuspended in the original TNT volume using 50mM HEPES to be added to the import mix.

3.2.2.8 Protein precipitation and denaturation

Following the ultracentrifugation to remove the ribosomes, the TNT mix was precipitated using two volumes of saturated $AmSO_4$ and left on 30 minutes on ice. The mix was centrifuged at 16,6000g for 30 minutes at 4°C to pellet the precipitated TNT mix. The pellet was resuspended in the desired buffer depending on the condition; native import buffer (50mM HEPES-KOH pH7.4),

native reducing buffer (50mM HEPES-KOH pH 7.4, 20mM DTT), denaturing buffer (50mM HEPES-KOH pH 7.4, 8M urea), or denaturing and reducing buffer (50mM HEPES-KOH pH 7.4, 20mM DTT, 8M urea).

3.2.2.9 Phosphorimage analysis

Radioactive proteins within the nitrocellulose membranes were visualised by incubating on an phosphorimage plate (Fujifilm) for 48 hours minimum to allow for decent exposure. The film was then scanned and visualised using a phosphoimager (Fujifilm FLA-7000).

3.2.3 *In organelle* assays

3.2.3.1 Isolation of yeast mitochondria

Mitochondria purification and isolation was completed as described by *Glick et al.*, 1991. A 100ml yeast preculture was grown overnight at 30°C, and 10 litres of YPLac media were inoculated with the preculture and grown at 30°C with shaking (120rpm) for 16 hours. The cells were collected by centrifugation at 3000g for 5 minutes RT and the resulting pellets resuspended in 300ml of ddH_20 and transferred to pre-weighed 250ml buckets. The 250ml buckets are centrifuged at 1850g for 5 minutes in a JA14, the supernatant removed and the cells weighed. Each of the two pellets were resuspended in Tris-DTT buffer (Tris-SO_4 pH 9.4, 10mM DTT) to weaken the yeast cell wall, then incubated for 30 minutes with gentle shaking. The cells are pelleted by centrifugation, 1850g, 5 minutes in a JA14 at 4°C and washed in sorbitol buffer (1.2M sorbitol, 20mM KP_i pH 7.4) and centrifuged as previously. To break down the cell wall, the yeast are incubated for 45 minutes at 30°C gentle shaking in sorbitol buffer (5ml per gram of cells) with zymolyase (3.5mg per gram of cells, AmsBio). The now spheroplasts were collected via centrifugation at 1480g 5 minutes and washed twice in 1.2M sorbitol buffer, every step from now on is completed on ice due to the sensitivity of spheroplasts. The cells are resuspended in a total of 100ml BB pH 6.0 (0.6M sorbitol, 20mM MES-KOH pH6) with 2mM PMSF added and broken by 15 strokes in a type B pestle to dounce the cells. A second round of douncing is carried out to break any cells that did not previously break. The dounced material is centrifuged for 5 minutes at 1480g, 4°C and the supernatants saved.

The supernatants are combined and centrifuged at 12,000g for 10 minutes, 4°C and the resulting mitochondria pellets resuspended in breaking buffer pH 6.0 (minus PMSF) using a PTFE dounce homogeniser and centrifuged at 1480g for 5minutes, 4°C. The supernatants are then centrifuged at 12,000g for 20 minutes and resuspended in 0.5ml breaking buffer pH 6.0 before the crude mitochondrial concentration is calculated with the conversion factor of an absorbance at 280 of 0.21 = 10mg/ml mitochondrial protein.

The mitochondria are further purified form the rude fraction by ultracentrifugation in a nycodenz gradient. The nycodenz gradient is prepared by layering a 14.5% nycodenz solution (1X breaking buffer pH 6, nycodenz and ddH_20) over a 20% nycodenz solution and the crude mitochondria are added. The gradient(s) are centrifuged in a SW-40Ti rotor (Beckman Coulter) at 283,807g for one hour, 4°C. After centrifugation, the purified mitochondria appear as a brown band around the 18%-14.5% and are removed via a syringe with a 19-gauge needle. The purified mitochondria are washed in breaking buffer pH 7.4 (0.6M sorbitol, 20mM HEPES-KOH pH 7.4) by a 10 minute spin, 12,500g, 4°C to remove any residual nycodenz. To measure the pure mitochondria concentration, the conversion factor of an absorbance at 280 of 0.21 = 10mg/ml protein. The mitochondria are diluted to 20mg/ml using breaking buffer pH 7.4 and 10mg/ml BSA is added to a final amount of 10% of the total volume. The mitochondria are stored in 25µl aliquots and flash frozen in liquid nitrogen before being stored at -80°C.

3.2.3.2 Yeast mitochondrial protein import

The concentration of mitochondria was determined using the conversion factor of an absorbance at 280 of 0.24 = 20mg/ml, and 50µg mitochondria were added per 100µl of import mix. For the import, the mitochondria were resuspended in import buffer (600mM sorbitol, KH_2PO_4, 50mM KCl, 50mM HEPES-KOH pH 7.4, 10mM $MgCl_2$, 2.5mM EDTA, 5mM L-methionine, 1mg/ml fatty free BSA), with the addition of 2mM ATP and 2.5mM NADH. The IMM potential was depleted with the addition of 25µM carbonyl cyanide m-chlorophenyl hydrazone (CCCP) instead of NADH. After the different import mixes are prepared, the radiolabelled protein of interest (as described in section 3.2.2.7) is added at an amount of 5µl TNT to 50µg mitochondria in 100µl. The mix is then incubated at 30°C for the

appropriate time (standard time of around 10 minutes). After the import is completed, the samples are placed on ice to terminate the reaction and then centrifuged at 16,600g for 5 minutes at 4°C (all centrifugation steps for this section are this, unless stated otherwise). Non-imported material was removed by the protease trypsin (0.1mg/ml) diluted in breaking buffer pH 7.4, and the resulting pellets from the above spin were resuspended in the trypsin solution and incubated on ice for 30 minutes. As a control for complete permeabilization of the mitochondria, a sample is resuspended in trypsin with 1% Triton-X100 and incubated for 30 minutes on ice. Following the 30 minute incubation with trypsin, the mixes are centrifuged as above and resuspended in the soybean trypsin inhibitor (SPTI, 1mg/ml) to inhibit protease degradation, and incubated for 10 minutes on ice. The mitochondria are pelleted by centrifugation and resuspended in 100µl of breaking buffer pH 7.4 to wash any residual trypsin/SPTI. Finally, the mitochondria are pelleted by centrifugation and resuspended in 10µl 2X SB.

Import experiments with purified Trx1 (in comparison to the standard RRL TNT reactions) were carried out as above however instead of using radiolabelled proteins, 100µg of the purified protein was precipitated with $AmSO_4$ at 2X the original volume. The mix was incubated for 30 minutes on ice and centrifuged for 30 minutes, 16,600g at 4°C. The supernatant was removed and the precipitated pellet resuspended in 50.6µl 50mM HEPES pH 7.4 buffer to give a concentration of 2µg/µl to use for subsequent imports.

3.2.3.3 Mitoplasting

Following the previous section, the mitochondria after trypsin treatment are resuspended in 20µl 1X import buffer (final concentration 5mg/ml) and then diluted in 8X mitoplast buffer (20mM HEPES-KOH pH 7.4) with and without proteinase K (0.1mg/ml) and incubated on ice for 30 minutes. After incubation, 1mM PMSF was added and the samples left to incubate on ice for a further 10 minutes. The mitoplasts are pelleted by centrifugation, 16,600g, 5 minutes at 4°C and the supernatant precipitated with trichloroacetic acid (TCA) (10% v/v final concentration), incubated on ice for 20 minutes and centrifuged at 16,600g for 20 minutes at 4°C. The supernatant containing soluble IMS proteins, and the

pellet containing outer/inner membrane and matrix proteins were resuspended in 10µl 2X SB.

3.2.3.4 Carbonate extraction

To separate the soluble IMS, matrix and any loose peripherally associated membrane proteins, Na_2CO_3 extraction was used. Na_2CO_3 at a concentration of 100mM was incubated with the samples (which contained 150µg mitochondria), and incubated on ice for 30 minutes. Following the incubation, the sample was pelleted at 131,440g for 30minutes at 4°C. The pellet was resuspended in 2X SB and the supernatant TCA precipitated as described in 3.2.3.3.

3.2.4 *In vivo* assays

3.2.4.1 Yeast spot test

Yeast colonies were selected for the strains being investigated and the OD_{600} values measured. The yeast were diluted to 0.1OD units in ddH_2O and the 0.1OD unit was then serial diluted four times to give a range of dilutions from 0.1-0.0001. From each dilution, 5µl were spotted onto YPD or YPLac plates and grown at 30°C for 24 hours.

3.2.5 *In silico* analysis

3.2.5.1 Illustration design

All figures in this report were designed using Adobe photoshop (version 13.0) and Adobe illustrator (version 16.0).

Chapter 4: Investigating components of the import mechanism of Trx1

4.1 Introduction: Trx1 in the IMS

As previously discussed in the introduction (1.4.5.1), Trx1 is a reductase with a role in aiding oxidative stress. Previously identified as being present in the IMS, both the function and import pathway of Trx1 remain unknown (Vögtle *et al.,* 2012). Erdogan *et al.,* in 2018 detailed that the redox state of Mia40, which is crucial for its optimal function, is semi-oxidised. Additionally, the authors reported that ALR/Erv1, which re-oxidises Mia40, is superstoichiometric (present at a greater then 1:1 ratio) over CHCHD4/Mia40 (Erdogan *et al.,* 2018). Whilst there is the capability to oxidise Mia40 in the IMS, no reductive system has yet been described and given the semi-oxidised state of Mia40 it could be reasoned that there is a reductive capacity in this sub-compartment. Unpublished data from the Tokatlidis lab group has shown that Trx1 may have an influence on the redox regulated MIA machinery.

Previous work from the Tokatlidis lab has identified a potential β-like IMS targeting signal (bITS) which may have a role in import into the IMS and is composed of the following residues; polar-X-G-X-X-hydrophobic-X-polar. The bITS is present in 22% of IMS proteins, and the ITS signal is present in 21% of IMS proteins with a 57% overlap in proteins that contain both the bITS and ITS. However, the bITS is also present in a large number of matrix and cytosolic proteins, making it a fairly redundant sequence. Proteins that contain the bITS include Gpx3, Trx1, Trx2 and Trr1 and it is highly conserved across yeast, human and bacteria (unpublished data, Tokatlidis Lab group 2021). All import reactions in this chapter were performed using the TNT coupled Wheat Germ extract system.

4.2 Import of Trx1 and double cysteine mutant C30/33S into wild type mitochondria

The majority of experiments carried out in this report are import experiments which are used to test if a protein has been imported into mitochondria. The protein was translated with ^{35}S-Methione for visualisation on a Phosphorimage plate, which was then scanned using a phosphoimager. Once the TNT quick coupled transcription/translation system (Promega) had been left to incubate

for 90 minutes, the mix was centrifuged to remove the ribosomes. Different import mixes were prepared in eppendorfs for the different conditions (e.g ΔΨ+, ΔΨ- and +Triton-X), 50µg mitochondria and 5µl of the TNT mix were added per 100µl of import mix. Once incubated for the appropriate time at 30°C, the eppendorfs were placed on ice to stop the reaction. Non-imported material was removed by the addition of the protease trypsin which cleaves components of the OMM. If the protein has been imported, it will be protected from the trypsin and a band will be present in the lane of this condition. Triton-X completely permeabilises the mitochondria and is included as a negative control, therefore no band should be present in the lane of this condition. Additionally, the first lane of each import is either a 2%, 5% or 10% control of the material used for import, which determines if the protein has been successfully translated in the TNT reaction.

As the majority of IMS proteins are imported via the MIA pathway, which relies on the presence of cysteine residues in substrates, the import of both Trx1 and the double cysteine mutant C30/33S were conducted into WT mitochondria (figure 5). As shown in figure 5, Trx1 and Trx1 C30/33S both appear to import, however the suggested import band does not appear to be present in the 5% TNT control lane. Overall, this result demonstrates that Trx1 can be imported into mitochondria and that cysteines 30 and 33 are not required for import.

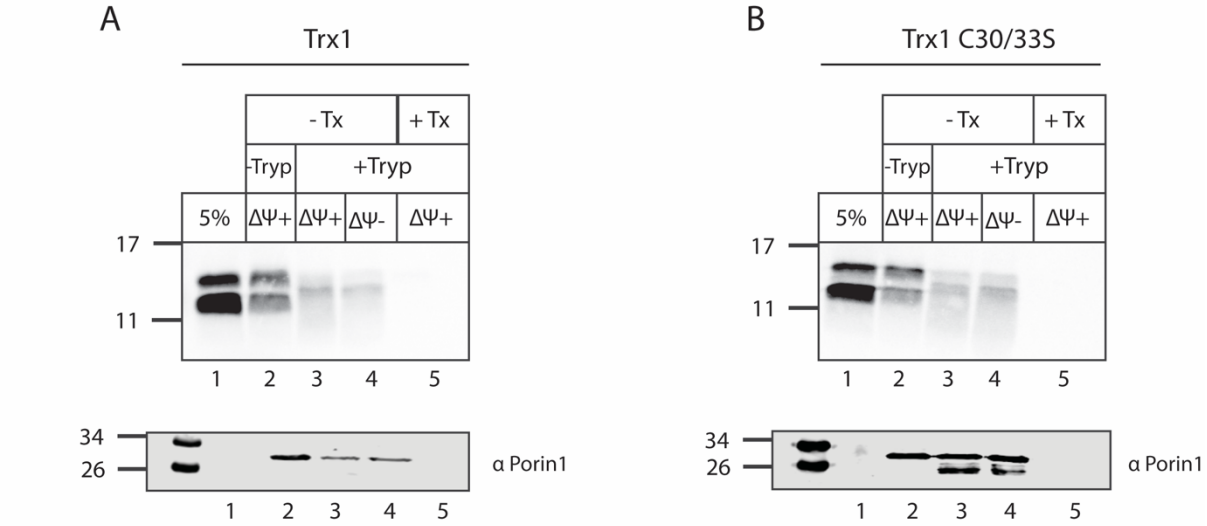

Figure 5: Import of radiolabelled (A) Trx1 and (B) Trx1 C30/33S into WT mitochondria shown via phosphorimage analysis. Lane 1 is a control for the TNT translation reaction, displaying 5% of total radiolabelled protein present in each condition. Proteins are imported with and without a membrane potential

(ΔΨ) and with and without Trypsin (Tryp). Triton-X solubilises the mitochondria and therefore is a negative control. The loading control Porin1 was used to observe mitochondria protein loaded in each lane.

4.3 Import of Trx1 into wild type, galMia40 and galErv1 mitochondria

As the cysteine residues were shown to be dispensable for the import of Trx1, it is unlikely that the MIA pathway is involved in import. To further strengthen this, galMia40 and galErv1 mitochondria were used to investigate the two major components of the MIA pathway. The expression of the respective proteins are under control of the gal promoter as Mia40 and Erv1 are essential genes. Firstly, to check the gal strains were reduced in the levels of Mia40 and Erv1 steady states of the proteins were checked via qualitative Western blotting (figure 6). It was observed that the galMia40 mitochondria had decreased levels of Mia40 and the galErv1 mitochondria had decreased levels of Erv1, both in comparison to WT. However, the galErv1 strain had reduced levels of Mia40 in comparison to WT and the galMia40 strain had reduced levels of Erv1 in comparison to WT. Overall, both the galMia40 and the galErv1 strain were reduced in the level of the respective protein.

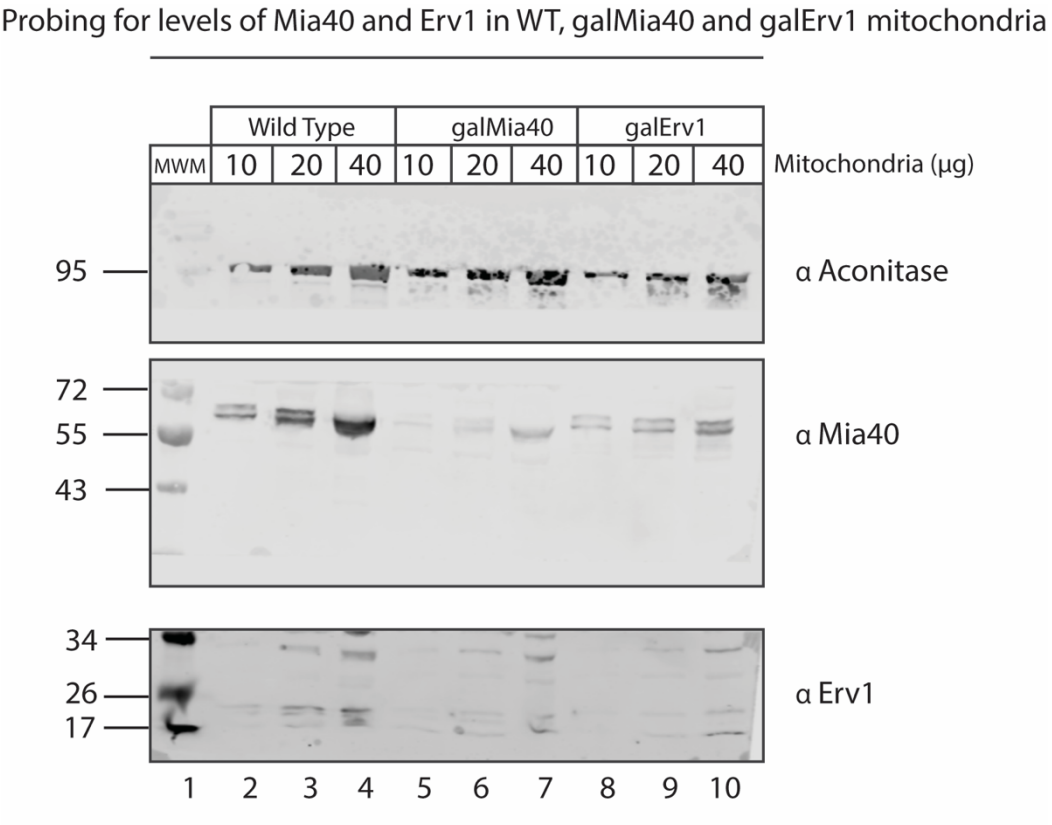

Figure 6: Steady state levels of Mia40 and Evr1 in WT, galMia40 and galErv1 stains. Levels of aconitase were included as a loading control. Three different amounts of mitochondria were loaded for each strain.

Once the gal strains had been checked, Trx1 was imported into the strains with WT mitochondria as a control (figure 7 A-C). Additionally, the import of Tim10 was carried out as a negative control as Tim10 is a substrate of the MIA pathway and therefore its import into the gal strains would be expected to be reduced (figure 7 D-F). The import of Trx1 into the gal strains appears to be slightly reduced, however, the imports across panels A-C of figure 7 do not appear to be a clear band, instead appearing more smeared. In contrast, the import of the MIA substrate Tim10 was decreased when comparing lane 3 of panels D-F in figure 7 as expected.

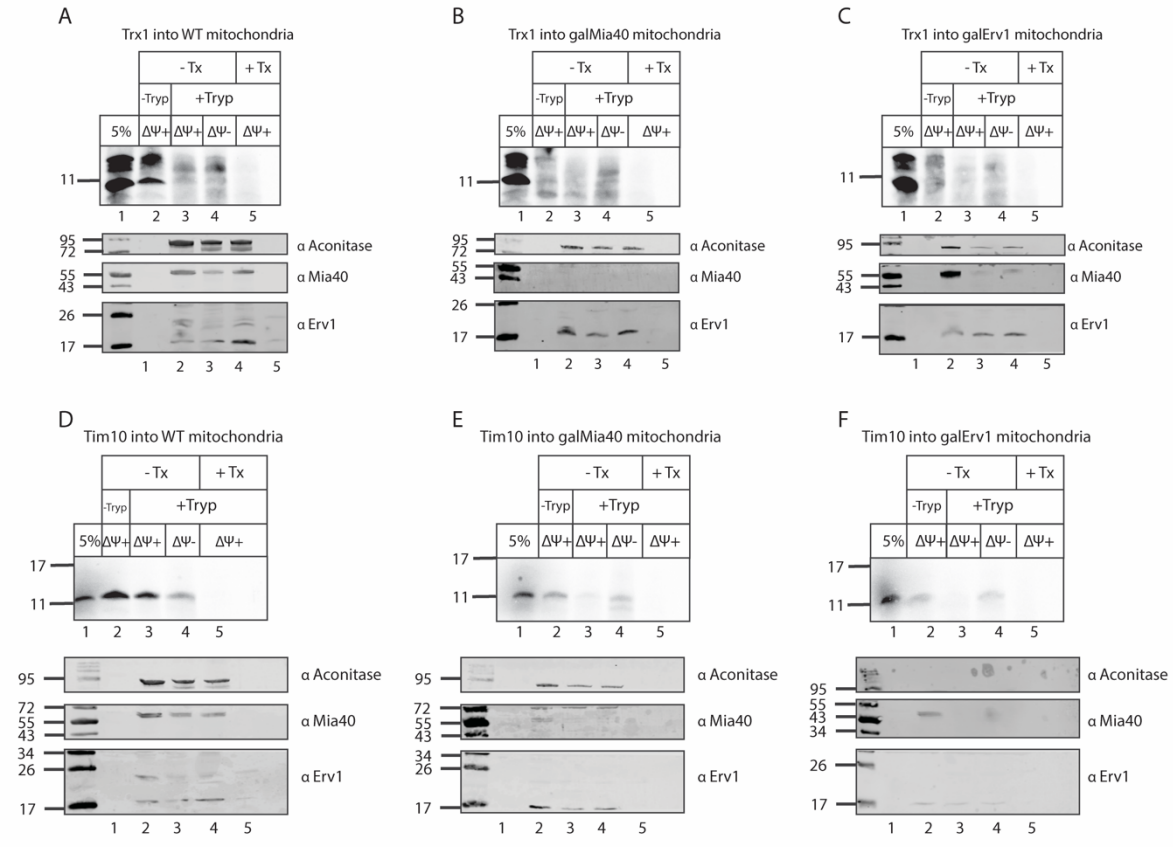

Figure 7: Import of (A-C) Trx1 and the MIA pathway substrate (D-F) Tim10 into (A+D) WT mitochondria, (B+E) galMia40 mitochondria and (C+F) galErv1 mitochondria. The import of radiolabelled Trx1 and Tim10 are shown via phosphorimage analysis. Lane 1 is a control for the TNT translation reaction, displaying 5% of total radiolabelled protein present in each condition. Proteins

are imported with and without a membrane potential (ΔΨ) and with and without Trypsin (Tryp). Triton-X solubilises the mitochondria and therefore is a negative control. The loading control aconitase was used to observe mitochondria protein loaded in each lane, and the levels of Mia40 and Erv1 were also probed for.

4.4 Import of Su9-DHFR and Trx1 into wild type mitochondria in the presence of increasing amounts of the oxidative phosphorylation uncoupler carbonyl cyanide m-chlorophenyl hydrazone (CCCP)

As the import pathway of Trx1 into the IMS is uncharacterised, and is not dependent on the MIA pathway, it would be expected that the import of Trx1 is also not dependent on membrane potential. However, Gpx3 has been recently identified as being targeted to the IMS and under H_20_2 stress an 18-amino acid N-terminal extension is alternatively translated which targets Gpx3 to the mitochondria (Kritsiligkou *et al.*, 2017). The import pathway of the non-extended form of Gpx3 is also unknown, and therefore it was tested to see if stressing the mitochondria with CCCP would have any effect on the import of Trx1. CCCP is used in standard imports at a concentration of 25μM where it uncouples mitochondrial oxidative phosphorylation, depolarising the IMM and therefore reducing ATP production.

The import of Su9-DHFR was abolished with a concentration of ≥25μM CCCP in contrast to the import of Trx1 which appeared unaffected by any concentration of CCCP (figure 8). Overall showing that the import of Trx1 is neither increased or decreased with increasing levels of CCCP.

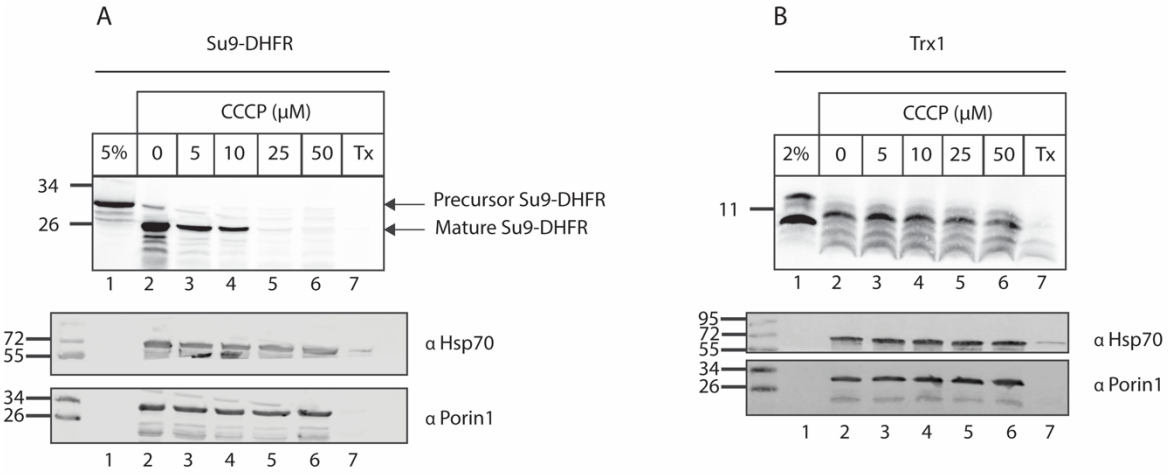

Figure 8: Import of (A) Su9-DHFR and (B) Trx1 into WT mitochondria with an increasing concentration (µM) of CCCP. The import of radiolabelled Su9-DHFR and Trx1 are shown via phosphorimage analysis. Lane 1 is a control for the TNT translation reaction, displaying 5% and 2% of total radiolabelled protein present in each condition. Triton-X solubilises the mitochondria and therefore is a negative control. The loading controls Hsp70 and Porin1 were used to observe mitochondria protein loaded in each lane.

4.5 Pulldown of His-tagged Trx1 with solubilised mitochondria

To investigate components of the Trx1 import pathway a pulldown experiment was conducted. This involved binding varying amounts of His-tagged Trx1 (µg) to Ni-NTA columns, solubilising mitochondria and passing this through the columns to see if any mitochondrial proteins would be bound to Trx1 on the column. No additional proteins were pulled down, with Trx1 being present in both elution lanes (+ and – DTT) which demonstrates that the protein was bound to the columns (figure 9).

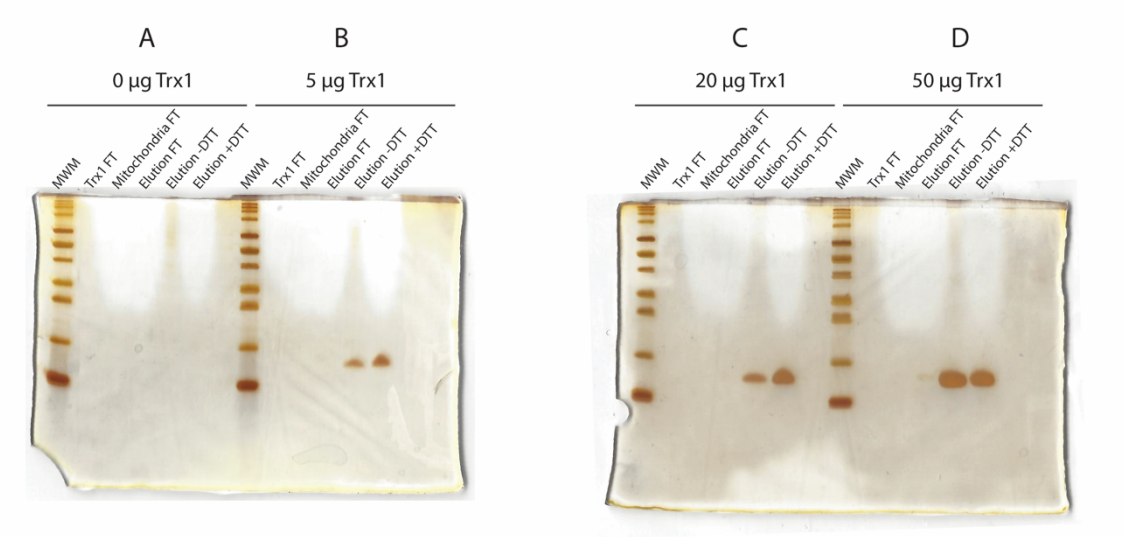

Figure 9: His-tagged Trx1 pulldown with NiNTA columns and varying amounts of Trx1 (µg). (A) With 0µg Trx1, (B) 5µg Trx1, (C) 20µg and (D) 50µg Trx1 present. The samples were ran on a Tris-Tricine gel which was then silver stained. Trx1 FT describes the sample that was collected after Trx1 was passed through the column. Mitochondria FT describes the sample that was collected after the solubilised mitochondria were passed through the column.

4.6 Investigating the import of Trx1 β-like IMS targeting signal (bITS) into wild type mitochondria

Identified by a previous lab member in the Tokatlidis lab group, the bITS is comprised of polar-X-G-X-X-hydrophobic-X-polar residues which in Trx is the following amino acids: K-N-G-K-E-V-A-K. The lysine residue at position 86 and the glycine residue at position 81 were mutated to alanine using side-directed mutagenesis and the import of both mutants into WT mitochondria were conducted. In comparison to Trx1 import, the import of both mutants appeared as a less defined band, although all three imports are not of great quality and steps to optimise the import will be investigated in the following chapter (figure 10).

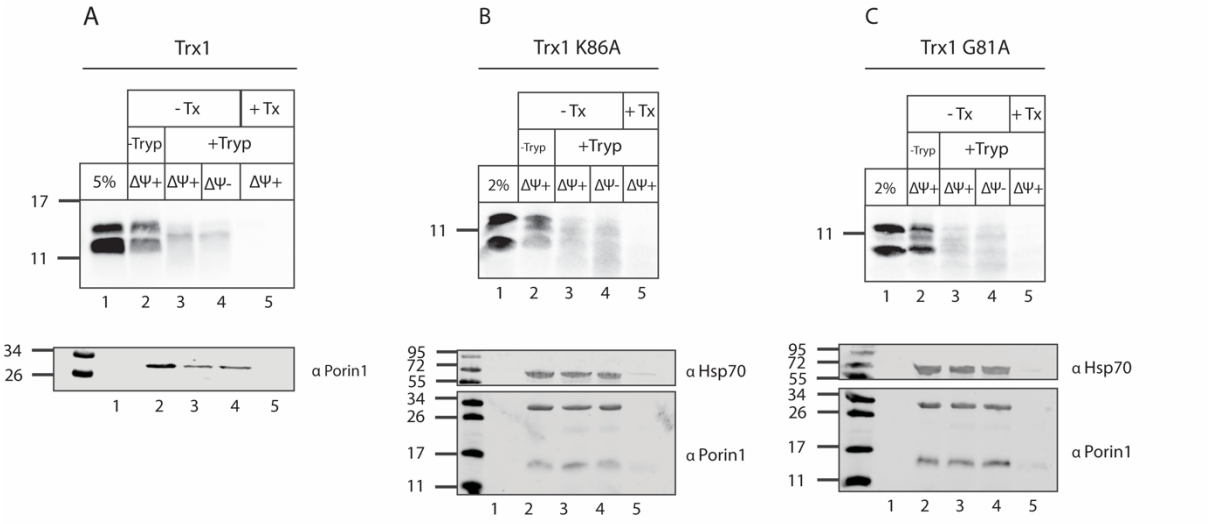

Figure 10: Import of (A) Trx1, (B) Trx1 K86A and (C) Trx1 G81A into WT mitochondria. The import of Trx1, Trx1 K86A and Trx1 G81A are shown via phosphorimage analysis. Lane 1 is a control for the TNT translation reaction, displaying 5% or 2% of total radiolabelled protein present in each condition. Proteins are imported with and without a membrane potential (ΔΨ) and with and without Trypsin (Tryp). Triton-X solubilises the mitochondria and therefore is a negative control. The loading controls Hsp70 and Porin1 were used to observe mitochondria protein loaded in each lane.

4.7 Import of Thioredoxin reductase 1 into wild type mitochondria

Whilst Trx1 has a broad substrate specificity, Trr1 specifically reduces the oxidised and inactive state of Trx1 to its active reduced form. Trr1 was

identified as being present in the IMS in the same study that identified Trx1 in the IMS (Vögtle *et al.*, 2012). An import experiment with Trr1 was conducted to see if this result could be repeated however no import of Trr1 into WT mitochondria was observed (figure 11).

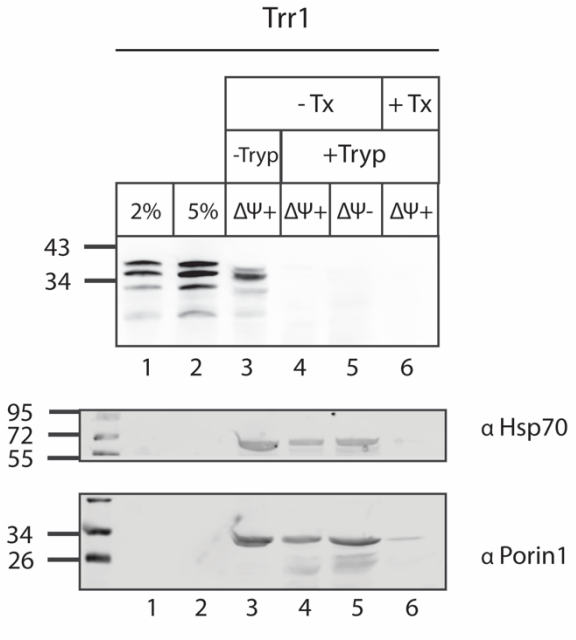

Figure 11: Import of radiolabelled Trr1 into WT mitochondria shown via phosphorimage analysis. Lane 1 is a control for the TNT translation reaction, displaying 2% of total radiolabelled protein present in each condition. Proteins are imported with and without a membrane potential (ΔΨ) and with and without Trypsin (Tryp). Triton-X solubilises the mitochondria and therefore is a negative control. The loading controls Hsp70 and Porin1 were used to observe mitochondria protein loaded in each lane.

4.8 Discussion

The aim of this chapter was to investigate components of the import pathway of Trx1. Trx1 and the C30/33S mutant could be imported into mitochondria (figure 5) which suggests that the MIA pathway is not involved in import. This independence of Mia40 for the import of Trx1 was further investigated by the use of gal strains (figure 6). GalMia40 mitochondria contain reduced levels of Mia40 however they contain functional Erv1, which reoxidises Mia40 back to its active form. GalErv1 mitochondria contain reduced levels of Erv1, which as mentioned previously is required for a functional Mia40 (Mesecke *et al.*, 2005; Banci *et al.*, 2011, 2013). Trx1 import appeared slightly decreased between the

WT and gal strains however a clear band is not visible (figure 7 A-C). This potential reduction could be because Trx1 may be interacting with components of the MIA pathway and substrates, which are reduced in the gal strains and therefore the requirement for Trx1 is deceased. In sharp contrast, the import of Tim10 is reduced in the galMia40 and galErv1 strains (figure 7D-F), however a faint band is still visible in the ΔΨ- lanes (lanes 4, figure 7E and F). Tim10 is a substrate of the MIA pathway and therefore it was expected that its import would be reduced in mitochondria with decreased levels of Mia40 and Erv1 (Stojanovski *et al.,* 2008). A control that is lacking from this set of experiments due to time constraints is a protein whose levels are unaffected by a reduction in Mia40 and/or Erv1 such as the matrix targeted protein Su9. Additionally in figure 7F, the aconitase loading control is not present. Overall, Trx1 does not appear to require the MIA pathway for its import, however additional controls and repeats are necessary.

As mentioned previously, the thioredoxin system is crucial for regulating oxidative stress and aiding in the removal of ROS/RNS (Cardenas-Rodriguez and Tokatlidis, 2017). On the one hand, as an IMS protein, Trx1 would not decrease upon reduction of membrane potential but could the import be increased upon mitochondrial stress caused by an uncoupler? It was observed that import of Trx1 was unaffected by the increasing concentrations of CCCP, in contrast to Su9 which is present in the matrix and requires membrane potential for its import (figure 8) (Schmidt *et al.,* 1983). A further control for this experiment would be to test the import of a protein where the import is known to be unaffected by CCCP. This could be the import of any OMM protein, for example Porin1, or an IMS protein such as a small Tim. Overall, this result suggests that Trx1 import is neither increased or decreased in the presence of oxidative phosphorylation uncoupling and therefore mitochondrial stress.

Next, a pulldown experiment involving His-tagged Trx1 and solubilised mitochondria was conducted to identify any protein components of import. As shown in figure 9, the pulldown experiment did not pull down any other proteins, however there are multiple improvements that could be made if a repeat had been carried out. Adjustments and optimisation steps include; increasing the incubation time of the solubilised mitochondria on the column and including varying the amount of mitochondria added to the columns.

Furthermore, a Cys-trapping Trx mutant could be used to stabilise any potential interacting partners and/or substrates in order to identify them. Additionally, the IMS fraction of mitochondria could be isolated and ran through the column as opposed to entire solubilised mitochondria. Once optimised, a pulldown experiment with Trx1 and mitochondria would allow for any interacting proteins to be identified, for example proteins in the IMS that are interactors.

To further investigate the import pathway of Trx1, import experiments of two bITS motif mutants were carried out. As mentioned previously, the bITS has been recently identified by a previous lab member, however the bITS motif is also present in a large number of proteins that contain the intermembrane space targeting signal and is present in many matrix and cytosolic proteins. The import of the bITS mutants appears smeared and the band that is seen in figure 10A lane 3 does not appear to be as defined in lane 3 of figure 10B and 10C. It is worth noting that work with the bITS motif is in preliminary stages, however a member of the Tokatlidis lab group has shown that when these residues were mutated in the bITS of Gpx3, import of Gpx3 was abolished. This suggests that residues in the bITS are important for import of Gpx3 and the results presented in figure 10 suggest that there may be a role of the bITS, maybe in conjunction with other internal targeting signals, in the import of Trx1, however further repeats are required.

Lastly, Trx1 requires recycling back to its active reduced state and this process is carried out by Trr1 (Collet and Messens, 2010). The same study identified both Trx1 and Trr1 as being present in the IMS and therefore an import of Trr1 was carried out to try and repeat this result (Vögtle *et al.*, 2012). Trr1 was unable to be imported, however in the future repeats should be carried out and the conditions of the import could be altered (e.g in denaturing and/or reducing conditions) to see if Trr1 could be imported (figure 11). No other protein has been identified that recycles Trx1 back to its reduced state, therefore it can be reasoned that Trr1 must also be present in the IMS.

Chapter 5: Optimising the import protocol of Trx1

5.1 Introduction: Why optimise the import protocol of Trx1 and background to the methods used to do so

Following the results presented in chapter 4, the quality of the import of Trx1 further decreased and appeared more smeared. Additionally, the apparent import band did not appear to be the predominant band in the TNT control lane. This multiple banding pattern that appears in the TNT has been observed by previous members of the Tokatlidis lab. The decline in import quality of Trx1 lead to a series of experiments to try and improve both the quality of the import on the phosphorimage scan and the intensity of the middle band in the TNT control lane which is assumed to be the Trx1 import band.

The Flexi RRL system was utilised to try and improve the import of Trx1 as the environment of the Flexi RRL system can be more easily controlled which allows for optimisation. The concentration of Mg^{2+} and K^{+} can be altered and there is the option to add or omit the reducing agent DTT. Additionally, the concentration of glucose-6-phosphate (G6P) could be altered which allows for more control over the redox state of the lysate system. It was hypothesised that the reducing environment of the lysate systems may be leading to aberrant disulfide bond formation which could be due to the lack of NADPH present. To prevent this, the concentration of G6P can be increased as the main mechanism of NADPH recycling is through the enzyme G6PDH, which converts G6P into 6-phosphoglucono-δ-lactone, producing NADPH in the process. Increasing the amount of G6P present in the environment increases the activity of NADPH recycling, and therefore the amount of NADPH present to act as the ultimate electron donor increases, and this may aid the prevention of aberrant disulfide bond formation (Poet *et al.*, 2017).

5.2 Use of the Flexi RRL system with increasing concentrations of G6P

Five concentrations of G6P were included in experiment in the hopes of increasing the strength of the middle of the three bands present in the TNT reaction. As shown in figure 12, 1mM of G6P did appear to slightly increase the presence of the middle band, however the intensity of the lower band also

appeared to increase. Between the different concentrations of G6P, the intensity of the uppermost band stayed constant.

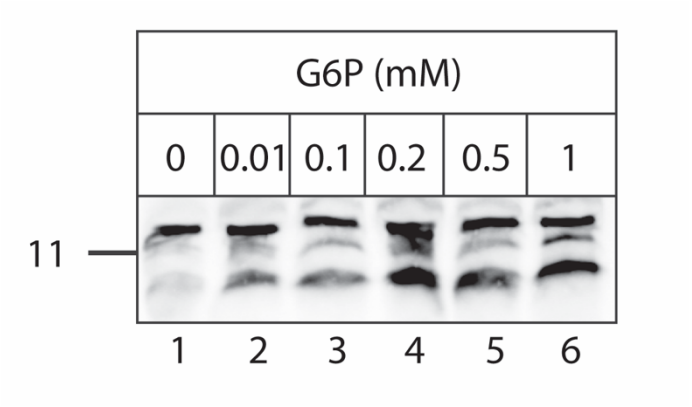

Figure 12: Radiolabelled Trx1 RNA 10% controls, treated with different concentrations (mM) of G6P. The above phosphorimage scan shows six lanes of 10% control of Trx1 RNA, with the sample containing no reducing agent (no DTT present in the 2X sample buffer).

5.3 Comparing import of Trx1 between the Wheat Germ lysate system and the Flexi RRL with 1mM G6P

Following the above experiment, an import experiment was conducted to compare the Flexi RRL containing 1mM G6P with the Wheat Germ lysate. The quality of import of Trx1 with the Flexi RRL system does not appear any different when compared to the Wheat Germ lysate, with import still appearing unclear and no clear import bands in lanes 4 and 5 present.

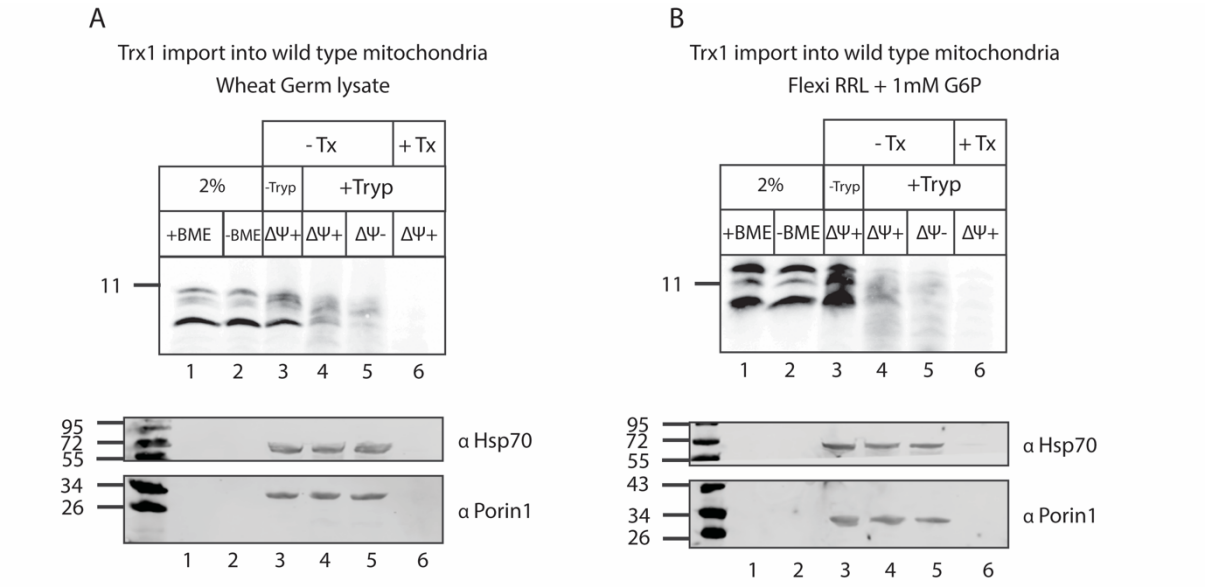

Figure 13: (A) Import of radiolabelled Trx1 into wild type mitochondria with the Wheat germ lysate system and (B) import of Trx1 RNA into wild type mitochondria with the Flexi RRL system with the addition of 1mM G6P. Lanes 1 and 2 are controls for the TNT translation reaction, displaying 2% of total radiolabelled protein present in each condition. Proteins are imported with and without a membrane potential (ΔΨ) and with and without Trypsin (Tryp). Triton-X solubilises the mitochondria and therefore is a negative control. The loading controls Hsp70 and Porin1 were used to observe mitochondria protein loaded in each lane.

5.4 Investigating the effect of denaturing and/or reducing conditions on the import of Trx1

Denatured conditions involve the addition of urea, final concentration of 8M, to denature the protein and reducing conditions involve the addition of DTT, final concentration 10mM, to reduce disulfide bonds in the protein. The following set of experiments were conducted to investigate any effects of these conditions on the import of Trx1. Comparing lane 4 between the four conditions, the native condition appears to be the most defined band with panels B-D appearing of lower quality. However, there is no clear difference between any of the four conditions investigated.

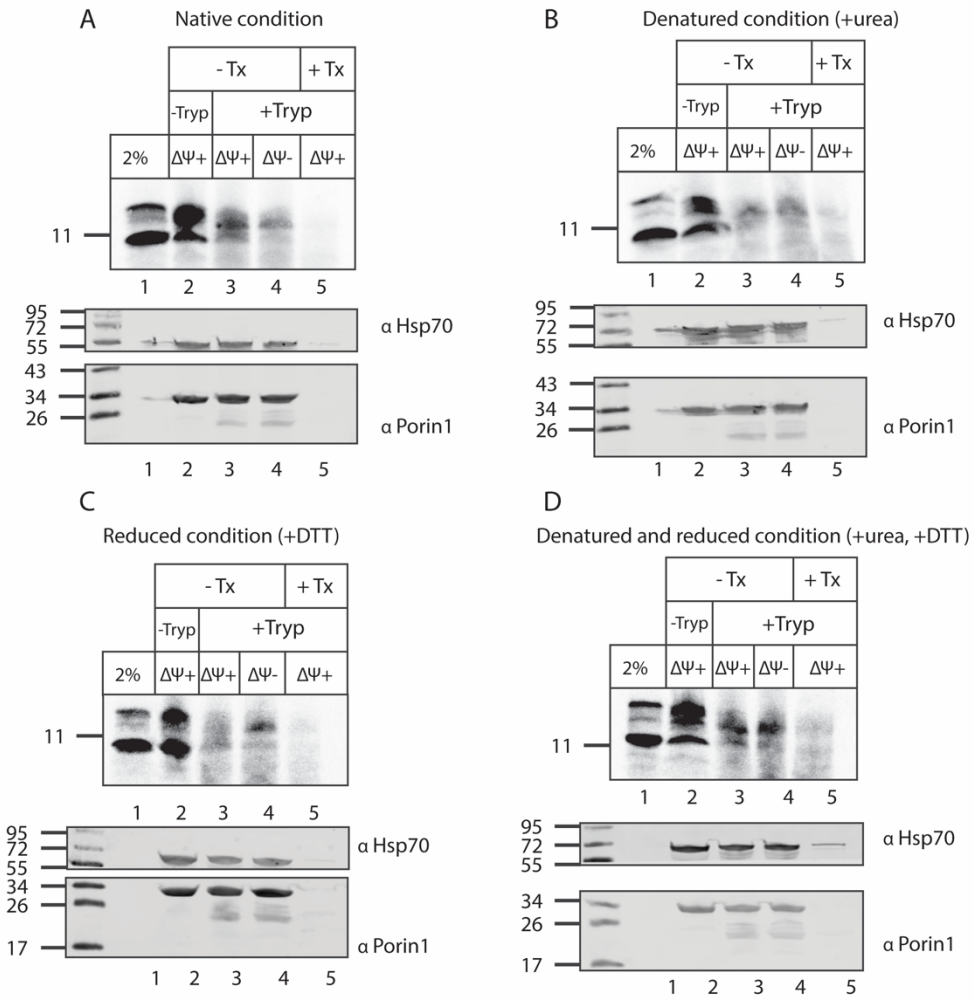

Figure 14: Import of radiolabelled Trx1 in (A) native condition, (B) denatured condition, (C) reduced conditions and (D) with reduced and denatured conditions into wild type mitochondria. Lane 1 is a control for the TNT translation reaction, displaying 2% of total radiolabelled protein present in each condition. Proteins are imported with and without a membrane potential (ΔΨ) and with and without Trypsin (Tryp). Triton-X solubilises the mitochondria and therefore is a negative control. The loading controls Hsp70 and Porin1 were used to observe mitochondria protein loaded in each lane.

5.5 Protein purification of Trx1 and import of the purified protein

Following a lack of effect on the import of radiolabelled Trx1 with the Flexi RRL, and any difference between denaturing and/or reducing conditions, it was decided to prepare freshly purified Trx1 protein and test its import. Trx1 had been previously cloned into the pET24 vector with a 6xHis tag and as Trx1 is soluble, the purification processes was straightforward. Figure 15A displays the

result of a small scale expression of two colonies from the transformation of BL21DE3 cells, induced with a final concentration of 0.4mM IPTG. From the small scale colony expression, it is evident that Trx1 was successfully expressed. Following this, Trx1 was successful purified as shown by the large band in the elution lane (lane 6, figure 15B). The protein was concentrated and stored in 400µg aliquots at -20°C and -80°C for subsequent import experiments.

Once Trx1 had been successfully purified, an import experiment was conducted into WT mitochondria (figure 16). The presence of Trx1 in lane 2 (figure 16) indicates that the protein is present on the OMM of mitochondria. However, in lanes 3 and 4 which are treated with trypsin the Trx1 import band is no longer present, this indicates that purified Trx1 was not imported.

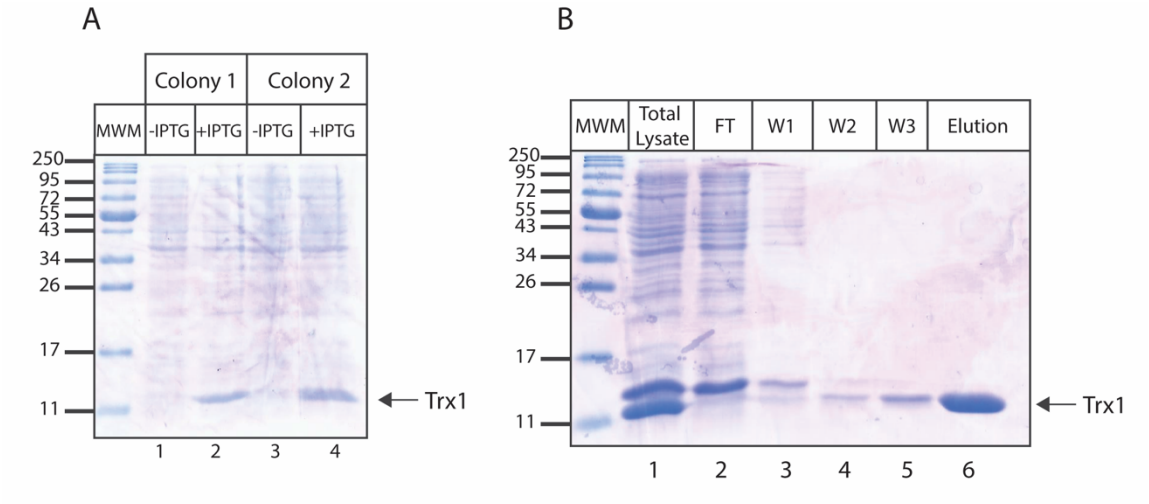

Figure 15: Protein purification of Trx1. (A) Small scale expression of transformed BL21DE3 cells and (B) Ni-NTA protein purification of Trx1. Samples were ran on 15% Tris-glycine gels at 80V through the stacking, 120V through the separating and then Coomassie stained.

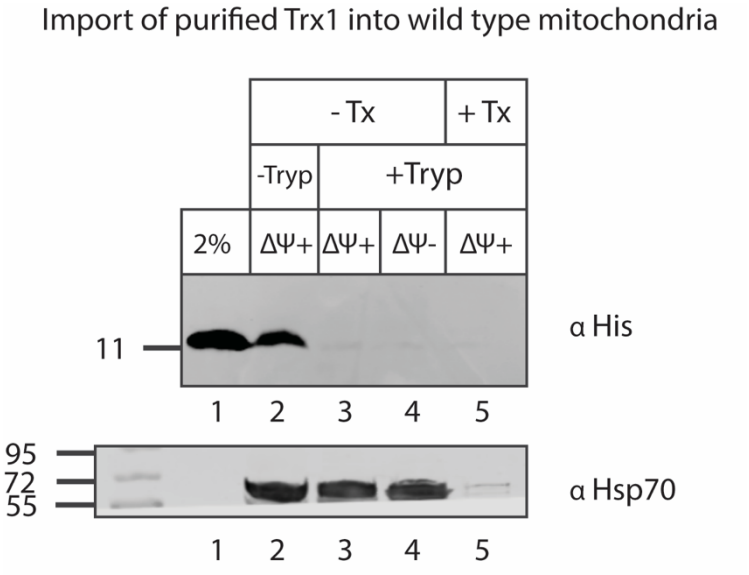

Figure 16: Import of purified Trx1 protein into wild type mitochondria. Lane 1 is a control lane, displaying a 2% control. A total of 100µg of purified protein was used which equates to 20µg per lane of the import. Proteins are imported with and without a membrane potential (ΔΨ) and with and without Trypsin (Tryp). Triton-X solubilises the mitochondria and therefore is a negative control. The loading controls Hsp70 and Porin1 were used to observe mitochondria protein loaded in each lane.

5.6 Discussion

The aim of this chapter was to optimise the import protocol of Trx1: firstly to increase the strength of the middle band in the TNT control, and secondly to investigate conditions that would improve the strength of the faint import band. As described in the introduction to this chapter, G6P was added to increase NADPH recycling to ultimately help prevent aberrant disulfide bond formation. It was previously described by Poet., *et al* (2017) that the reducing environment could be re-established by the addition of 0.2mM G6P. With the addition of 1mM G6P to the TNT mixture, the intensity of the middle band appears to increase between lanes 1-6 of figure 12, however the intensity of the lower band also appears to increase. This increase appears to be due to the increasing presence of G6P, however it remains unclear what these additional bands are. As an additional precaution the construct of Trx1 used in this report was sequenced with no abnormalities or mutations reported. Looking at the sequence of Trx1,

the bands are unlikely to stem from alternative start codons as other methionine residues present in the sequence do not have ribosome binding sites upstream. It would be interesting to analyse these other bands present in the TNT by mass spectrometry to identify exactly what they are. If the bands are other translation products, the additional methionine residues could be mutated to see if the presence of these bands in the TNT are prevented. Overall, the presence of G6P in the TNT reaction appears to increase the intensity of the middle Trx1 import band however it remains unclear exactly what these additional bands are.

Next, an import was conducted to compare the effect of the addition of 1mM G6P in the Flexi system compared to the Wheat germ system previously used for Trx1 import experiments (figure 13). Between the two panels there does not appear to be a great difference in the import lanes (lanes 4-5, figure 13), indicating that the quality of import of Trx1 has not been improved. Whilst figure 12, mentioned above, showed a slight increase in intensity of this middle (and upper) band in the control lane, this does not appear to have translated into improved import of the protein.

Following this result, the impact of denaturing and/or reducing conditions on the import of Trx1 was investigated. In denatured conditions the protein loses its structure and shape but the redox active bonds are still present. In reduced conditions, the protein retains its structure however the redox active disulfide bonds are no longer present. In the case of Tim10 these redox active bonds also have a structural role and the protein will lose its structure in reduced conditions. This is not the case for yeast Trx1, which contains two redox active cysteines at position 30 and 33 that form the conserved CGPC motif (Cardenas-Rodriguez and Tokatlidis, 2017). Between the four conditions investigated (native, reduced, denatured and denatured/reduced), there appears to be little difference between the import of Trx1 (figure 14). The molecular weight of Trx1 is 11.2kDa, therefore denaturing the relatively small protein is unlikely to affect import which is indeed what is observed (figure 14B and 14D). Additionally, as described in the previous chapter, the redox active cysteines are not required for the import of Trx1 and therefore reducing this bond is unlikely to have an effect when compared to import in a native condition. The lack of effect on import is also observed in the experiments carried out (figure 14C-D). From this

set of experiments, it can be concluded that denaturing and/or reducing conditions have no effect on the import of Trx1.

Due to the lack of success in improving the quality of import with the Wheat germ system or the Flexi RRL, the Trx1 protein was freshly purified. As Trx1 is soluble, the protein purification was straight forward and the protein was successfully purified (figure 15). The next working day, an import was conducted using the freshly prepared purified protein (20µg per import lane, as per a previous lab members protocol). The purified protein was unable to be imported into WT mitochondria, shown by the disappearance of the band visible in lane 2 (without trypsin treatment) compared to lanes 3-4 (with trypsin treatment). This result is in contrast to previous results gathered by the lab, where the purified protein could be imported and warrants further investigation in the forms of repeats.

Overall, the quality of import of Trx1 could not be optimised despite the various conditions and systems that were tested. The paper which identified Trx1 as being present in the IMS reported a clear, well-defined single import band that is the same between the TNT control lane and the import lanes. The import experiment carried out by the group is very similar to the protocol used in this report, however Proteinase K instead of trypsin was used to test import and no final solubilised Triton-X lane is present (Vögtle *et al.*, 2012). Triton-X100 is a critical control, as it solubilises the mitochondria making the whole mitochondria content accessible to the externally added protease and therefore no band should be present in this lane.

Chapter 6: Investigating components of the import mechanism of Gpx3

6.1 Introduction – Gpx3 in the IMS and background to the proteins investigated in this chapter

Gpx3 was first identified in the IMS in 2012, and in 2017 was reported to undergo alternative translation under stress which produces an N18 extended form of the protein (Vögtle *et al.,* 2012; Kritsiligkou *et al.,* 2017). Gpx3 with and without the N18 extension is imported into the IMS however the presence of the N18 extension increases the efficiency of import into mitochondria. Gpx3 has previously been reported to interact with Mia40, oxidising its inactive reduced form back to the active oxidised form of Mia40 (Kritsiligkou *et al.,* 2017). Therefore, it is likely that Gpx3 has a role in maintaining the redox state of the IMS, where the redox state is crucial for the import of the majority of IMS proteins which relay on the MIA pathway. However, both the import pathway of Gxp3 and the function of the non N18 extended form of Gpx3 remain unknown.

Work by current members of the Tokatlidis lab has involved systematically conducting imports using delta, gal and temperature sensitive strains of the main OMM import machinery components (e.g all TOM complex subunits and all SAM complex subunits). As no effect was seen from these imports, focus shifted to the OMM proteins Om14 and Om45. Interestingly, both Om14 and 45 are some of the most abundant OMM proteins, have no human homolog and the function of Om45 remains unknown. Om45 contains 363 residues, only 5 of which are present in the cytoplasm with the majority in the IMS (Wu, Li and Jiang, 2018). It is the most abundant signal anchored protein of the OMM and follows components of the presequence pathway. It has previously been reported that the precursor form of Om45 is recognised by the TOM receptors 20 and 22, then the TIM23 complex and Mim1 have a role in translocating the large C-terminal domain into the IMS (Wenz *et al.,* 2014). Additionally, delta strains of Om45 have no defects in cell viability, growth or mitochondrial protein import (Yaffes, Jensenp and Guido, 1989). Om14 contains 134 amino acids and has three transmembrane domains in the OMM and similar to Om45, delta Om14 strains show no obvious growth defects. Previous data has shown that the steady state levels of Om14 and Om45 are co-regulated, which could suggest that the function(s) of these proteins is linked (Burri *et al.,* 2006). Om14 has been

previously identified as a receptor for the nascent chain-associated complex (NAC) as ΔOm14 *S. cerevisiae* cells had lower amounts of ribosomes and associated NACs. The NAC was shown to specifically interact with Om14 whilst the NAC is associated with the ribosome (Lesnik *et al.*, 2014). Additionally, Porin1 has been shown to form a complex with Om14 and Om45 in a monomeric manner. Om45 and Om14 interact together resulting in the formation of a stable oligomeric structure only in the presence of Porin1 with Om14 mediating binding to Porin1. The formation of the complex was suggested to aid the binding of Porin1 to specific channels, assisting the transport of metabolites (figure 17) (Lauffer *et al.*, 2012).

Additionally, glucose grown mitochondria were used in this chapter as the levels of both Om45 and Om14 had been previously been reported to decrease when cells were grown on glucose (Burri *et al.*, 2006; Bruckmann *et al.*, 2009). This provided a system where both the levels of Om45 and Om14 were reduced, allowing the effects of a reduction in both proteins to be investigated.

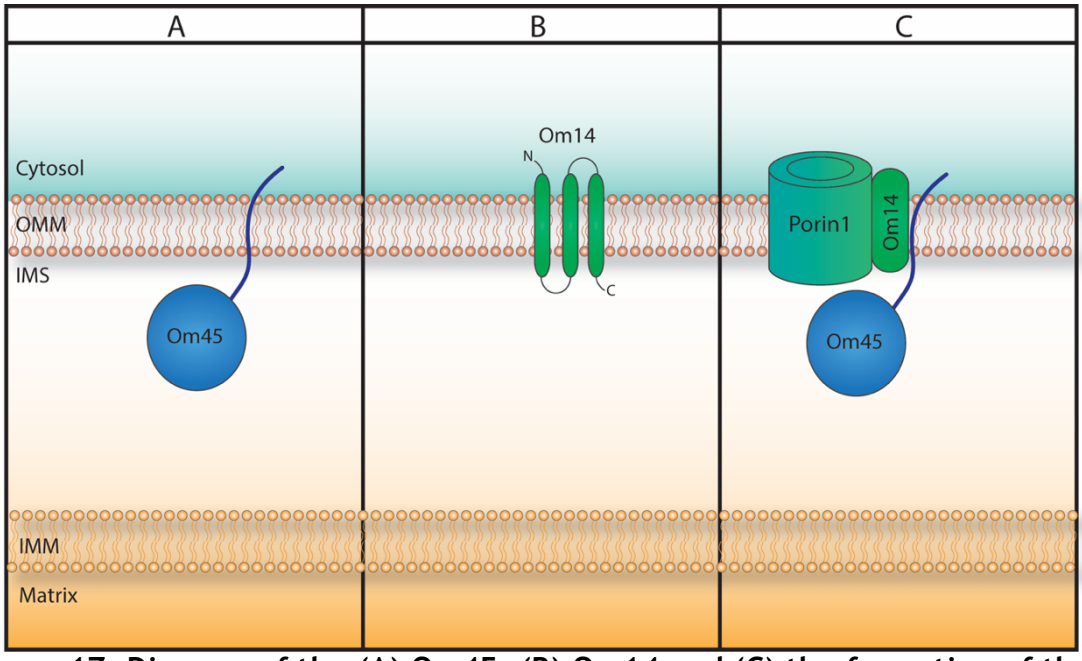

Figure 17: Diagram of the (A) Om45, (B) Om14 and (C) the formation of the monomeric complex of Om14, Om45 and Porin1.

6.2 Localisation of Gpx3 into wild type mitochondria

To confirm the presence of non-extended Gpx3 in the IMS, a localisation experiment was conducted using mitoplasting and carbonate extraction to identify the protein of interest in a specific sub-compartment. For mitoplasting,

if the protein band is visible in the supernatant (S), then the protein is present in the IMS. If the band is visible in the pellet (P), then the protein is present in the IMM or the matrix. $NaCO_3$ (carbonate extraction) determines if the protein is soluble or is in/or associated with a membrane. If there is a band present in the supernatant (S) of the $NaCO_3$ then the protein is soluble and not bound to a lipid bilayer, if there is a band present in the pellet (P) of the $NaCO_3$ then the protein is a membrane protein.

From figure 18, comparing lane 5 (S mitoplasting -PK) and lane 7 (S mitoplasting +PK), the band disappears indicating that mitoplasting was successful as the IMS band was able to be degraded by PK. There is a faint band in lane 9 and no band in lane 10 of figure 18, indicating that Gpx3 is a soluble protein. As Gpx3 is a known soluble protein perhaps the band in lane 9 would be expected to be more clear. Looking at the western blot controls, Aconitase (a matrix localised protein) appears to have 'spilled' over into neighbouring lanes, however the Tom40 (an OMM protein) bands are present where an OMM protein would be expected. Erv1 (an IMS protein) should be present in the supernatant lanes, however it is visible in the pellet lanes.

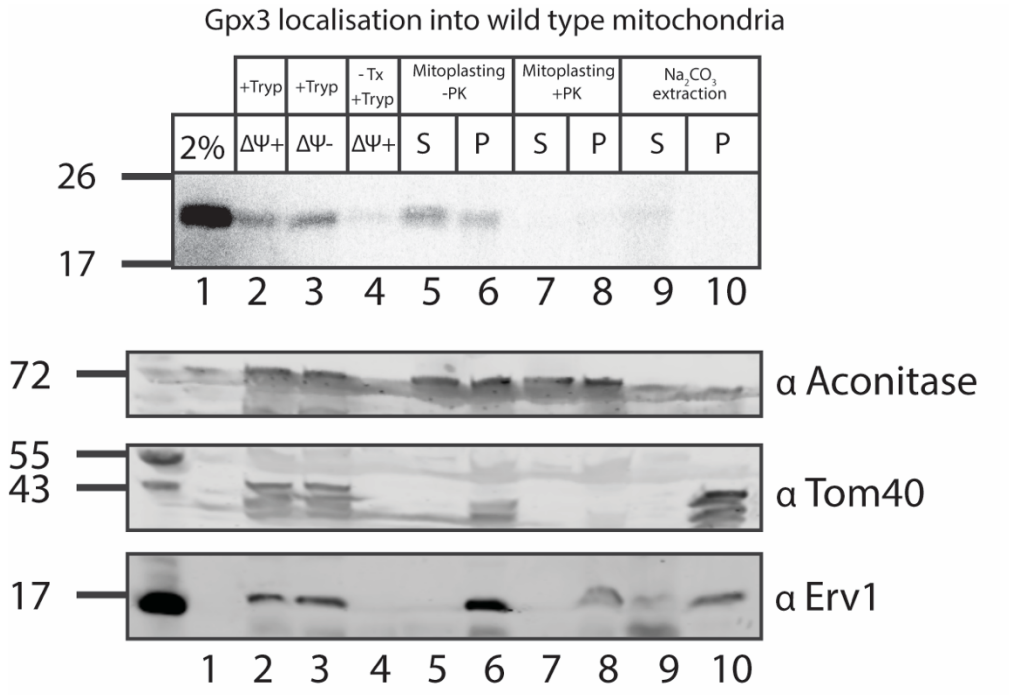

Figure 18: Import and localisation of radiolabelled Gpx3 into wild type mitochondria. Import was conducted over a 10 minute period, followed by trypsin treatment (to remove unimported material) or trypsin and Triton-X (Tx) as a control. Lane 1 is a control for the TNT translation reaction, displaying 2% of

total radiolabelled protein present in each condition. The mitochondrial outer membrane is ruptured by an osmotic shock which creates mitoplasts consisting of the inner membrane and matrix pellet (P) and the soluble IMS supernatant (S). Proteinase K (PK) is added as a control (+PK) for mitoplasting as PK would cleave mitochondrial proteins in the IMS. $NaCO_3$ extraction (carbonate extraction) separates the soluble matrix and IMS fraction from membrane associated proteins of the OMM and IMM. A western blot probing for proteins in different compartments were used as controls; Aconitase in the matrix, Tom40 in the outer membrane and Erv1 in the intermembrane space.

6.3 Investigating the effect of denaturing and/or reducing conditions on the import of Gpx3

As was previously investigated for Trx1 (chapter 5.4), the effect of the same conditions (native, denatured, reduced and denatured/reduced) were investigated for any effects on the import of Gpx3. This set of experiments was conducted to investigate whether the denatured and/or reduced state of Gpx3 would affect the import (either an increase or decrease). As mentioned previously, denatured conditions involve the addition of urea (final concentration of 8M) to denature the protein and reducing conditions involve the addition of DTT (final concentration 10mM) to reduce disulfide bonds in the protein. Comparing lane 3 to the different conditions, there does not appear to be a difference in import. However, between all conditions, import in $\Delta\Psi$- (lanes 4) conditions appears greater than in $\Delta\Psi$+ (lane 3) condition.

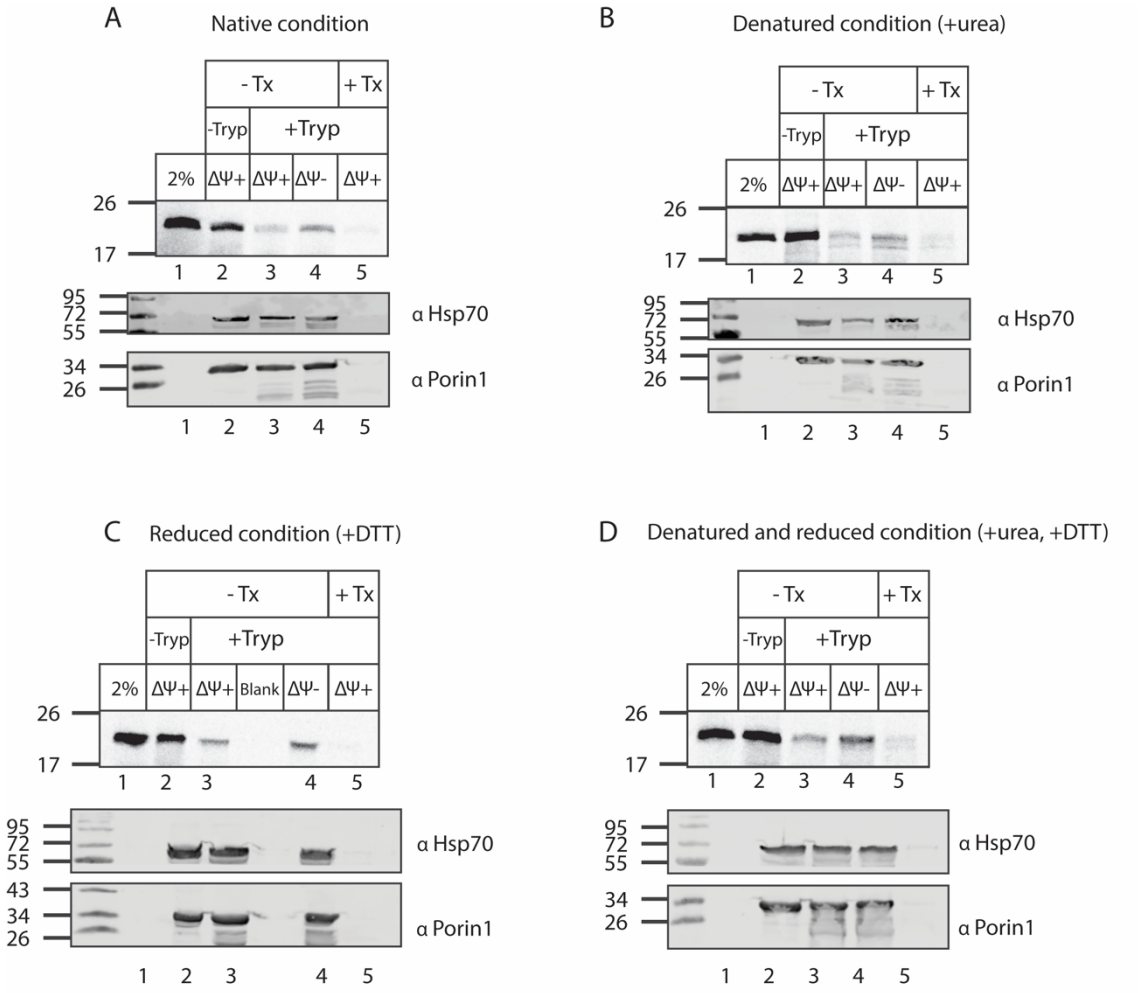

Figure 19: Import of radiolabelled Gpx3 in (A) native condition, (B) denatured condition, (C) reduced conditions and (D) with reduced and denatured conditions into wild type mitochondria. Lane 1 is a control for the TNT translation reaction, displaying 2% of total radiolabelled protein present in each condition. Proteins are imported with and without a membrane potential (ΔΨ) and with and without Trypsin (Tryp). Triton-X solubilises the mitochondria and therefore is a negative control. The loading controls Hsp70 and Porin1 were used to observe mitochondria protein loaded in each lane.

6.4 Confirming the delta strains ΔOm45 and ΔOm14 and a phenotypic assessment of the strains

Following a successful mitoprep, steady state level protein analysis using immunoblotting were conducted to confirm the delta strains used in this report. The delta strains were observed to be knocked out for their respective proteins (figure 20) with Hsp70 included as a loading control. To see if either Om45 and Om14 had an effect on growth of the yeast cells, a spot test assay was

conducted in both fermentative and respiratory conditions. No great difference between the strains was observed for any dilution in either condition (figure 21).

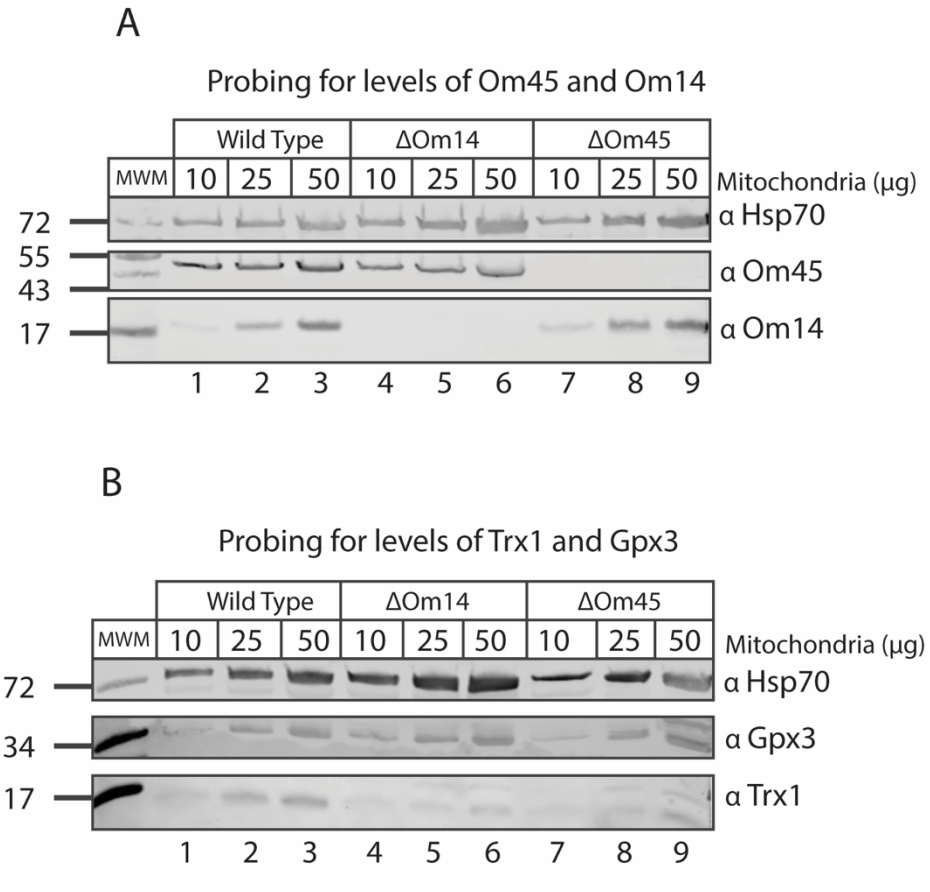

Figure 20: Steady state levels of (A) Om45 and Om14 and (B) Gpx3 and Trx1 in ΔOm45 and ΔOm14 strains compared to wild type mitochondria. Three different quantities of mitochondria were loaded, 10µg, 25µg and 50µg with Hsp70 included as a loading control.

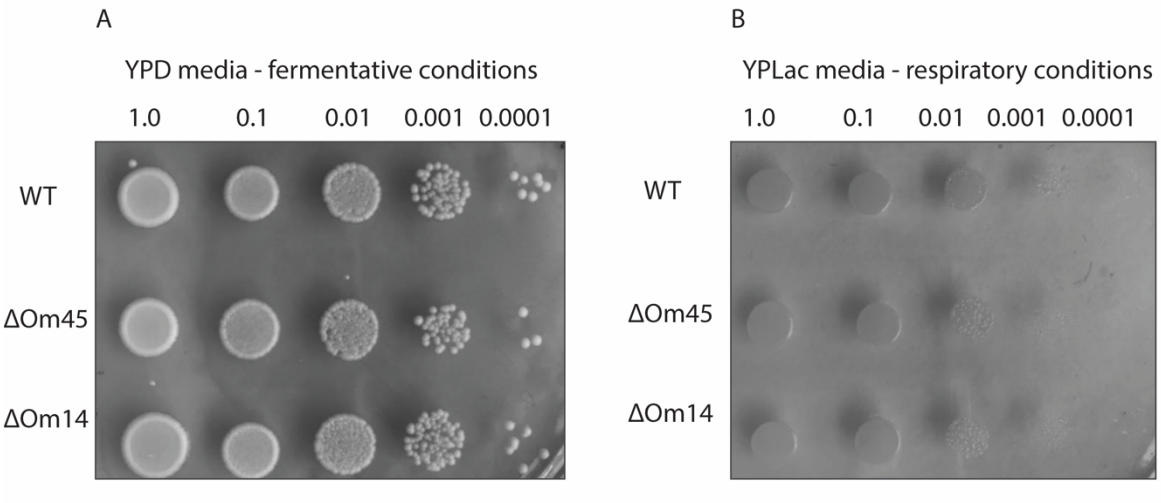

Figure 21: Spot test assay of ΔOm45 and ΔOm14 yeast strains compared to a wild type yeast strain, grown on (A) YPD media (fermentative conditions) or (B) YPLac media (respiratory conditions). Four different serial dilutions from a stock of 0.1OD units (left to right) were made and pipetted onto the respective plates for each yeast strain. The plates were placed in a 30°C incubator and checked after 24 hours.

6.5 Import of Gpx3 into ΔOm14 mitochondria with Su9-DHFR, AAC and Tim10 as controls

The import of Gpx3 does not appear greatly affected in ΔOm14 mitochondria compared to WT mitochondria (figure 22 A-B). Controls for this experiment included proteins that are present in the matrix (Su9-DHFR), the IMM (AAC) and the IMS (Tim10). The import of Su9-DHFR appears slightly decreased in ΔOm14 mitochondria when compared to wild type (lanes 2-4 vs lanes 8-10, figure 22C). The import of AAC does not appear to be affected between the different mitochondria (lanes 2-4 vs lanes 7-9, figure 22D). However, the import of Tim10 does appear to be reduced when comparing wild type and ΔOm14 mitochondria (lanes 2-5 vs lanes 7-10, figure 22E).

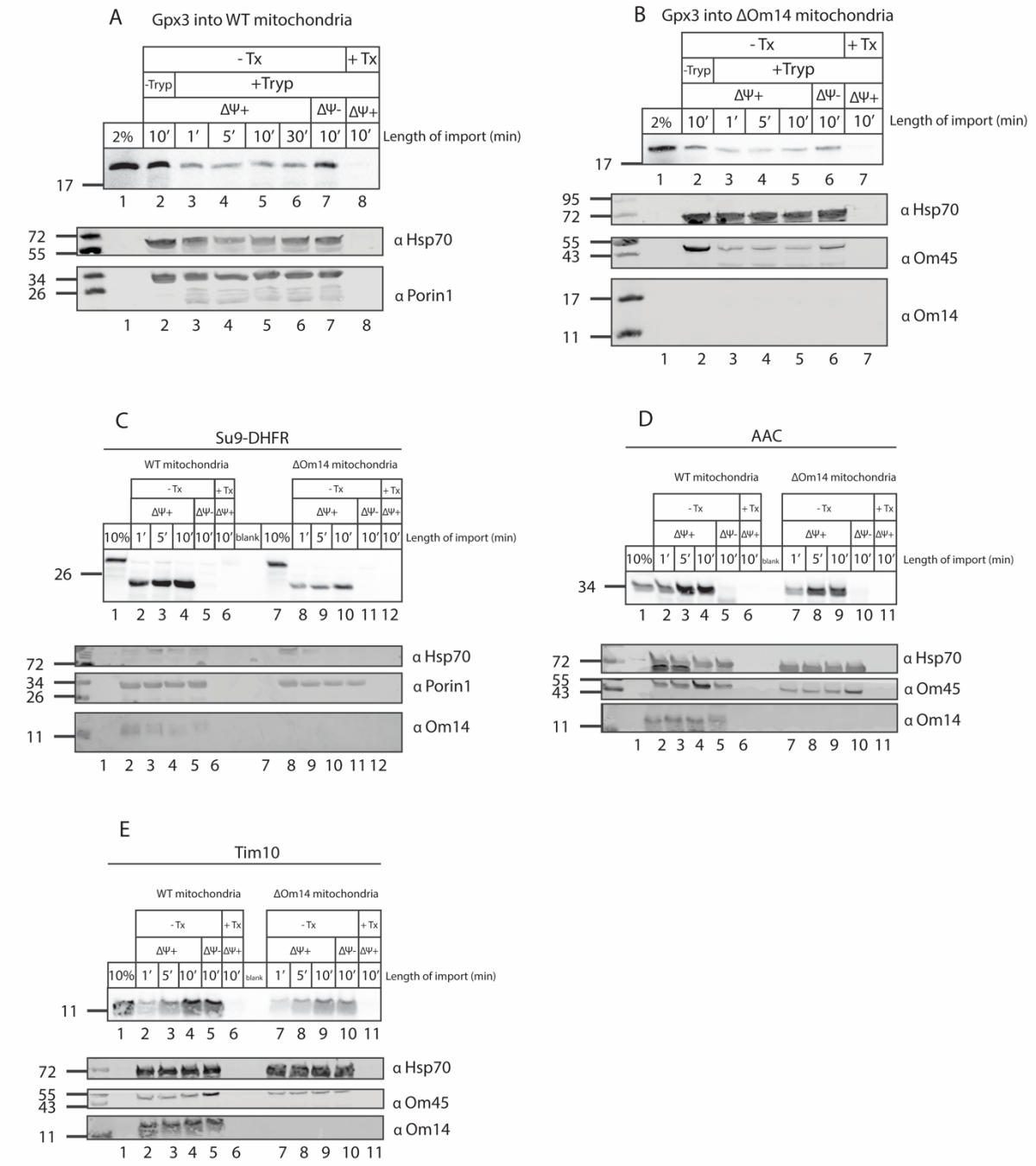

Figure 22: Imports of radiolabelled (A-B) Gpx3, (C) Su9-DHFR, (D) ATP-ADP carrier (AAC) and (E) Tim10 into wild type and ΔOm14 mitochondria. Lane 1 is a control for the TNT translation reaction, displaying 2% or 10% of total radiolabelled protein present in each condition. Proteins are imported with and without a membrane potential (ΔΨ) and with trypsin or trypsin and Triton-X (Triton-X solubilises the mitochondria and therefore is a negative control). The loading controls Hsp70 and Porin1 were used to observe mitochondria protein loaded in each lane, additional western blot controls include probing for Om45 and Om14 to check their levels.

6.6 Import of Gpx3 into ΔOm45 mitochondria with Su9-DHFR, AAC and Tim10 as controls

Import of Gpx3 remains unchanged between wild type and ΔOm45 mitochondria (lanes 2-5 vs lanes 8-11, figure 23A) as does the import of Su9-DHFR (lanes 2-4 vs lane 8-10, figure 23B). In contrast, both the import of AAC (lanes 2-4 vs lanes 7-9, figure 23C) and Tim10 (lanes 2-5 vs lanes 8-11, figure 23D) appear reduced in ΔOm45 mitochondria.

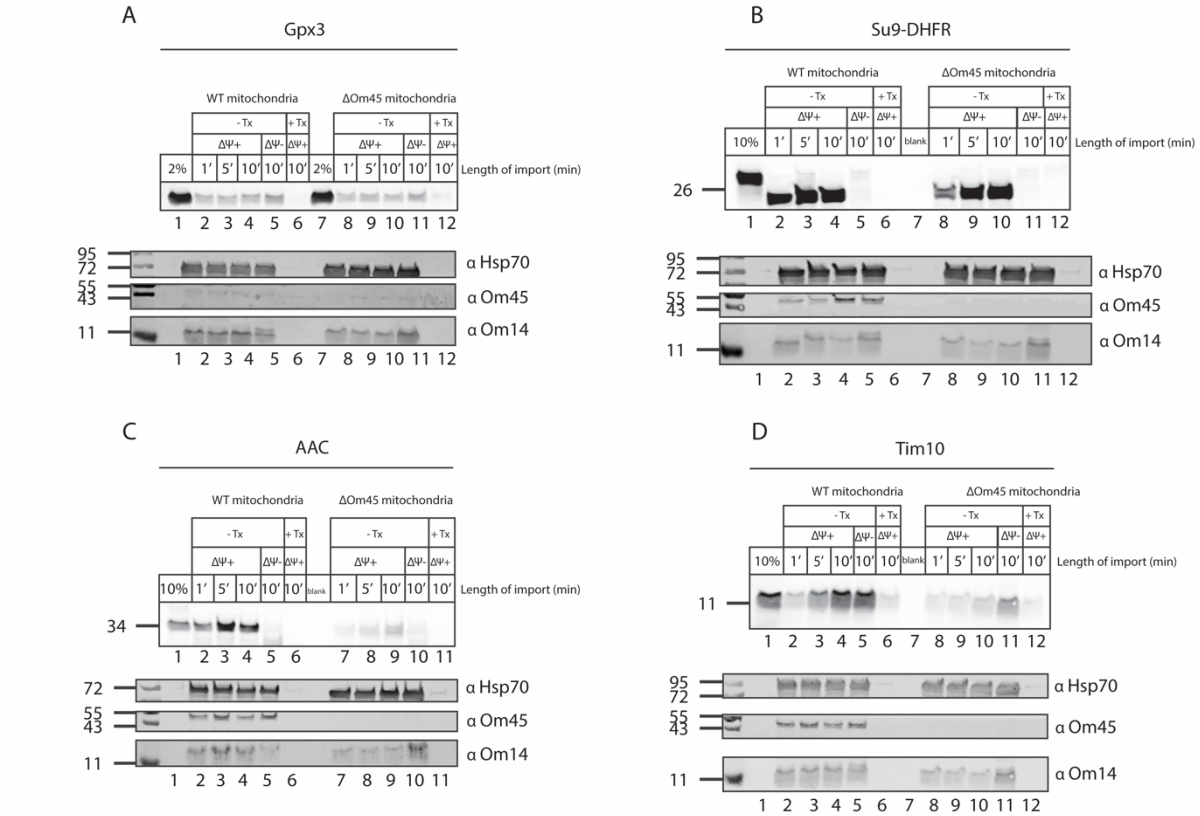

Figure 23: Imports of radiolabelled (A) Gpx3, (B) Su9-DHFR, (C) ATP-ADP carrier (AAC) and (D) Tim10 into wild type and ΔOm45 mitochondria. Lane 1 is a control for the TNT translation reaction, displaying 2% or 10% of total radiolabelled protein present in each condition. Proteins are imported with and without a membrane potential (ΔΨ) and with trypsin or trypsin and Triton-X (Triton-X solubilises the mitochondria and is therefore a negative control). The loading controls Hsp70 and Porin1 were used to observe mitochondria protein loaded in each lane, additional western blot controls include probing for Om45 and Om14 to check their levels.

6.7 Investigating the import of Gpx3 into glucose grown mitochondria

As mentioned in the introduction, mitochondria were grown on glucose as the levels of both Om45 and Om14 have previously been reported to decrease when cells were grown on glucose (Burri *et al.*, 2006; Bruckmann *et al.*, 2009). It was observed that when probing for Om45 and Om14, the levels appear reduced when comparing wild type and glucose grown mitochondria (figure 24).

Import of Gpx3 appears unaffected between wild type and glucose grown mitochondria (lanes 2-5 vs lanes 8-11, figure 25A). The import of Su9-DHFR appears slightly increased when comparing lanes 2-4 of figure 25 B-C. Lastly, the import of both AAC (lanes 2-4 vs lanes 8-10, figure 25D) and Tim10 (lanes 2-5 vs lanes 8-11, figure 25E) do not appear affected comparing wild type and glucose grown mitochondria.

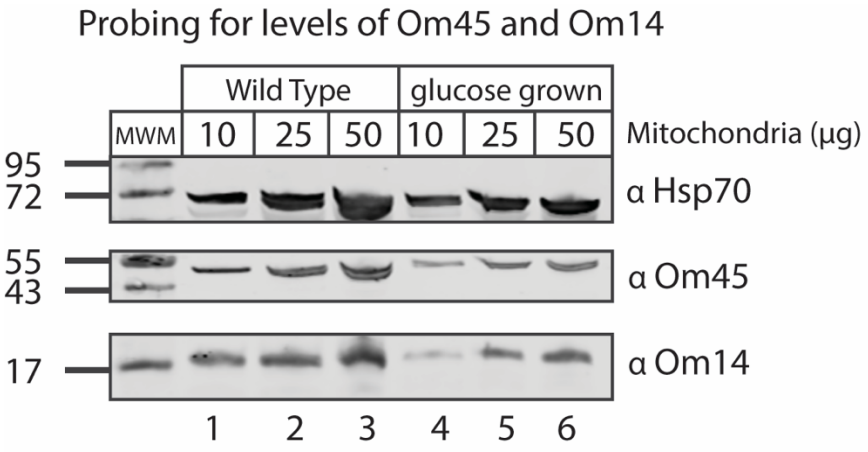

Figure 24: Steady state levels of Om45 and Om14 in wild type and glucose grown mitochondria. Three different amounts of mitochondria were loaded, 10µg, 25µg and 50µg with Hsp70 included as a loading control.

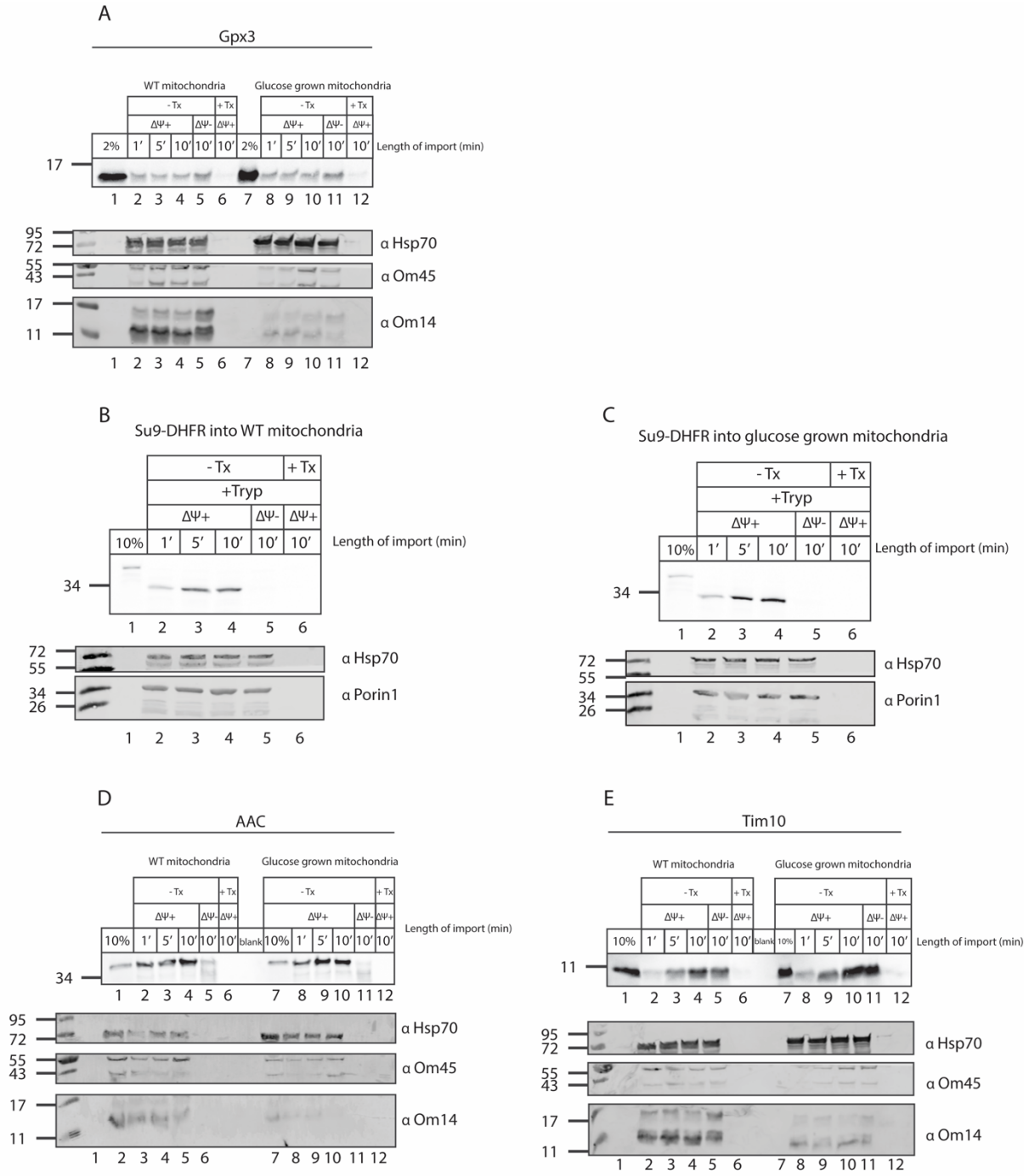

Figure 25: Imports of radiolabelled (A) Gpx3, (B-C) Su9-DHFR, (d) ATP-ADP carrier (AAC) and (E) Tim10 into wild type and glucose grown mitochondria. Lane 1 is a control for the TNT translation reaction, displaying 2% or 10% of total radiolabelled protein present in each condition. Proteins are imported with and without a membrane potential (ΔΨ) and with trypsin or trypsin and Triton-X (Triton-X solubilises the mitochondria and therefore is a negative control). The loading controls Hsp70 and Porin1 were used to observe mitochondria protein loaded in each lane, additional western blot controls include probing for Om45 and Om14 to check their levels.

6.8 Discussion

The aim of this chapter was to try and investigate components of the import pathway of Gpx3. Firstly, a localisation was conducted to confirm the presence of the non-extended Gpx3 in the IMS. A stronger band would perhaps have been expected in the $NaCO_3$ extraction supernatant (lane 9, figure 18) as Gpx3 is a soluble protein. Additionally, the Western blot probe for aconitase appears to have leaked into neighbouring wells and probing for Tom40 (an integral OMM protein) identified its presence in the mitoplasting -PK pellet fraction (lane 6, figure 18). Mitoplasting ruptures the OMM but does not destroy it which could account for the presence of Tom40 here. The last control probed for was Erv1, a soluble IMS protein, and as Erv1 is soluble it would be expected to observe bands in the supernatant fractions. This is the case in the $NaCO_3$ extraction supernatant fraction (lane 9, figure 18) however the Erv1 bands in the pellet fractions (lanes 6, 8 and 10, figure 18) are more predominant. This observation that Erv1 is found mainly in the pellet fractions could be because Erv1 is binding IMM tethered Mia40 but this does not account for the band still present upon addition of PK. Overall, due to inconsistencies with the Western blot probing controls this experiment should be repeated. An interesting experiment would have been to conduct a localisation with hydrogen peroxide stressed mitochondria to investigate if a stronger band is seen in the $NaCO_3$ extraction supernatant fraction: current literature has reported that Gpx3 is an IMS soluble protein (Vögtle *et al.,* 2012; Kritsiligkou *et al.,* 2017).

Next, the same denaturing and/or reducing experiments that were conducted for Trx1 were carried out with Gpx3. Just as was observed Trx1, no difference in import between the four conditions was observed (figure 19). Similar to Trx1, Gpx3 is a relatively small protein (~18kDa) and therefore denaturing is unlikely to have an impact on import which is indeed what is observed (figure 19B and D). Additionally, as the redox active cysteines are not required for import, reducing conditions are unlikely to have an effect which is also observed (figure 19C and D). Overall, denaturing and/or reducing conditions have no effect on the import of Gpx3 however in all cases, import in ΔΨ- conditions appears to be greater than ΔΨ+ conditions. This is strange as a decrease in membrane potential has not previously been reported to affect Gpx3 import, however, N18 Gpx3 import into mitochondria is increased upon H_20_2 stress (Kritsiligkou *et al.,* 2017). Perhaps a decrease in membrane potential, which ultimately stresses

mitochondria, is somehow increasing the import of the non-extended form of Gpx3 into mitochondria. A future experiment could be to conduct a CCCP titration with Gpx3, as was done for Trx1 (figure 8), investigating both the extended and non-extended forms of the protein for any differences. Although no effect was seen for Trx1, it would be interesting to carry out this titration with a greater range of CCCP concentrations and see if the same was observed for Gpx3 or at what concentration this increase in import is observed.

The rest of this chapter focuses on the proteins Om14 and Om45, the latter of which has an unknown function other than participating in a complex with Porin1, and more recently as an interactor of the OMM protein Mcp3, a high-copy suppressor of loss of ER-mitochondria encounter structure (ERMES) (Lauffer *et al.*, 2012; Sinzel, Zeitler and Dimmer, 2018). Firstly, delta strains were prepared by mitopreps and steady states conducted to check that the strains were delta, which was the case (figure 20A). Additionally, the levels of Gpx3 and Trx1 were probed for via Western blot and the level of Gpx3 appears unaffected between WT, ΔOm14 and ΔOm45 mitochondria. Although, a slight reduction in the level of Trx1 was observed when comparing the delta strains to WT mitochondria (figure 20B). However, due to the high homology between Trx1 and Trx2, the antibody used to probe for Trx1 is not just specific for Trx1 and may be detecting levels of Trx2 as well. Furthermore, additional repeats of both steady state Western blots are required to carry out a semi-quantitative analysis of the level of reduction of any proteins. It would also have been interesting to carry out additional steady states, probing for a greater range of proteins in different mitochondrial subcompartments such as Su9, AAC, Tim9 or Tim10 and an OMM protein such as Tom40 or Sam50 to see if any of their levels are affected in the delta strains. In conclusion, the delta strains used in this report are indeed reduced in the level of their respective protein and in both delta strains a decrease in the level of Trx1 is observed.

A spot test assay in respiratory and fermentative conditions was conducted to see if there were any obvious growth defects of the delta strain yeast cells (figure 21). Comparing the delta strains to the WT yeast strain, there is no difference between growth. This is in agreement with previous studies that also observed no obvious growth defect in Om14 or Om45 mutant strains (Yaffes, Jensenp and Guido, 1989; Lesnik *et al.*, 2014). It would have been interesting to

try additional conditions of spot test assay such as including hydrogen peroxide to stress the mitochondria and observe growth. Overall, there is no difference between the mutant strains and WT between the two conditions on growth.

A delta Om14 yeast strain was used to investigate the effect of this protein on the import of Gpx3. No obvious difference was observed for the import of Gpx3 between ΔOm14 and WT mitochondria (figure 22A-B). However, as the import was not conducted on the same gel, this would need to be repeated for a more accurate comparison of the import between the WT and mutant strain. The way imports are conducted in the lab through the RRL system is post-translationally and as Om14 is a receptor for cytosolic ribosomes, Om14 is involved in co-translational import (Lesnik *et al.,* 2014). This may explain why there is no effect on import of Gpx3 in ΔOm14 mitochondria. In comparison, the import of Su9-DHFR appears to decrease in ΔOm14 mitochondria when compared to WT (figure 22C). The import of AAC appears unaffected between the different mitochondria which is surprising considering that the import of Tim10 appears decreased (figure 22D and E). Tim10 is involved in the import pathway of AAC, functioning as part of a chaperone complex with Tim9 when AAC is passing through the IMS, ad aiding in the transfer of AAC to the TIM22 complex (Koehler *et al.,* 1998; Rehling *et al.,* 2003; Vasiljev *et al.,* 2004; Webb *et al.,* 2006). Therefore, it would be expected that when a decrease in the import of Tim10 is observed, the import of AAC would also be negatively affected. It would be interesting to carry out an import of Tim9 into ΔOm14 and WT mitochondria to see if the same decrease observed for Tim10 is also seen for Tim9. These imports would need to be repeated multiple times for quantification to be sure of any effect seen.

Om14 has previously been reported as a receptor for NAC, as discussed in the introduction to this chapter, with ΔOm14 showing a decrease in import efficiency. This decrease was observed particularly for the co-translated protein Mdh1 where import was decreased in ΔOm14 mitochondria. A reduction in protein import was also observed for Su9-DHFR with the authors concluding that Om14 contributes to co-translational import into yeast mitochondria (Lesnik *et al.,* 2014). This decrease in the import of Su9-DHFR is in agreement with the result presented in figure 22C. Additionally, an effort was made to clone Mdh1 into pSP64 for import experiments to try and replicate the results by Lesnik *et*

al, however in the time frame the attempt was unsuccessful. It would have been interesting to conduct an import experiment with Mdh1 into WT and ΔOm14 mitochondria and observe any difference. In conclusion, between ΔOm14 and WT mitochondria the import of Gpx3 and AAC remained unchanged (figure 22A, B and D), the import of Su9-DHFR was increased (figure 22C) and the import of Tim10 was decreased (figure 22E). However, replicates of all these imports would need to be conducted.

Next, the import of Gpx3, Su9-DHFR, AAC and Tim10 were conducted with a ΔOm45 yeast strain. No difference was observed in the import of Gpx3 between the WT and ΔOm45 mitochondria (figure 23A), as was observed with ΔOm14 mitochondria. The import of Su9-DHFR was also unaffected between the different mitochondria (figure 23B). Interestingly, the import of both AAC and Tim10 were decreased in ΔOm45 mitochondria in comparison to WT (figure 23C-D). Unlike what was observed in imports with ΔOm14 mitochondria where there was a decrease in the import of Tim10 but not AAC (figure 22D-E), a decrease in the imports of Tim10 and AAC were observed (figure 23C-D). This decrease in both AAC and Tim10 import is more logical as AAC is reliant on Tim10 as part of its import pathway into the IMM, and therefore any decrease in Tim10 would likely have an effect on AAC. Likewise, with ΔOm14 it would be interesting to carry out an import with Tim9 and see if a similar decrease is seen. In conclusion, the import of AAC and Su9-DHFR is unaffected in ΔOm45 mitochondria (figure 23A-B), whilst the import of AAC and Tim10 is decreased in ΔOm45 mitochondria (figure 23C-D).

The aim of using the glucose grown mitochondria was to have a system where both the levels of Om45 and Om14 were reduced, as previously reported when yeast were grown on glucose (Burri *et al.*, 2006). From a steady state Western blot, a difference in levels of Om45 and Om14 was observed between WT and glucose grown mitochondria, although this steady state experiment should be carried out in triplicate in order for quantification (figure 24). After it was confirmed that there was a difference in levels of Om14 and Om45, import experiments were conducted. No difference in import was observed for Gpx3, AAC or Tim10 into glucose grown mitochondria when compared to WT (figure 25A, D, E). Finally, a slight increase in the import of Su9-DHFR was observed between the two mitochondria however this experiment should be repeated and

samples run on the same gel for a more accurate comparison (figure 25B-C). The glucose grown mitochondria, in addition to having reduced levels of levels of Om45 and Om14, have altered levels of other genes and therefore there may be other factors involved (Burri *et al.*, 2006; Bruckmann *et al.*, 2009). As neither Om14 or Om45 are essential, it would have been interesting to test a double mutant of the two proteins and carry out quantitative proteomics on all mutants to see if any proteins are up/down regulated when two of the most abundant OMM proteins are not present.

Overall, as there was no difference in the import of Gpx3 with either of the delta strains or the glucose grown mitochondria, it is therefore unlikely that either Om45 or Om14 have a role in the import of Gpx3. No clear function of Om45 has been identified, however as it has been shown to participate in a complex with Porin1 and Om14 it would be interesting to carry out mutagenesis experiments (Lauffer *et al.*, 2012). These mutagenesis experiments with Om45 could involve removing the bulky IMS domain completely and to different degrees: and subsequent investigation of any effects on mitochondria in case Om45 has a potential function in plugging Porin1.

Chapter 7: Use of truncated Gpx3 mRNA to investigate co-translational import

7.1 Introduction – background to the use of ribosome-stalled RNA

As mentioned briefly in the previous chapter, the manner imports are conducted in the RRL system is that the protein is imported in a post-translational manner. This led to the use of ribosome stalled Gpx3 RNA to provide a co-translational system for the investigation of the import of Gpx3 into Om14, which has been previously reported to have a role in co-translational import (Lesnik *et al.*, 2014) (figure 26). RNA was generated as described in the materials and methods section 3.2.1.3, Gpx3 was forced to stay attached in the ribosome by removal of its stop codon using a reverse primer to generate stalled ribosome/nascent chain complexes.

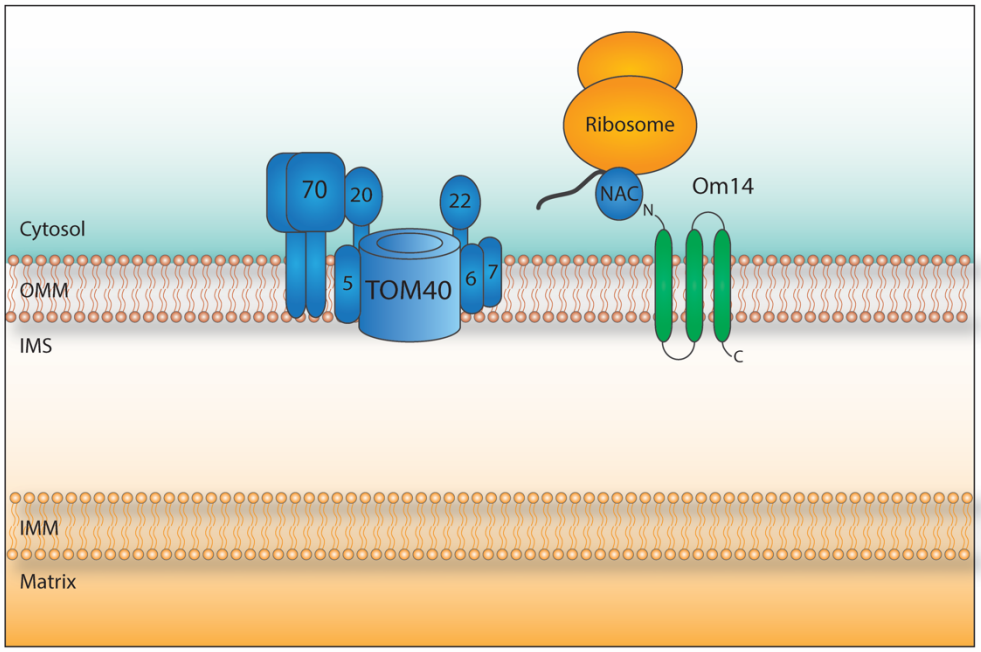

Figure 26: Diagram of Om14 mediated co-translational import with Om14 interacting with the nascent chain-associated complex (NAC). Adapted from Lesnick *et al.*, 2014.

7.2 Optimising conditions for the import of ribosome stalled Gpx3

Before import experiments were conducted with ΔOm14 and ΔOm45 mitochondria on the Gpx3 ribosome-stalled RNA, the conditions of the import

were investigated (figure 27). Between lanes 1-3 (no spin) and lanes 4-6 (116,717g spin for 15 minutes), the Gpx3 protein bands appear fainter with both conditions having bands at ~15kDa which could be a partial translation product or radiolabelled tRNA. In the third condition (189,062g 30 minute spin with a 30% sucrose gradient), the bands appear the most clear with no bands present at ~15kDa. Overall, this result indicates that the third condition, the 30-minute spin at 189,062g with a 30% sucrose gradient, provides the clearest result and this condition will be used for the following import experiments.

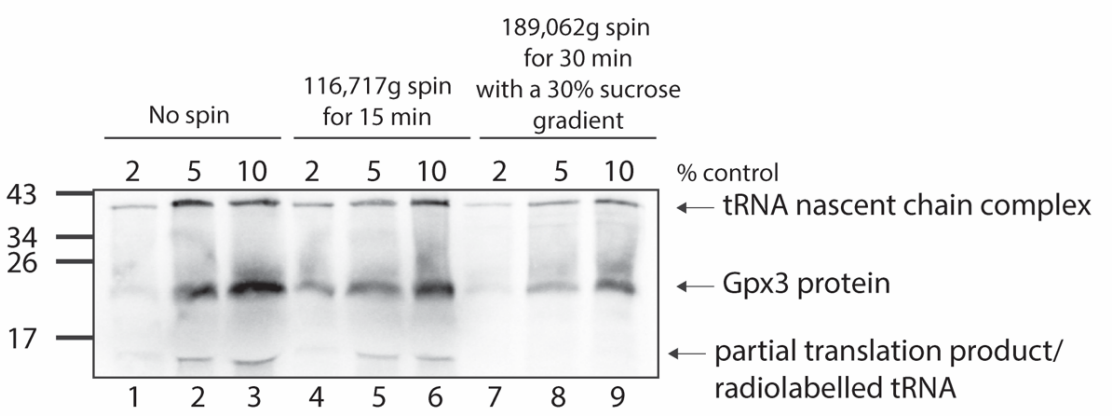

Figure 27: Different percentage (2%, 5% and 10%) controls of a Gpx3 Flexi RRL reaction in three different conditions. The Flexi RRL TNT reaction was incubated for 90 minutes and the pellet fraction resuspended in 2X sample buffer to give either a 2%, 5% or 10% control. Samples in lanes 1-3 have had no additional treatment, lanes 4-5 have undergone centrifugation at 116,717g (55,000 rpm) for 15 minutes and samples in lanes 7-8, samples have been centrifuged at 189,0662g (70,000 rpm) for 30 minutes in a 30% sucrose gradient. All centrifugation steps were conducted at 4°C.

7.3 Import experiments into ΔOm14 and ΔOm45 mitochondria with ribosome stalled Gpx3

Following the results gathered from figure 27, ribosome-stalled Gpx3 used in import experiments with ΔOm14 (figure 28A) and ΔOm45 mitochondria (figure 28B). There appears to be no difference in import between WT and ΔOm14 mitochondria (figure 28A). However, a slight increase in import was observed between WT and ΔOm45 mitochondria (figure 28B).

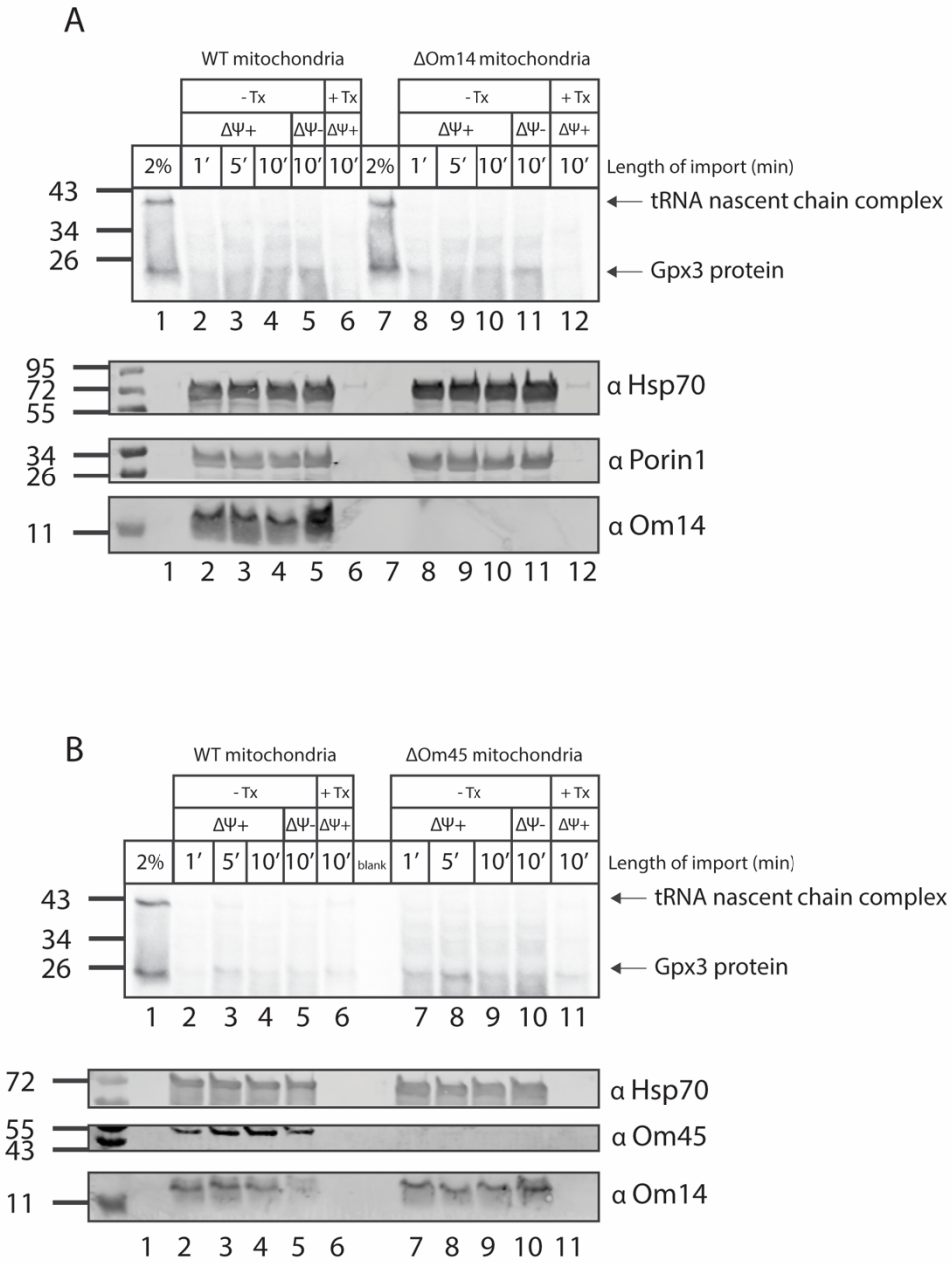

Figure 28: Import of radiolabelled, ribosome-stalled Gpx3 using the Flexi RRL system into (A) ΔOm14 and (B) ΔOm45 mitochondria. Lane 1 (and lane 7 of B) is a control for the TNT translation reaction, displaying 2% of total radiolabelled protein present in each condition. Proteins are imported with and without a membrane potential (ΔΨ) and with trypsin or trypsin and Triton-X (Triton-X solubilises the mitochondria and therefore is a negative control). The loading control Hsp70 was used to observe mitochondria protein loaded in each lane, additional western blot controls include probing for Om45 and Om14 to check levels.

7.4 Discussion

The aim of this chapter was to use ribosome-stalled Gpx3 to investigate Om14 and Om45 in a more co-translational manner using the Flexi RRL, in comparison to the post-translational manner of import with the RRL. Firstly, the TNT conditions were optimised with the clearest band observed at the highest speed spin (70,000 rpm) with a 30% sucrose gradient (figure 27). Once this had been established, imports were conducted with Gpx3 ribosome stalled RNA using WT, ΔOm14 and ΔOm45 mitochondria (figure 28). With the ΔOm14 mitochondria, no difference was observed in comparison with WT mitochondria (figure 28A). This supports data seen in the previous chapter where under post-translational conditions, there was no change in the import of Gpx3 synthesised in the RRL system between ΔOm14 and WT mitochondria (figure 22A-B). However, with ΔOm45 mitochondria, an increase in import was observed in comparison to WT (figure 28B) which is in disagreement with the post-translational import of Gpx3 where no difference in import was observed between WT and ΔOm45 mitochondria (figure 23A). This result indicates that Om45 may play a role in the import of Gpx3 by modulating the co-translational mode of import rather than the post-translational mode. Om45 may have a role in limiting the import of Gpx3 into mitochondria, as Gpx3 has an influence on the redox state of the IMS. In conclusion, both these import experiments should be repeated multiple times to allow for a quantification of any differences between mutants in comparison to the WT.

This method of using stalled ribosome nascent chain complexes (RNCs) to investigate the role of Om14 has been previously utilised by Lesnik *et al.,* 2015. The method they reported for the generation of RNCs was the same as the one used in this report and a sucrose cushion used in the centrifugation step was of a similar composition (Lesnik *et al.,* 2014). The paper investigated the protein malate dehydrogenase 1 (Mdh1) which catalyses the reversible oxidation of malate to oxaloacetate in post-translational imports and an import using RNCs (McAlister-Henn and Thompson, 1987). In co-translational import conditions (RNCs with purified mitochondria), the import of MDH1 is decreased. Although the authors report that Om14 is a mitochondrial receptor for cytosolic ribosomes though interacting with the NAC, this interaction is not detailed. The authors speculate that this interaction may occur directly through the cytoplasmic

domains of Om14 or Om14 may require an additional protein to stabilise the interaction with NAC (Lesnik *et al.*, 2014). A future experiment could be to carry out the import of Mdh1 RNCs into ΔOm14 and ΔOm45 mitochondria to see if the same observation as Lesnik *et al.*, can be made.

There are multiple improvements that could have been made to the experiments carried out in figure 28. In addition to carrying out imports with ribosome stalled Mdh1 and Su9-DHFR, EDTA could have been included to disassemble ribosomes as a further control. Overall, the aim of this chapter was to investigate whether Gpx3 is imported into cells in an intact state or if it is imported in co-translationally, the results presented in this chapter suggest that Gpx3 is not imported co-translationally however further repeats are required for certainty.

Chapter 8: General discussion, conclusions and future work

8.1 General thoughts

Due to restrictions in place during the practical lab time of this report, time constraints had a major impact on the collection of results and the ability to conduct repeats. During the months of January to early April, practical lab work could not be conducted due to the pandemic lockdown.

The redox state of the IMS is crucial as the major import pathway into this sub compartment, the MIA pathway, is subject to redox regulation. Therefore, the presence of the oxidase Gpx3 and the reductase Trx1 in the IMS raises questions about the fine-tuning of the redox state. Although the oxidised form of Mia40 is the active form, previous research has detailed that Mia40 is present in a semi-oxidised state. This could be indicative of a reductive presence in the IMS, as unlike other locations of disulfide bond formation (the ER and the periplasm), no reducing capacity has been described here. The import pathways of Gpx3 and Trx1 remain unknown and the overall aim of this report was to further understanding of these import pathways into mitochondria.

8.2 Investigating components of the import of Trx1 – conclusions and future work

The aim of chapter 4 was to investigate components of the import pathway of Trx1, first identified in the IMS in 2012 (Vögtle *et al.,* 2012). It was found that the import of Trx1 does not appear to require cysteines or depend on the MIA pathway. If time had permitted, it would have been interesting to repeat the pull-down experiment with solubilised mitochondria and purified Trx1. If any additional bands had appeared, it would have been suggestive of any interactors with Trx1. Additionally, if time had permitted if would have been interesting to create mitochondrial OMM vesicles to investigate import components and requirements of Trx1. The OMM vesicles would have allowed different components of import machinery to be present on the membrane of the vesicle, or for different components to be encapsulated. Thereby allowing the minimum/required requirements of the import pathway to be observed. Another future experiment could involve interactions studies between Mia40 and Trx1,

and even perhaps between Gpx3 and Trx1. If an interaction between either Mia40 and Gpx3 was observed, this would provide further evidence that Trx1 has a role in helping maintaining the redox balance of the IMS. Lastly, it would have been interesting to carry out more experiments with Trr1 as no other protein has been identified that reduces Trx1 back to its reduced and active form. Overall, this chapter concluded that the cysteines of Trx1, components of the MIA pathway and denaturing and/or reducing conditions have no effect on the import of Trx1 in the IMS.

8.3 Optimising the import protocol of Trx1 – conclusions and future work

Following a decline in the quality of import in the previous chapter, focus shifted towards investigating if the import protocol could be improved. One of the goals was to investigate the multiple banding pattern in the TNT reaction, the weakest of which appeared to be the band that was imported. A future experiment to investigate this multiple banding pattern would be to send the samples for mass spectrometry to determine what those additional bands are. Additionally, the other methionine residues in Trx1 could be mutated to see if there is an effect on the TNT reaction. Reducing and/or denaturing conditions also had no effect on the import of Trx1, and the purified protein was unable to be imported. Overall, the quality of import of Trx1 could not be improved, however the future experiments mentioned above may have an effect.

8.4 Investigating components of the import of Gpx3

The aim of chapter 6 was to investigate the import pathway of Gpx3, with focus shifting to the abundant OMM proteins, Om45 and Om14. Imports with either delta strain had no effect on the import of Gpx3, with Su9 import decreasing in ΔOm14, AAC import decreasing in ΔOm45 and Tim10 decreasing in both. All these imports should be repeated to confirm the effects observed, and any differences quantified. As both Om45 and Om14 are non-essential, it would be interesting to obtain a double mutant and conduct import experiments with both the proteins not present. To reduce the levels of Om14 and Om45 the cells were grown on glucose, however no effect on the import of Gpx3, AAC and Tim10 was observed with the import of Su9 appearing slightly increased. A further

experiment with the delta strains could be to conduct quantitative proteomics to see if the levels of any proteins are affected when the two most abundant OMM proteins are not present. A blue native PAGE (BN-PAGE) could also be conducted to see if there is any difference in complex formation between ΔOm14 and ΔOm45. Additionally, as the function of Om45 is yet to be determined, mutagenesis experiments could be conducted on the protein. This could involve mutating the large bulky IMS domain of the protein, both to completely remove it and to remove it to varying degrees. Mutagenesis experiments could also be conducted to disrupt the formation of the monomeric complex of Om45, Om14 and Porin1, observing any differences in the viability of mitochondria.

In conclusion for this chapter the following had no effect on the import of Gpx3; denaturing/reducing conditions, the delta strains ΔOm14 and ΔOm45, and a reduction in the levels of Om14 and Om45 through glucose grown mitochondria. It is therefore unlikely that Om14 and/or Om45 have a role in the import of Gpx3 but it would be interesting to see the results of the experiments mentioned above.

8.5 Use of ribosome-stalled Gpx3 RNA to investigate import

Due to the post-translational manner of RRL imports, and the role of Om14 in co-translational import, ribosome-stalled Gpx3 was created to investigate import in a co-translational manner. Whilst no effect on the import of Gpx3 was observed in ΔOm14, curiously an increase in import was seen in ΔOm45 mitochondria and this result should be repeated to be certain. Further studies could involve investigating the role of GTP hydrolysis rather than ATP hydrolysis, as GTP is the energy source for the binding of an amino bound tRNA to the A site of the ribosome (Maracci *et al.*, 2014) that could therefore be used to power protein import, and would indicate a co-translational mode of import. Future experiments would involve repeating the import of ribosome stalled Gpx3 into ΔOm14 and ΔOm45 mitochondria as well as importing ribosome stalled Mdh1 into the delta strains to see if a the same result as Lesnik *et al.*, is observed (Lesnik *et al.*, 2014).

8.6 Closing remarks

To conclude, whilst the import mechanism of Trx1 and Gpx3 remain to be fully elucidated, this report has identified components and parameters which were found to have no effect and can be excluded. Some of these include denaturing and/or reducing conditions, different strains of mitochondria and a co-translational import environment. Additionally, whilst the import of Trx1 could not be improved, progress was made in terms of trying different conditions. In the future, it will be interesting to further detail the role of Gpx3 and Trx1 in maintaining the balance of the redox state in the IMS which is crucial for overall mitochondria viability.

List of References

Abe, Y. *et al.* (2000) 'Structural basis of presequence recognition by the mitochondrial protein import receptor Tom20', *Cell*. doi: 10.1016/S0092-8674(00)80691-1.

Allen, S. *et al.* (2005) 'Erv1 mediates the Mia40-dependent protein import pathway and provides a functional link to the respiratory chain by shuttling electrons to cytochrome c', *Journal of Molecular Biology*, 353(5), pp. 937–944. doi: 10.1016/j.jmb.2005.08.049.

Backes, S. and Herrmann, J. M. (2017) 'Protein translocation into the intermembrane space and matrix of mitochondria: Mechanisms and driving forces', *Frontiers in Molecular Biosciences*. Frontiers Media S.A., p. 83. doi: 10.3389/fmolb.2017.00083.

Banci, L. *et al.* (2009) 'MIA40 is an oxidoreductase that catalyzes oxidative protein folding in mitochondria', *Nature Structural and Molecular Biology*, 16(2), pp. 198–206. doi: 10.1038/nsmb.1553.

Banci, L. *et al.* (2010) 'Molecular chaperone function of Mia40 triggers consecutive induced folding steps of the substrate in mitochondrial protein import', *Proceedings of the National Academy of Sciences of the United States of America*, 107(47), pp. 20190–20195. doi: 10.1073/pnas.1010095107.

Banci, L. *et al.* (2011) 'Molecular recognition and substrate mimicry drive the electron-transfer process between MIA40 and ALR', *Proceedings of the National Academy of Sciences of the United States of America*, 108(12), pp. 4811–4816. doi: 10.1073/pnas.1014542108.

Banci, L. *et al.* (2013) 'An intrinsically disordered domain has a dual function coupled to compartment-dependent redox control', *Journal of Molecular Biology*, 425(3), pp. 594–608. doi: 10.1016/j.jmb.2012.11.032.

Becker, T. *et al.* (2008) 'Biogenesis of the mitochondrial TOM complex: Mim1 promotes insertion and assembly of signal-anchored receptors', *Journal of Biological Chemistry*, 283(1), pp. 120–127. doi: 10.1074/jbc.M706997200.

Bien, M. *et al.* (2010) 'Mitochondrial Disulfide Bond Formation Is Driven by Intersubunit Electron Transfer in Erv1 and Proofread by Glutathione', *Molecular*

Cell, 37(4), pp. 516–528. doi: 10.1016/j.molcel.2010.01.017.

Bihlmaier, K. *et al.* (2007) 'The disulfide relay system of mitochondria is connected to the respiratory chain', *Journal of Cell Biology*, 179(3), pp. 389–395. doi: 10.1083/jcb.200707123.

Bock, F. J. and Tait, S. W. G. (2020) 'Mitochondria as multifaceted regulators of cell death', *Nature Reviews Molecular Cell Biology*. Nature Research, pp. 85–100. doi: 10.1038/s41580-019-0173-8.

Braun, H. P. and Schmitz, U. K. (1997) 'The mitochondrial processing peptidase', *International Journal of Biochemistry and Cell Biology*, 29(8–9), pp. 1043–1045. doi: 10.1016/S1357-2725(97)00032-0.

Bruckmann, A. *et al.* (2009) 'Proteome analysis of aerobically and anaerobically grown Saccharomyces cerevisiae cells', *Journal of Proteomics*, 71(6), pp. 662–669. doi: 10.1016/J.JPROT.2008.11.012.

Burri, L. *et al.* (2006) 'Integral membrane proteins in the mitochondrial outer membrane of Saccharomyces cerevisiae', *The FEBS Journal*, 273(7), pp. 1507–1515. doi: 10.1111/J.1742-4658.2006.05171.X.

Calabrese, G., Morgan, B. and Riemer, J. (2017) 'Mitochondrial Glutathione: Regulation and Functions', *Antioxidants and Redox Signaling*. Mary Ann Liebert Inc., pp. 1162–1177. doi: 10.1089/ars.2017.7121.

Calvo, S. E. and Mootha, V. K. (2010) 'The mitochondrial proteome and human disease', *Annual Review of Genomics and Human Genetics*. Annual Reviews , pp. 25–44. doi: 10.1146/annurev-genom-082509-141720.

Cardenas-Rodriguez, M. and Tokatlidis, K. (2017) 'Cytosolic redox components regulate protein homeostasis via additional localisation in the mitochondrial intermembrane space', *FEBS Letters*, 591(17), pp. 2661–2670. doi: 10.1002/1873-3468.12766.

Cárdenas Rodríguez, M. (2019) 'Regulation of protein import by a thioredoxin reductive pathway in the intermembrane space of mitochondria'.

Ceh-Pavia, E. *et al.* (2020) 'Redox characterisation of Erv1, a key component for protein import and folding in yeast mitochondria', *The FEBS Journal*, 287(11), pp. 2281–2291. doi: 10.1111/febs.15136.

Chacinska, A. *et al.* (2004) 'Essential role of Mia40 in import and assembly of mitochondrial intermembrane space proteins', *EMBO Journal*, 23(19), pp. 3735–3746. doi: 10.1038/sj.emboj.7600389.

Chacinska, A. *et al.* (2009) 'Importing Mitochondrial Proteins: Machineries and Mechanisms', *Cell*. Cell Press, pp. 628–644. doi: 10.1016/j.cell.2009.08.005.

Chatzi, A. *et al.* (2013) 'Biogenesis of yeast Mia40 - uncoupling folding from import and atypical recognition features', *FEBS Journal*, 280(20), pp. 4960–4969. doi: 10.1111/febs.12482.

Collet, J. F. and Messens, J. (2010) 'Structure, function, and mechanism of thioredoxin proteins', *Antioxidants and Redox Signaling*. Mary Ann Liebert, Inc. 140 Huguenot Street, 3rd Floor New Rochelle, NY 10801 USA , pp. 1205–1216. doi: 10.1089/ars.2010.3114.

Collins, Y. *et al.* (2012) 'Mitochondrial redox signalling at a glance', *Journal of Cell Science*, 125(4), pp. 801–806. doi: 10.1242/jcs.098475.

Cremers, C. M. and Jakob, U. (2013) 'Oxidant sensing by reversible disulfide bond formation', *Journal of Biological Chemistry*. American Society for Biochemistry and Molecular Biology, pp. 26489–26496. doi: 10.1074/jbc.R113.462929.

Curran, S. P. *et al.* (2002) 'The role of the Tim8p-Tim13p complex in a conserved import pathway for mitochondrial polytopic inner membrane proteins', *Journal of Cell Biology*, 158(6), pp. 1017–1027. doi: 10.1083/jcb.200205124.

Curran, S. P. *et al.* (2004) 'The role of Hot13p and redox chemistry in the mitochondrial TIM22 import pathway', *Journal of Biological Chemistry*, 279(42), pp. 43744–43751. doi: 10.1074/jbc.M404878200.

Cvetko, F. *et al.* (2020) 'Nrf2 is activated by disruption of mitochondrial thiol homeostasis but not by enhanced mitochondrial superoxide production', *Journal of Biological Chemistry*, p. jbc.RA120.016551. doi: 10.1074/jbc.ra120.016551.

Dabir, D. V. *et al.* (2007) 'A role for cytochrome c and cytochrome c peroxidase in electron shuttling from Erv1', *EMBO Journal*, 26(23), pp. 4801–4811. doi: 10.1038/sj.emboj.7601909.

Daithankar, V. N., Farrell, S. R. and Thorpe, C. (2009) 'Augmenter of liver regeneration: Substrate specificity of a flavin-dependent oxidoreductase from the mitochondrial intermembrane space', *Biochemistry*, 48(22), pp. 4828–4837. doi: 10.1021/bi900347v.

Delaunay, A. *et al.* (2002) 'A thiol peroxidase is an H2O2 receptor and redox-transducer in gene activation', *Cell*, 111(4), pp. 471–481. doi: 10.1016/S0092-8674(02)01048-6.

Diekert, K. *et al.* (1999) 'An internal targeting signal directing proteins into the mitochondrial intermembrane space', *Proceedings of the National Academy of Sciences of the United States of America*, 96(21), pp. 11752–11757. doi: 10.1073/pnas.96.21.11752.

Diekert, K. *et al.* (2001) 'Apocytochrome c requires the TOM complex for translocation across the mitochondrial outer membrane', *EMBO Journal*, 20(20), pp. 5626–5635. doi: 10.1093/emboj/20.20.5626.

Dumont, M. E. *et al.* (1991) 'Role of cytochrome c heme lyase in mitochondrial import and accumulation of cytochrome c in Saccharomyces cerevisiae.', *Molecular and Cellular Biology*, 11(11), pp. 5487–5496. doi: 10.1128/mcb.11.11.5487.

Edwards, R., Eaglesfield, R. and Tokatlidis, K. (2021) 'The mitochondrial intermembrane space: the most constricted mitochondrial sub-compartment with the largest variety of protein import pathways', *Open biology*, 11(3), p. 210002. doi: 10.1098/rsob.210002.

Edwards, R., Gerlich, S. and Tokatlidis, K. (2020) 'The biogenesis of mitochondrial intermembrane space proteins', *Biological Chemistry*. De Gruyter, pp. 737–747. doi: 10.1515/hsz-2020-0114.

Edwards, R. and Tokatlidis, K. (2019) 'The Yeast Voltage-Dependent Anion Channel Porin: More IMPORTant than Just Metabolite Transport', *Molecular Cell*. Cell Press, pp. 861–862. doi: 10.1016/j.molcel.2019.02.028.

Ellenrieder, L. *et al.* (2019) 'Dual Role of Mitochondrial Porin in Metabolite Transport across the Outer Membrane and Protein Transfer to the Inner Membrane', *Molecular Cell*, 73(5), pp. 1056-1065.e7. doi: 10.1016/j.molcel.2018.12.014.

Erdogan, A. J. *et al.* (2018) 'The mitochondrial oxidoreductase CHCHD4 is present in a semi-oxidized state in vivo', *Redox Biology*, 17, pp. 200–206. doi: 10.1016/j.redox.2018.03.014.

Esaki, M. *et al.* (1999) 'Two distinct mechanisms drive protein translocation across the mitochondrial outer membrane in the late step of the cytochrome b2 import pathway', *Proceedings of the National Academy of Sciences of the United States of America*, 96(21), pp. 11770–11775. doi: 10.1073/pnas.96.21.11770.

Esser, K. *et al.* (2004) 'The mitochondrial IMP peptidase of yeast: Functional analysis of domains and identification of Gut2 as a new natural substrate', *Molecular Genetics and Genomics*, 271(5), pp. 616–626. doi: 10.1007/s00438-004-1011-y.

Fischer, M. and Riemer, J. (2013) 'The mitochondrial disulfide relay system: Roles in oxidative protein folding and beyond', *International Journal of Cell Biology*. Hindawi Publishing Corporation. doi: 10.1155/2013/742923.

Frey, T. G. and Mannella, C. A. (2000) 'The internal structure of mitochondria', *Trends in Biochemical Sciences*. Elsevier Current Trends, pp. 319–324. doi: 10.1016/S0968-0004(00)01609-1.

Gabriel, K. *et al.* (2007) 'Novel Mitochondrial Intermembrane Space Proteins as Substrates of the MIA Import Pathway', *Journal of Molecular Biology*, 365(3), pp. 612–620. doi: 10.1016/j.jmb.2006.10.038.

Geissler, A. *et al.* (2002) 'The mitochondrial presequence translocase: An essential role of Tim50 in directing preproteins to the import channel', *Cell*, 111(4), pp. 507–518. doi: 10.1016/S0092-8674(02)01073-5.

Gerashchenko, M. V., Lobanov, A. V. and Gladyshev, V. N. (2012) 'Genome-wide ribosome profiling reveals complex translational regulation in response to oxidative stress', *Proceedings of the National Academy of Sciences of the United States of America*, 109(43), pp. 17394–17399. doi: 10.1073/pnas.1120799109.

Glick, B. S. *et al.* (1992) 'Cytochromes c1 and b2 are sorted to the intermembrane space of yeast mitochondria by a stop-transfer mechanism', *Cell*. doi: 10.1016/0092-8674(92)90292-K.

Gold, V. A. *et al.* (2017) 'Visualization of cytosolic ribosomes on the surface of mitochondria by electron cryo-tomography', *EMBO reports*, 18(10), pp. 1786–

1800. doi: 10.15252/embr.201744261.

Gomes, F. *et al.* (2017) 'Proteolytic cleavage by the inner membrane peptidase (IMP) complex or Oct1 peptidase controls the localization of the yeast peroxiredoxin Prx1 to distinct mitochondrial compartments', *Journal of Biological Chemistry*, 292(41), pp. 17011–17024. doi: 10.1074/jbc.M117.788588.

Grevel, A., Pfanner, N. and Becker, T. (2019) 'Coupling of import and assembly pathways in mitochondrial protein biogenesis', *Biological Chemistry*, 401(1), pp. 117–129. doi: 10.1515/hsz-2019-0310.

Haas, R. H. (2019) 'Mitochondrial dysfunction in aging and diseases of aging', *Biology*, 8(2). doi: 10.3390/biology8020048.

Habich, M. *et al.* (2019) 'Vectorial Import via a Metastable Disulfide-Linked Complex Allows for a Quality Control Step and Import by the Mitochondrial Disulfide Relay', *Cell Reports*, 26(3), pp. 759-774.e5. doi: 10.1016/j.celrep.2018.12.092.

Habich, M., Salscheider, S. L. and Riemer, J. (2019) 'Cysteine residues in mitochondrial intermembrane space proteins: more than just import', *British Journal of Pharmacology*. John Wiley and Sons Inc., pp. 514–531. doi: 10.1111/bph.14480.

Hangen, E. *et al.* (2015) 'Interaction between AIF and CHCHD4 Regulates Respiratory Chain Biogenesis', *Molecular Cell*, 58(6), pp. 1001–1014. doi: 10.1016/j.molcel.2015.04.020.

Herrmann, J. M. and Hell, K. (2005) 'Chopped, trapped or tacked - Protein translocation into the IMS of mitochondria', *Trends in Biochemical Sciences*. Elsevier Ltd, pp. 205–212. doi: 10.1016/j.tibs.2005.02.005.

Hill, K. *et al.* (1998) 'Tom40 forms the hydrophilic channel of the mitochondrial import pore for preproteins', *Nature*, 395(6701), pp. 516–521. doi: 10.1038/26780.

Hofhaus, G. *et al.* (2003) 'The N-terminal cysteine pair of yeast sulfhydryl oxidase Erv1p is essential for in vivo activity and interacts with the primary redox centre', *European Journal of Biochemistry*, 270(7), pp. 1528–1535. doi: 10.1046/j.1432-1033.2003.03519.x.

Hofmann, S. *et al.* (2005) 'Functional and mutational characterization of human MIA40 acting during import into the mitochondrial intermembrane space', *Journal of Molecular Biology*, 353(3), pp. 517–528. doi: 10.1016/j.jmb.2005.08.064.

Hoppins, S. C. and Nargang, F. E. (2004) 'The Tim8-Tim13 Complex of Neurospora crassa Functions in the Assembly of Proteins into Both Mitochondrial Membranes', *Journal of Biological Chemistry*, 279(13), pp. 12396–12405. doi: 10.1074/jbc.M313037200.

Hu, J., Dong, L. and Outten, C. E. (2008) 'The redox environment in the mitochondrial intermembrane space is maintained separately from the cytosol and matrix', *Journal of Biological Chemistry*, 283(43), pp. 29126–29134. doi: 10.1074/jbc.M803028200.

Hulett, J. M. *et al.* (2008) 'The Transmembrane Segment of Tom20 Is Recognized by Mim1 for Docking to the Mitochondrial TOM Complex', *Journal of Molecular Biology*, 376(3), pp. 694–704. doi: 10.1016/j.jmb.2007.12.021.

Hüttemann, M. *et al.* (2011) 'The multiple functions of cytochrome c and their regulation in life and death decisions of the mammalian cell: From respiration to apoptosis', *Mitochondrion*. Mitochondrion, pp. 369–381. doi: 10.1016/j.mito.2011.01.010.

Hutu, D. P. *et al.* (2008) 'Mitochondrial protein import motor: Differential role of Tim44 in the recruitment of Pam17 and J-complex to the presequence translocase', *Molecular Biology of the Cell*, 19(6), pp. 2642–2649. doi: 10.1091/mbc.E07-12-1226.

Ieva, R. *et al.* (2014) 'Mgr2 functions as lateral gatekeeper for preprotein sorting in the mitochondrial inner membrane', *Molecular Cell*, 56(5), pp. 641–652. doi: 10.1016/j.molcel.2014.10.010.

Kallergi, E. *et al.* (2012) 'Targeting and maturation of Erv1/ALR in the mitochondrial intermembrane space', *ACS Chemical Biology*, 7(4), pp. 707–714. doi: 10.1021/cb200485b.

Kawano, S. *et al.* (2009) 'Structural basis of yeast Tim40/Mia40 as an oxidative translocator in the mitochondrial intermembrane space', *Proceedings of the National Academy of Sciences of the United States of America*, 106(34), pp.

14403–14407. doi: 10.1073/pnas.0901793106.

Koehler, C. M. *et al.* (1998) 'Import of mitochondrial carriers mediated by essential proteins of the intermembrane space', *Science*, 279(5349), pp. 369–373. doi: 10.1126/science.279.5349.369.

Kojer, K. *et al.* (2012) 'Glutathione redox potential in the mitochondrial intermembrane space is linked to the cytosol and impacts the Mia40 redox state', *The EMBO Journal*, 31(14), pp. 3169–3182. doi: 10.1038/emboj.2012.165.

Komiya, T. *et al.* (1998) 'Interaction of mitochondrial targeting signals with acidic receptor domains along the protein import pathway: Evidence for the "acid chain" hypothesis', *EMBO Journal*, 17(14), pp. 3886–3898. doi: 10.1093/emboj/17.14.3886.

Kritsiligkou, P. *et al.* (2017) 'Unconventional Targeting of a Thiol Peroxidase to the Mitochondrial Intermembrane Space Facilitates Oxidative Protein Folding', *Cell Reports*, 18(11), pp. 2729–2741. doi: 10.1016/j.celrep.2017.02.053.

Kuan, J. and Saier, M. H. (2008) 'The Mitochondrial Carrier Family of Transport Proteins: Structural, Functional, and Evolutionary Relationships', *https://doi.org/10.3109/10409239309086795*, 28(3), pp. 209–233. doi: 10.3109/10409239309086795.

Kühlbrandt, W. (2015) 'Structure and function of mitochondrial membrane protein complexes', *BMC Biology*. BioMed Central Ltd., p. 89. doi: 10.1186/s12915-015-0201-x.

Kutik, S. *et al.* (2008) 'Dissecting Membrane Insertion of Mitochondrial ß-Barrel Proteins', *Cell*, 132(6), pp. 1011–1024. doi: 10.1016/j.cell.2008.01.028.

van der Laan, M. *et al.* (2007) 'Motor-free mitochondrial presequence translocase drives membrane integration of preproteins', *Nature Cell Biology*, 9(10), pp. 1152–1159. doi: 10.1038/ncb1635.

Lauffer, S. *et al.* (2012) 'Saccharomyces cerevisiae Porin Pore Forms Complexes with Mitochondrial Outer Membrane Proteins Om14p and Om45p', *The Journal of Biological Chemistry*, 287(21), p. 17447. doi: 10.1074/JBC.M111.328328.

Lesnik, C. *et al.* (2014) 'OM14 is a mitochondrial receptor for cytosolic ribosomes that supports co-translational import into mitochondria', *Nature*

Communications 2014 5:1, 5(1), pp. 1–11. doi: 10.1038/ncomms6711.

Lill, R. *et al.* (1992) 'Import of cytochrome c heme lyase into mitochondria: A novel pathway into the intermembrane space', *EMBO Journal*, 11(2), pp. 449–456. doi: 10.1002/j.1460-2075.1992.tb05074.x.

Lionaki, E. *et al.* (2010) 'The N-terminal Shuttle Domain of Erv1 Determines the Affinity for Mia40 and Mediates Electron Transfer to the Catalytic Erv1 Core in Yeast Mitochondria', *Antioxidants & Redox Signaling*, 13(9), pp. 1327–1339. doi: 10.1089/ars.2010.3200.

Liu, X. *et al.* (1996) 'Induction of apoptotic program in cell-free extracts: Requirement for dATP and cytochrome c', *Cell*, 86(1), pp. 147–157. doi: 10.1016/S0092-8674(00)80085-9.

Lu, H. *et al.* (2004) 'Functional TIM10 Chaperone Assembly Is Redox-regulated in Vivo', *Journal of Biological Chemistry*, 279(18), pp. 18952–18958. doi: 10.1074/jbc.M313045200.

Magnani, N. D. *et al.* (2020) 'Role of Mitochondria in the Redox Signaling Network and Its Outcomes in High Impact Inflammatory Syndromes', *Frontiers in Endocrinology*. Frontiers Media S.A., p. 568305. doi: 10.3389/fendo.2020.568305.

Manganas, P., MacPherson, L. and Tokatlidis, K. (2017) 'Oxidative protein biogenesis and redox regulation in the mitochondrial intermembrane space', *Cell and Tissue Research*. Springer Verlag, pp. 43–57. doi: 10.1007/s00441-016-2488-5.

Mannella, C. A. (2006) 'Structure and dynamics of the mitochondrial inner membrane cristae', *Biochimica et Biophysica Acta - Molecular Cell Research*. Biochim Biophys Acta, pp. 542–548. doi: 10.1016/j.bbamcr.2006.04.006.

Maracci, C. *et al.* (2014) 'Ribosome-induced tuning of GTP hydrolysis by a translational GTPase', *Proceedings of the National Academy of Sciences*, 111(40), pp. 14418–14423. doi: 10.1073/PNAS.1412676111.

McAlister-Henn, L. and Thompson, L. M. (1987) 'Isolation and expression of the gene encoding yeast mitochondrial malate dehydrogenase.', *Journal of Bacteriology*, 169(11), p. 5157. doi: 10.1128/JB.169.11.5157-5166.1987.

Meisinger, C. *et al.* (2004) 'The mitochondrial morphology protein Mdm10 functions in assembly of the preprotein translocase of the outer membrane', *Developmental Cell*, 7(1), pp. 61–71. doi: 10.1016/j.devcel.2004.06.003.

Mesecke, N. *et al.* (2005) 'A disulfide relay system in the intermembrane space of mitochondria that mediates protein import', *Cell*, 121(7), pp. 1059–1069. doi: 10.1016/j.cell.2005.04.011.

Mesecke, N. *et al.* (2008) 'The zinc-binding protein Hot13 promotes oxidation of the mitochondrial import receptor Mia40', *EMBO Reports*, 9(11), pp. 1107–1113. doi: 10.1038/embor.2008.173.

Milenkovic, D. *et al.* (2007) 'Biogenesis of the essential Tim9-Tim10 chaperone complex of mitochondria: Site-specific recognition of cysteine residues by the intermembrane space receptor Mia40', *Journal of Biological Chemistry*, 282(31), pp. 22472–22480. doi: 10.1074/jbc.M703294200.

Milenkovic, D. *et al.* (2009) 'Identification of the signal directing Tim9 and Tim10 into the intermembrane space of mitochondria', *Molecular Biology of the Cell*, 20(10), pp. 2530–2539. doi: 10.1091/mbc.E08-11-1108.

Mokranjac, D. and Neupert, W. (2010) 'The many faces of the mitochondrial TIM23 complex', *Biochimica et Biophysica Acta - Bioenergetics*. Elsevier, pp. 1045–1054. doi: 10.1016/j.bbabio.2010.01.026.

Monzio Compagnoni, G. *et al.* (2020) 'The Role of Mitochondria in Neurodegenerative Diseases: the Lesson from Alzheimer's Disease and Parkinson's Disease', *Molecular Neurobiology*. Springer, pp. 2959–2980. doi: 10.1007/s12035-020-01926-1.

Nakao, L. S. *et al.* (2015) 'Mechanism-based proteomic screening identifies targets of thioredoxin-like proteins', *Journal of Biological Chemistry*, 290(9), pp. 5685–5695. doi: 10.1074/jbc.M114.597245.

Naoé, M. *et al.* (2004) 'Identification of Tim40 that mediates protein sorting to the mitochondrial intermembrane space', *Journal of Biological Chemistry*, 279(46), pp. 47815–47821. doi: 10.1074/jbc.M410272200.

Neal, S. E. *et al.* (2017) 'Osm1 facilitates the transfer of electrons from Erv1 to fumarate in the redox-regulated import pathway in the mitochondrial intermembrane space', *Molecular Biology of the Cell*, 28(21), pp. 2773–2785.

doi: 10.1091/mbc.E16-10-0712.

Nuebel, E., Manganas, P. and Tokatlidis, K. (2016) 'Orphan proteins of unknown function in the mitochondrial intermembrane space proteome: New pathways and metabolic cross-talk', *Biochimica et Biophysica Acta - Molecular Cell Research*. Elsevier B.V., pp. 2613–2623. doi: 10.1016/j.bbamcr.2016.07.004.

Otera, H. *et al.* (2007) 'A novel insertion pathway of mitochondrial outer membrane proteins with multiple transmembrane segments', *Journal of Cell Biology*, 179(7), pp. 1355–1363. doi: 10.1083/jcb.200702143.

Patterson, H. C. *et al.* (2015) 'A respiratory chain controlled signal transduction cascade in the mitochondrial intermembrane space mediates hydrogen peroxide signaling', *Proceedings of the National Academy of Sciences*, 112(42), pp. E5679–E5688. doi: 10.1073/PNAS.1517932112.

Peker, E. *et al.* (2021) 'Erv1 and Cytochrome c Mediate Rapid Electron Transfer via A Collision-Type Interaction', *Journal of Molecular Biology*, 433(15), p. 167045. doi: 10.1016/j.jmb.2021.167045.

Poet, G. J. *et al.* (2017) 'Cytosolic thioredoxin reductase 1 is required for correct disulfide formation in the ER', *The EMBO Journal*, 36(5), pp. 693–702. doi: 10.15252/EMBJ.201695336.

Poyton, R. O. and McEwen, J. E. (1996) 'Crosstalk between nuclear and mitochondrial genomes', *Annual Review of Biochemistry*. Annual Reviews Inc., pp. 563–607. doi: 10.1146/annurev.bi.65.070196.003023.

Rampelt, H. *et al.* (2020) 'The mitochondrial carrier pathway transports non-canonical substrates with an odd number of transmembrane segments', *BMC Biology*, 18(1), p. 2. doi: 10.1186/s12915-019-0733-6.

Rassow, J. *et al.* (1994) 'Mitochondrial protein import: Biochemical and genetic evidence for interaction of matrix hsp70 and the inner membrane protein MIM44', *Journal of Cell Biology*, 127(6 I), pp. 1547–1556. doi: 10.1083/jcb.127.6.1547.

Rath, S. *et al.* (2020) 'MitoCarta3.0: an updated mitochondrial proteome now with sub-organelle localization and pathway annotations', *Nucleic Acids Research*, (1). doi: 10.1093/nar/gkaa1011.

Rehling, P. *et al.* (2003) 'Protein insertion into the mitochondrial inner membrane by a twin-pore translocase', *Science*, 299(5613), pp. 1747–1751. doi: 10.1126/science.1080945.

Reinhardt, C. *et al.* (2020) 'AIF meets the CHCHD4/Mia40-dependent mitochondrial import pathway', *Biochimica et Biophysica Acta - Molecular Basis of Disease*, 1866(6), p. 165746. doi: 10.1016/j.bbadis.2020.165746.

Roise, D. and Schatz, G. (1988) 'Mitochondrial presequences', *Journal of Biological Chemistry*.

Sagan, L. (1967) 'On the origin of mitosing cells', *Journal of Theoretical Biology*, 14(3), pp. 225-IN6. doi: 10.1016/0022-5193(67)90079-3.

Sakaue, H. *et al.* (2019) 'Porin Associates with Tom22 to Regulate the Mitochondrial Protein Gate Assembly', *Molecular Cell*, 73(5), pp. 1044-1055.e8. doi: 10.1016/j.molcel.2019.01.003.

Schendzielorz, A. B. *et al.* (2018) 'Motor recruitment to the TIM23 channel's lateral gate restricts polypeptide release into the inner membrane', *Nature Communications*, 9(1), pp. 1–10. doi: 10.1038/s41467-018-06492-8.

Schieber, M. and Chandel, N. S. (2014) 'ROS function in redox signaling and oxidative stress', *Current Biology*. Cell Press, p. R453. doi: 10.1016/j.cub.2014.03.034.

Schmidt, B. *et al.* (1983) 'Biosynthetic pathway of mitochondrial ATPase subunit 9 in Neurosporacrassa', *The Journal of Cell Biology*, 96(1), p. 248. doi: 10.1083/JCB.96.1.248.

Schmidt, O., Pfanner, N. and Meisinger, C. (2010) 'Mitochondrial protein import: From proteomics to functional mechanisms', *Nature Reviews Molecular Cell Biology*. Nature Publishing Group, pp. 655–667. doi: 10.1038/nrm2959.

Shiota, T. *et al.* (2015) 'Molecular architecture of the active mitochondrial protein gate', *Science*, 349(6255), pp. 1544–1548. doi: 10.1126/science.aac6428.

Sideris, D. P. *et al.* (2009) 'A novel intermembrane space-targeting signal docks cysteines onto Mia40 during mitochondrial oxidative folding', *Journal of Cell Biology*, 187(7), pp. 1007–1022. doi: 10.1083/jcb.200905134.

Sideris, D. P. and Tokatlidis, K. (2007) 'Oxidative folding of small Tims is

mediated by site-specific docking onto Mia40 in the mitochondrial intermembrane space', *Molecular Microbiology*, 65(5), pp. 1360–1373. doi: 10.1111/j.1365-2958.2007.05880.x.

Sinzel, M., Zeitler, A. and Dimmer, K. S. (2018) 'Interaction network of the mitochondrial outer membrane protein Mcp3', *FEBS Letters*, 592(19), pp. 3210–3220. doi: 10.1002/1873-3468.13243.

Skuratovskaia, D. *et al.* (2020) 'Mitochondrial destiny in type 2 diabetes: The effects of oxidative stress on the dynamics and biogenesis of mitochondria', *PeerJ*, 8. doi: 10.7717/peerj.9741.

Spinelli, J. B. and Haigis, M. C. (2018) 'The multifaceted contributions of mitochondria to cellular metabolism', *Nature Cell Biology*. Nature Publishing Group, pp. 745–754. doi: 10.1038/s41556-018-0124-1.

Stehling, O. and Lill, R. (2013) 'The role of mitochondria in cellular iron-sulfur protein biogenesis: Mechanisms, connected processes, and diseases', *Cold Spring Harbor Perspectives in Biology*, 5(8). doi: 10.1101/cshperspect.a011312.

Steiner, H. *et al.* (1995) 'Biogenesis of mitochondrial heme lyases in yeast. Import and folding in the intermembrane space', *Journal of Biological Chemistry*, 270(39), pp. 22842–22849. doi: 10.1074/jbc.270.39.22842.

Stiller, S. B. *et al.* (2016) 'Mitochondrial OXA Translocase Plays a Major Role in Biogenesis of Inner-Membrane Proteins', *Cell Metabolism*, 23(5), pp. 901–908. doi: 10.1016/j.cmet.2016.04.005.

Stojanovski, D. *et al.* (2007) 'Alternative function for the mitochondrial SAM complex in biogenesis of α-helical TOM proteins', *Journal of Cell Biology*, 179(5), pp. 881–893. doi: 10.1083/jcb.200706043.

Stojanovski, D. *et al.* (2008) 'The MIA system for protein import into the mitochondrial intermembrane space', *Biochimica et Biophysica Acta (BBA) - Molecular Cell Research*, 1783(4), pp. 610–617. doi: 10.1016/J.BBAMCR.2007.10.004.

Sztolsztener, M. E. *et al.* (2013) 'Disulfide Bond Formation: Sulfhydryl Oxidase ALR Controls Mitochondrial Biogenesis of Human MIA40', *Traffic*, 14(3), pp. 309–320. doi: 10.1111/tra.12030.

Takeda, H. *et al.* (2021) 'Mitochondrial sorting and assembly machinery operates by ß-barrel switching', *Nature*, 12, pp. 1–7. doi: 10.1038/s41586-020-03113-7.

Tang, X. *et al.* (2020) 'Kinetic characterisation of Erv1, a key component for protein import and folding in yeast mitochondria', *The FEBS Journal*, 287(6), pp. 1220–1231. doi: 10.1111/febs.15077.

Terziyska, N. *et al.* (2007) 'The sulfhydryl oxidase Erv1 is a substrate of the Mia40-dependent protein translocation pathway', *FEBS Letters*, 581(6), pp. 1098–1102. doi: 10.1016/j.febslet.2007.02.014.

Thornton, N. *et al.* (2010) 'Two Modular Forms of the Mitochondrial Sorting and Assembly Machinery Are Involved in Biogenesis of α-Helical Outer Membrane Proteins', *Journal of Molecular Biology*, 396(3), pp. 540–549. doi: 10.1016/j.jmb.2009.12.026.

Tucker, K. and Park, E. (2019) 'Cryo-EM structure of the mitochondrial protein-import channel TOM complex at near-atomic resolution', *Nature Structural and Molecular Biology*, 26(12), pp. 1158–1166. doi: 10.1038/s41594-019-0339-2.

Vasiljev, A. *et al.* (2004) 'Reconstituted TOM Core Complex and Tim9/Tim10 Complex of Mitochondria Are Sufficient for Translocation of the ADP/ATP Carrier across Membranes', *Molecular Biology of the Cell*, 15(3), pp. 1445–1458. doi: 10.1091/mbc.E03-05-0272.

Voelker, D. R. (2004) 'Lipid synthesis and transport in mitochondrial biogenesis', in. Springer, Berlin, Heidelberg, pp. 267–291. doi: 10.1007/b95719.

Vögtle, F. N. *et al.* (2012) 'Intermembrane space proteome of yeast mitochondria', *Molecular and Cellular Proteomics*, 11(12), pp. 1840–1852. doi: 10.1074/mcp.M112.021105.

Webb, C. T. *et al.* (2006) 'Crystal structure of the mitochondrial chaperone TIM9•10 reveals a six-bladed α-propeller', *Molecular Cell*, 21(1), pp. 123–133. doi: 10.1016/j.molcel.2005.11.010.

Wenz, L.-S. *et al.* (2014) 'The presequence pathway is involved in protein sorting to the mitochondrial outer membrane', *EMBO reports*, 15(6), pp. 678–685. doi: 10.1002/EMBR.201338144.

Wiedemann, N. *et al.* (2003) 'Biogenesis of yeast mitochondrial cytochrome c: A

unique relationship to the TOM machinery', *Journal of Molecular Biology*, 327(2), pp. 465–474. doi: 10.1016/S0022-2836(03)00118-9.

Wiedemann, N. *et al.* (2004) 'Biogenesis of the protein import channel Tom40 of the mitochondrial outer membrane: Intermembrane space components are involved in an early stage of the assembly pathway', *Journal of Biological Chemistry*, 279(18), pp. 18188–18194. doi: 10.1074/jbc.M400050200.

Wiedemann, N. and Pfanner, N. (2017) 'Mitochondrial Machineries for Protein Import and Assembly', *Annual Review of Biochemistry*, 86(1), pp. 685–714. doi: 10.1146/annurev-biochem-060815-014352.

Wiedemann, N., Pfanner, N. and Ryan, M. T. (2001) 'The three modules of ADP/ATP carrier cooperate in receptor recruitment and translocation into mitochondria', *EMBO Journal*, 20(5), pp. 951–960. doi: 10.1093/emboj/20.5.951.

Wolf, D. M. *et al.* (2019) 'Individual cristae within the same mitochondrion display different membrane potentials and are functionally independent', *The EMBO Journal*, 38(22). doi: 10.15252/embj.2018101056.

Wu, C.-K. *et al.* (2003) 'The crystal structure of augmenter of liver regeneration: A mammalian FAD-dependent sulfhydryl oxidase', *Protein Science*, 12(5), pp. 1109–1118. doi: 10.1110/ps.0238103.

Wu, X., Li, L. and Jiang, H. (2018) 'Mitochondrial inner-membrane protease Yme1 degrades outer-membrane proteins Tom22 and Om45', *Journal of Cell Biology*, 217(1), pp. 139–149. doi: 10.1083/JCB.201702125.

Yaffes, M. P., Jensenp, R. E. and Guido, E. C. (1989) 'The Major 45-kDa Protein of the Yeast Mitochondrial Outer Membrane Is Not Essential for Cell Growth or Mitochondrial Function*', *The Journal of Biological Chemistry*, 264(35), pp. 21091–21096. doi: 10.1016/S0021-9258(19)30050-X.

Yamano, K. *et al.* (2008) 'Tom20 and Tom22 share the common signal recognition pathway in mitochondrial protein import', *Journal of Biological Chemistry*, 283(7), pp. 3799–3807. doi: 10.1074/jbc.M708339200.

Yamano, K., Tanaka-Yamano, S. and Endo, T. (2010) 'Mdm10 as a dynamic constituent of the TOB/SAM complex directs coordinated assembly of Tom40', *EMBO Reports*, 11(3), pp. 187–193. doi: 10.1038/embor.2009.283.

Yano, M., Terada, K. and Mori, M. (2004) ‘Mitochondrial Import Receptors Tom20 and Tom22 Have Chaperone-like Activity’, *Journal of Biological Chemistry*. doi: 10.1074/jbc.M311710200.

Young, J. C., Hoogenraad, N. J. and Hartl, F. U. (2003) ‘Molecular chaperones Hsp90 and Hsp70 deliver preproteins to the mitochondrial import receptor Tom70’, *Cell*. Cell Press, pp. 41–50. doi: 10.1016/S0092-8674(02)01250-3.

Zong, W. X., Rabinowitz, J. D. and White, E. (2016) ‘Mitochondria and Cancer’, *Molecular Cell*. Cell Press, pp. 667–676. doi: 10.1016/j.molcel.2016.02.011.